



ISSN 1433-559X  
ESS/INST/P1/01  
May 2001

## **Performance of a Suite of Generic Instruments on ESS**

**ESS Instrumentation Group  
Reports  
SAC Workshop, 3.-5. May 2001**

F. Mezei and R. Eccleston,  
ESS Instrumentation Task Leaders

Compiled by T. Gutberlet



## Content:

<b>Introduction</b>	
<b>Direct geometry spectrometers</b> <i>R. Eccleston et al.</i>	1
<b>Indirect geometry spectrometers</b> <i>K. Andersen et al.</i>	11
<b>NSE instruments</b> <i>M. Monkenbusch et al.</i>	23
<b>Single crystal diffraction and protein crystallography instruments</b> <i>C. Wilson et al.</i>	33
<b>Powder diffraction instruments</b> <i>P. Radaelli et al.</i>	41
<b>Materials science and engineering instruments</b> <i>P. Withers et al.</i>	57
<b>Reflectometry instruments</b> <i>H. Fritzsche et al.</i>	67
<b>SANS instruments</b> <i>R. Heenan et al.</i>	71
<b>Total scattering diffractometers</b> <i>A. Soper et al.</i>	83
<b>ESS Instrument Performance Sheets</b>	91



## Introduction

The goal of the ESS project is to build a neutron source that provides by far enhanced opportunities for the whole of neutron scattering research than any existing source does today. This implies a major change of paradigm. As of today continuous reactor sources and pulsed spallation sources are complementary, some applications are best served by one and others by the other approach. It has become clear, however, that there is no way to further improve the neutronic performance of fission reactors at reasonable costs, while spallation is far from its technical limits. Thus the progress to come will move beyond the complementarity of the two techniques and advanced spallation sources will offer superior potentials in all applications of neutron scattering, including those much better served today by reactor sources. This decisive progress will necessarily be achieved by combining instrumental techniques well established by now at either of the two types of sources with innovative approaches not yet implemented or even proposed. This process, by its very nature and time scale defined by an envisaged start of ESS operation in 2010, will be a multi-stage, successive approximation, in which each step will build on what has been learned and accomplished in the previous ones, and the final stages will eventually largely surpass what could be envisaged at the beginning.

The current report summarises the results of the first stage of this successive approach: to evaluate the expected performance of a set of generic instruments on ESS on the basis of currently available or conservatively envisaged technology. This evaluation was aimed at serving a dual purpose: to provide input data for the basic design choices to be made in the early stages of the project (in particular concerning target station options) and to support the work of the ESS Scientific Advisory Council (SAC) in establishing the scientific case for ESS.

The ESS Instrumentation Task has adopted a low technical risk approach to accomplishing this first study. The cornerstones of this approach are as follows:

- a) A reference ESS target-moderator performance has been established on the basis of experience at current spallation sources and the most detailed Monte Carlo neutron transport calculations available by now as results of the design studies performed in the framework of other next generation spallation source projects, primarily SNS at Oak Ridge. The final neutron parameters of ESS will certainly be different from, and in all likelihood quite superior to, these assumptions as the ESS target-moderator team progresses with design optimisation. In this context the current ESS reference can be considered as lower limit in expected performance. Enhanced options that are being explored include both improving the performance of the 6 types of moderators considered now, and implementing other types of moderators, not yet explored or feasible today. The ESS reference neutron beam performance is summarised in two documents available on the web site of the ESS Instrumentation Task, ESS-Instr-04.12.00 and ESS-Instr-31-12-00, together with further background information.
- b) The performance of a set of generic instruments, compared to those we are familiar with today, was primarily evaluated by assuming by now established instrumentation know how. In a few cases the techniques envisaged were conservatively innovative, i.e. not yet implemented, but already carefully studied and based on established hardware solutions and components. In particular, technologies in current use on continuous reactors sources have occasionally been assumed, even if they have not been implemented on pulsed sources. The most significant examples of this kind in the present report is the use of fast disc choppers to cut out very short pulses from high intensity (coupled moderator) source pulses for the use in high resolution backscattering spectroscopy. Here the choppers allow us to obtain cold neutron pulses several times shorter than the shortest ones possibly provided by a target-moderator system without mechanical pulse shaping.

The technical objectives of the study were also two-fold. On the one hand side, to establish the expected gains in instrument performance exclusively due to the enhanced neutronic performance of ESS compared to the most powerful existing neutron sources ("source gain"). On the other hand, to conservatively estimate the absolute performance of the instruments built at ESS, which will benefit both from the higher performance of the source and the more advanced design of the instruments and their components ("total gain"). These two aspects play essentially different roles. The source gains reflect the part of the progress which cannot be achieved without building an ESS class facility, they are crucial to justify the realisation of the new, advanced technical concepts of ESS. In contrast, estimates of the total gains allow us to assess what kind of new scientific opportunities ESS will offer. In order to just give a arbitrary numerical example: a 30 fold source gain combined with a foreseeable 30 fold improvement in instrument efficiency will offer 3 orders of magnitude gain of sensitivity for ESS. This will open up fully different, qualitatively new scientific opportunities compared to those 30 times more efficient instruments could offer using existing sources or source technology.

In this respect, special care was taken to compare apples with apples, i.e. well optimised instruments on existing neutron sources with essentially equally optimised machines assumed for ESS. Indeed, many of the instruments operating today are of older design or have been built with insufficient funds, and they do not properly reflect the potentials of the neutron sources themselves. One obvious example is the small detector solid angle coverage on most of the less recent machines. We have therefore often assumed hypothetical best possible instruments on existing sources (some of which will be or are being realised in the near future). Thus the source gain factors given in the report truly reflect the increase in performance ESS will offer beyond all other enhancements that can be envisaged by improving the instruments at current, state of the art neutron sources.

The present report is the result of the dedicated effort of a group of experts, who appear as authors of the various contributions, and of the support of institutions they belong to. We would like to thank very much both for their help to make the ESS project advance, to the benefit of the several thousand European scientist, who rely on neutron scattering experiments in their quest for understanding condensed matter in its various forms from structural materials to living organisms.

Feri Mezei

Roger Eccleston

Thomas Gutberlet

# Direct Geometry Spectrometers

**R.I.Bewley<sup>1</sup>, R.S.Eccleston<sup>1</sup>, R.Lechner<sup>2</sup>, F.Mezei<sup>2</sup>, H.Mutka<sup>3</sup>**

<sup>1</sup>ISIS Facility, Rutherford Appleton Laboratory, Chilton, Didcot, Oxfordshire OX11 0QX, United Kingdom

<sup>2</sup>Hahn-Meitner-Institut Berlin GmbH, Abt. SF1, Glienicker Str. 100, 14109 Berlin, Germany

<sup>3</sup>Institute Laue Langevin, 6 Rue Jules Horowitz, BP 156, 38042 Grenoble Cedex 9, France

We have investigated the performance of a reference suite of chopper spectrometers for the European Spallation Source (ESS). For thermal to high neutron energies, the instrument of choice is a Fermi chopper spectrometer design similar to MAPS at ISIS viewing a decoupled poisoned water moderator on a 50Hz short pulse source. For the thermal neutron regime (<100 meV) the use of guides offers the opportunity to build a longer instrument which will utilise the high flux available for a coupled moderator. This instrument is ideally suited to the 50Hz short pulse target station. A multi chopper spectrometer viewing a coupled hydrogen moderator on a 50Hz short pulse target would offer dramatic performance enhancements over existing instruments in terms of both flux and resolution. A similar instrument on the long pulse target station would offer a low-resolution, high-intensity capability.

## High and Thermal Energy Spectrometers

### Resolution

The energy resolution at the elastic line of a chopper spectrometer is given by

$$\frac{\Delta e}{E_i} = 8.7478 \times 10^{-4} \frac{\sqrt{E_i(\text{meV})}}{L_2(\text{m})} \Delta t(\text{m}) \quad (1)$$

where  $L_2$  is the flight path between the sample and the detector and  $\Delta t$  is the pulse width at the detector.  $\Delta t$  comprises a component ( $\Delta t_{md}$ ) arising from the moderator pulse width at the detector and a component from the chopper pulse width at the detector ( $\Delta t_{cd}$ ).

We can consider the two components as follows assuming we are restricting the discussion to elastic scattering for the time being for the sake of simplicity.

$$\Delta t_{md} = \frac{L_2 + L_3}{L_1} \Delta t_{mm} \quad (2)$$

$$\Delta t_{cd} = \frac{L_2 + L_1 + L_3}{L_1} \Delta t_{cc} \quad (3)$$

$\Delta t_{md}$  and  $\Delta t_{mm}$  is the moderator pulse width at the detector and the moderator pulse width at the moderator respectively. Similarly,  $\Delta t_{cd}$  and  $\Delta t_{cc}$  represent the chopper pulse width at the detector and at the chopper.  $L_1$  is the moderator to chopper distance and  $L_3$  the chopper to sample distance.

Clearly, to optimise resolution  $L_2$  is made as long as possible. The only limit being the expense of large detector arrays and the availability of space. For high incident energies large portions of Q space can be accessed at relatively low angles, at thermal to low energies however large detector areas are important to provide reasonable Q coverage.

In considering the optimal configuration for a chopper spectrometer one can calculate the minimum value of  $L_1$  which will give the desired resolution for the given moderator pulse width. We assume the resolution is dominated by the moderator contribution, therefore

$$\frac{\Delta e}{E_i} = 8.7478 \times 10^{-4} \frac{\sqrt{E_i}}{L_1} \Delta t_{mm} \left( 1 + \frac{L_3}{L_2} \right). \quad (4)$$

Table 1 gives the minimum values of  $L_1$  required to give a minimum (i.e. best) resolution of 1% and 2% for a range of energies for the poisoned de-coupled, un-poisoned de-coupled, and coupled ambient water moderators respectively.

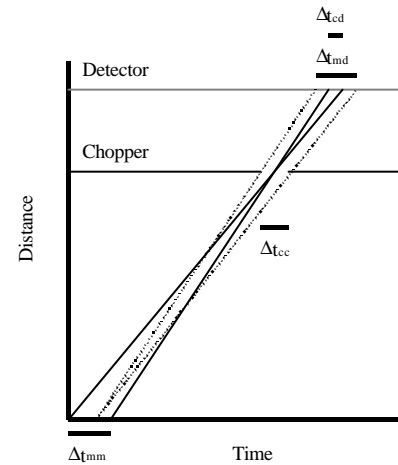


**Fig. 1:** Distance time plot for a chopper spectrometer.

2% Energy resolution	$E_i$ (meV)	Decoupled poisoned	Decoupled unpoisoned	Coupled
	10	3.4	5.5	12.3
	20	4.9	7.7	17.4
	50	7.2	11.7	26.0
	75	7.6	12.6	26.1
	100	7.1	12.1	22.3
	150	5.7	9.9	14.7
	200	4.7	8.0	10.3
	250	4.0	6.8	7.9
	300	3.5	5.9	6.4
	600	2.4	3.8	3.5

1% Energy resolution	$E_i$ (meV)	Decoupled poisoned	Decoupled unpoisoned	Coupled
	10	6.9	10.9	24.6
	20	9.7	15.5	34.8
	50	14.4	23.3	51.9
	75	15.1	25.2	52.2
	100	14.2	24.2	44.7
	150	11.4	19.8	29.4
	200	9.3	16.1	20.6
	250	7.9	13.5	15.8
	300	7.0	11.8	12.8
	600	4.8	7.7	7.0

**Table 1.** Minimum moderator-chopper distances (m) required to achieve 2% and 1% energy resolution when viewing three types of ambient water moderator.

### Flux

The flux at the sample for a given incident energy is proportional to the solid angle of the moderator as seen by the sample and the open time of the chopper as a fraction of the flight-time from moderator to chopper.

$$\Phi = \left( \frac{p}{d} \right) \left( \frac{WmHm}{(L_1 + L_3)^2} \right) \left( \frac{\Delta t_{cc}}{L_1} \right) \quad (5)$$

The term  $(p/d)$  refers to the ratio of the width of the chopper transmitting slits to the width of the absorbing slats. For high incident energies supermirrors will not reduce the  $(L_1+L_3)^2$  flux loss. It is clear that to optimise flux  $L_1$  should be as short as possible (10m is the practical minimum allowing for choppers etc.) and consequently the de-coupled poisoned moderator provides acceptable resolution. The Fermi chopper is a source of background, so  $L_3$  should be sufficiently long so as to remove the chopper from the direct line of sight of the detectors. As stated earlier  $L_2$  should be as long as reasonably possible, consistent with the desired detector solid angle and practical and financial constraints.

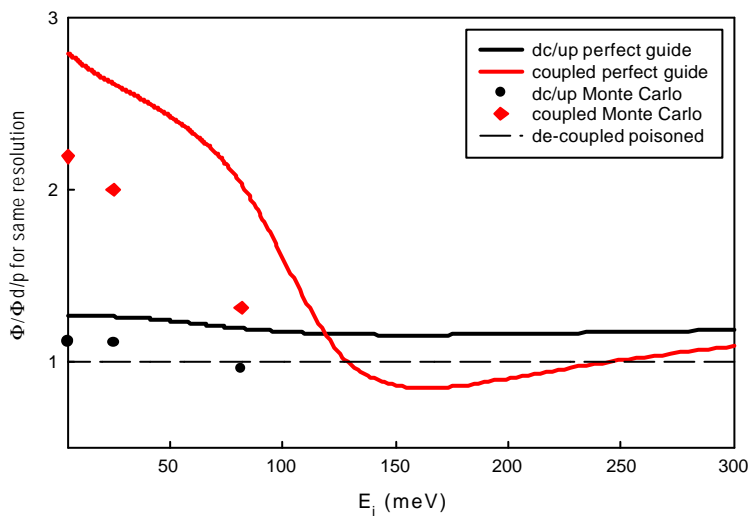


**Fig. 2:** Ratio of flux available from the de-coupled un-poisoned moderator and the coupled moderator to the de-coupled poisoned moderator as a function of temperature, for a perfect guide and based on Monte Carlo simulations of an  $m=3$  converging guide.

From figure 2 it is clear that the de-coupled un-poisoned moderator offers only marginal benefits over the de-coupled poisoned moderator, below ~50 meV. The coupled moderator on the other hand offers a flux enhancement for incident energies below 100 meV that rises to approximately a factor of two at 10 meV. Further, the additional length of the instrument make pulse rate replication<sup>i</sup> more feasible.

Bragg optics is used to good effect on steady state sources, for example IN6 and IN4 at the ILL, where focussing crystal monochromator and high repetition rate provide high flux. Previous work (Mutka in Ref,iii) has shown that the advantages of this concept do not transfer easily to short pulse spallation sources. However, due to the relaxed incident divergence (a few degrees horizontal and vertical) IN4 provides a benchmark for a thermal instrument, offering high flux ( $>10^5$  n cm<sup>-2</sup> s<sup>-1</sup> in the 30 to 70 meV range, at 4% resolution). At 50 meV, the thermal instrument will offer a flux of  $\sim 9 \cdot 10^5$  n cm<sup>-2</sup> s<sup>-1</sup> (2.5% resolution).

### Summary

- For high-energy spectroscopy  $L_1$  should be as short as possible and  $L_2$  as long as possible consistent with the desired solid angle. The de-coupled poisoned moderator is required
- For thermal neutron spectroscopy, the de-coupled un-poisoned moderator can offer marginal flux enhancement below 50 meV.
- A coupled moderator offers better flux for energies up to 100 meV than can be achieved at equivalent resolution viewing the de-coupled poisoned moderator.
- The later option also offers the capability of rep rate multiplication.
- A tail cutting chopper will almost certainly need to be used on a spectrometer viewing a coupled moderator.
- Position sensitive detectors are essential on all instruments.
- All these instruments are well suited to a 50Hz source.
- Chopper spectrometers on the ESS will out-perform all present state-of-the-art instruments on any source.

***Chopper spectrometers on the ESS will out-perform all present state-of-the-art instruments on any source.***

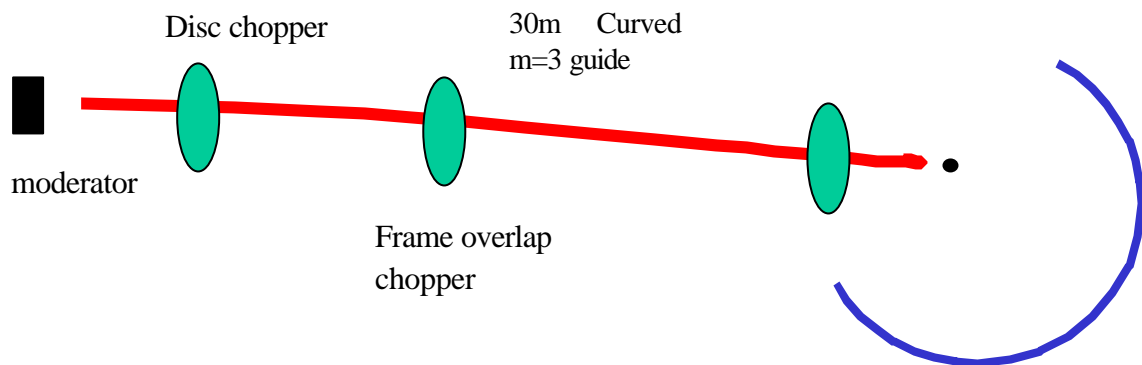
## Low Energy Chopper Spectrometers

### A Multi-Chopper Spectrometer (MCS)

The aim of this work is to study the performance of a multi-chopper spectrometer (MCS) optimised for cold neutrons ( $E_i$  range 1-30 meV) which, in this document will be called LET (low energy transfer). At present MCSs only exist on reactor sources such as NEAT (HMI) and IN5 (ILL). However, unlike many neutron instruments, the flux on a direct geometry spectrometer is directly related to the peak flux of the moderator and not the time-averaged flux. This vastly favours spallation sources over reactor sources for such an instrument.

Multi-chopper spectrometers have the advantage of giving the user complete flexibility over resolution and lineshape. Two components: the moderator time width and the chopper opening time essentially define the resolution of a direct geometry spectrometer. On instruments like HET and MAPS one has no control over the moderator component of the resolution (other than deciding on the type of moderator the instrument views). The resolution can be controlled, only by changing the chopper opening time. This not only limits the lowest resolution that can be achieved, but it also means that the two resolution components are not 'matched' and hence it is not possible to achieve the optimum configuration for flux for any given resolution. A MCS allows both resolution components to be adjusted. The lowest resolution is limited only by the physical limits of the chopper speed.

## Schematic of a MCS



<b>Moderator</b>	coupled H
<b>Incident energy</b>	1-80 meV
<b>Best resolution</b>	1% at 1 meV - 5% at 80 meV
<b>Primary length</b>	30m
<b>Sample-detector</b>	2.5m
<b>Flight path</b>	m=3 supermirror curved guide
<b>Choppers</b>	2 pairs of counter-rotating disc choppers (5-330Hz)+frame overlap chopper
<b>Detectors</b>	position sensitive, angular range -30 to 150 degrees

**Fig.3:** Schematic diagram of a MCS.

## Energy Resolution

The energy resolution can be easily calculated and has been written in many forms but the most intuitive representation is

$$R = \frac{\sqrt{E_i \Delta t_{\text{det}}}}{1142 L_{\text{sd}}} \quad (6)$$

where  $\Delta t_{\text{det}}$  is the time uncertainty at the detectors in  $\mu\text{s}$  and  $L_{\text{sd}}$  is the sample to detector distance. There are other contributions to  $R$ , such as uncertainties in path length due to detector depths and sample size, but these tend to be very small compared to the contributions from the moderator and chopper. Equation 6 gives the energy resolution at the elastic line. The resolution improves with energy transfer  $\Delta E$  by multiplying the above equation by  $(1 - \Delta E / E_i)^{3/2}$ . In the following all the resolutions quoted will be at the elastic line.

The schematic diagrams (Figure 4) show the contributions of the moderator and chopper components to  $\Delta t_{\text{det}}$

From figure 4 it is easy to see from geometric considerations that the time width at the detector due to the moderator is

$$\Delta t_{\text{det}}^{\text{mod}} = \frac{L_2}{L_1} \Delta t_{\text{chop1}} \quad (7)$$

where  $\Delta t_{\text{chop1}}$  is the opening time of the 1st chopper.  $L_2 = L_{\text{sd}} + L_{\text{cs}}$  where  $L_{\text{cs}}$  is the distance from chopper2 to the sample.  $\Delta t_{\text{chop1}}$  can be controlled of course so we have control over the moderator width at the detector. If  $\Delta t_{\text{chop1}}$  is larger than the natural width of the moderator then the detector will only see the natural width of course. For the chopper contribution we have

$$\Delta t_{\text{det}}^{\text{chop}} = \frac{L_2 + L_0}{L_0} \Delta t_{\text{chop2}} \quad (8)$$

The two time contributions need to be convoluted together to give the total time width at the detector  $\Delta t_{\text{total}}$ . A good approximation to this is to add the two components in quadrature such that

$$\Delta t_{\text{tot}} = \left( \Delta t_{\text{det}}^{\text{mod}} \right)^2 + \left( \Delta t_{\text{det}}^{\text{chop}} \right)^2 \quad (9)$$

From this equation it is clear that one component only has to get slightly larger and it will dominate the resolution.

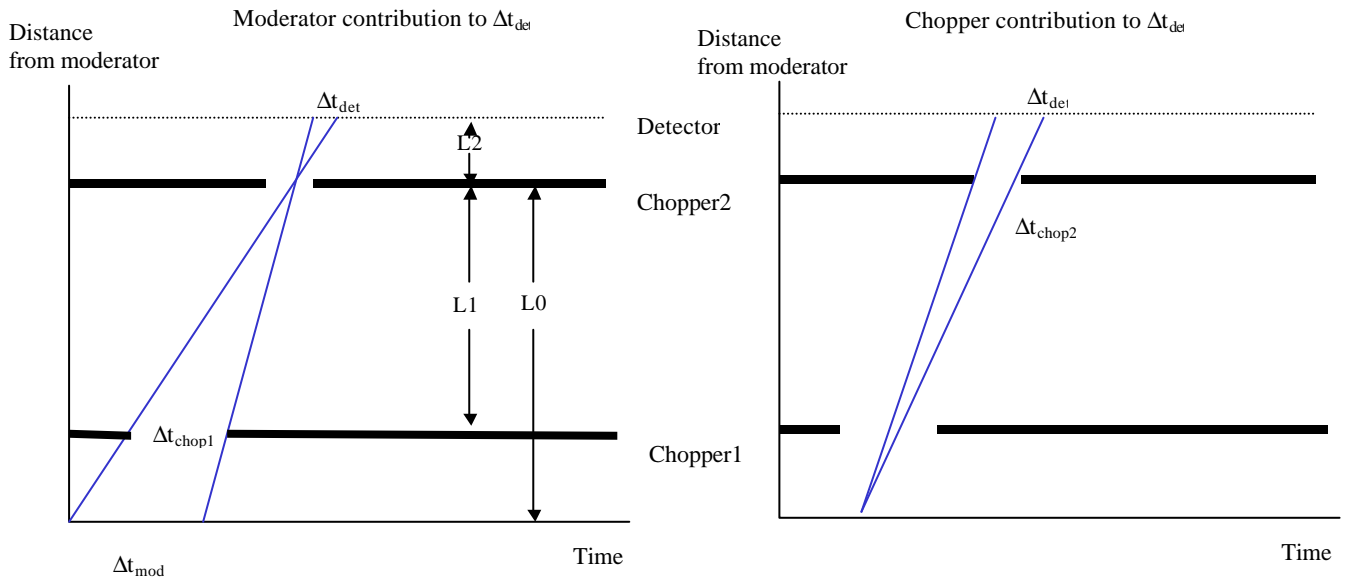


**Fig. 4:** Moderator and chopper components to the resolution of a MCS.

### Chopper optimisation (PWR)

To optimise the total flux for a particular resolution ideally one needs to match the two resolution components at the detector, i.e.  $\Delta t_{\text{det}}^{\text{mod}} = \Delta t_{\text{det}}^{\text{chop}}$ . On doing this one gets a condition for the opening times for both choppers to give the maximum possible flux

$$\frac{\Delta t_{\text{chop1}}}{\Delta t_{\text{chop2}}} = \frac{L_2 + L_0}{L_0} \frac{L_1}{L_2} \quad (10)$$

R. Lechner who designed NEAT at HMI, calls this Pulse-Width Ratio (PWR)<sup>ii</sup> optimisation. The expression above is

slightly different from his expression, as at a reactor the opening time of the 1<sup>st</sup> chopper directly defines the effective moderator width whereas on a spallation source you need to account for the distance from the moderator to the 1<sup>st</sup> chopper. If  $L_1=L_0$  the same result is obtained.

### **Choice of moderator**

As the design of LET is for energies below 30 meV then a hydrogen moderator is the dear choice for maximum flux. Since chopper1 provides control of the moderator time width, the important parameter is the peak height of the flux. A coupled moderator can typically give almost double the peak flux of a de-coupled moderator and the extra pulse width provides the flexibility to shape the pulse to triangular or trapezoidal resolution line shape or to relax the resolution to gain more flux. Consequently a coupled H moderator would be preferred.

### **Optimum primary flight path**

Higher energy instruments like HET and MAPS tend to be in as close to the moderator as is realistically possible considering biological shielding etc. A typical primary flight path is of around 10m because of the large  $1/r^2$  drop off in flux on these instruments. As LET is a low energy spectrometer the use of a guide changes this argument considerably. In the following discussion and calculation we will show that the optimum  $L_0$  is around 20m.

Before continuing to display the results of simulations it is informative to discuss the various parameters affecting the flux on LET. If  $L_0$  is very small then to get a particular resolution one finds that  $\Delta t_{\text{chop1}}$  has to be very small, i.e. we are only chopping a small amount of the available time width of the moderator pulse.  $\Delta t_{\text{chop1}}$  gets larger in direct proportion with  $L_0$  for the same instrument resolution. Therefore we are cutting more flux from the moderator with increasing  $L_0$ . As losses down a guide are small, it is clear that there is an optimum length, at which, for a given resolution we are utilising the whole moderator width. On increasing  $L_0$  further the flux decreases, not only because of the flux losses of the guide but also because the flux accepted from the moderator by chopper2 decreases as  $1/L_0$ . If  $\Delta t_{\text{chop2}}$  is kept constant such that the chopper contribution to the resolution is approximately constant, then one can see the acceptance angle of velocities getting through chopper2 is directly proportional to  $1/L_0$ .

Figure 5 shows the flux at the sample position calculated for various values of  $L_0$ . The resolution was kept fixed for each  $L_0$  by varying the values of  $\Delta t_{\text{chop1}}$  and  $\Delta t_{\text{chop2}}$ . The ratio of the chopper opening times was set to maximise the flux at each  $L_0$  using the matching condition given in equation 10. The relative opening times of the two choppers was also set to focus in time on the peak of the moderator flux. In this case the moderator parameters were for a coupled H<sub>2</sub> moderator using the parameters supplied by F. Mezei. Although the resolution calculated from the program at shorter values of  $L_0$

was in excellent agreement with the value expected, at longer values of  $L_0$  where the full moderator width has already been utilised the program gave a better resolution than calculated. This is to be expected of course as the moderator component contributes less and less to the resolution now. In order to keep a fixed resolution the matching condition was relaxed and the chopper2 opening time increased by an amount necessary to keep the resolution fixed. In the data shown the values of  $L_{cs}$  and  $L_{sd}$  were fixed at 1m and 2.5m respectively. We can see from the figure that the optimum flux for a LET spectrometer would be obtained with a primary path length of about 20m. It is interesting to note that the optimum path length is similar for both values of  $E_i$  at 2.31 and 20meV. This is rather fortunate as one length of spectrometer is optimised for the whole energy range of LET. This arises because as  $E_i$  increases, the time width on the detector must decrease to keep the same resolution. This decrease comes about naturally because moderator width also decreases with  $E_i$  and consequently  $L_0$  does not need to be increased.

The absolute values of flux given in the figures were obtained from normalising everything to a Monte-Carlo simulation. The simulation was done for  $L_0=20m$ , an  $m=3$  converging guide starting 1m from coupled  $H_2$  moderator (10cm x10cm cross section at moderator down to 4.5cm x4.5cm at sample).

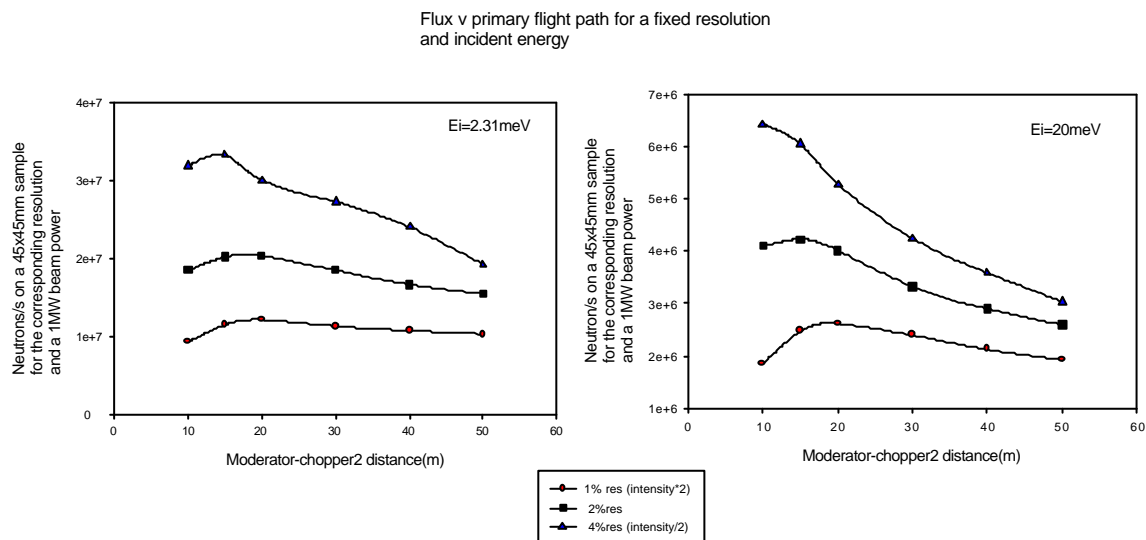


**Fig. 5:** Optimise flux vs. primary flight path for LET.

### Fluxes on LET compared to other instruments

In order to make a direct comparison of the capabilities of LET the flux at the sample position was simulated by Monte Carlo measurements. The parameters for the instrument were as follows:

- a 10cm x10cm coupled  $H_2$  moderator
- an  $m=3$  guide starting 1m from moderator and ending 20m from moderator, converging from 97mm x97mm down to 45mm x45mm at sample position with a reflectivity of 80% at a critical angle of  $3 \cdot m_{Ni}$ .

- chopper1 was at 5m from moderator
- chopper2 at 20m from moderator
- the chopper opening times were optimised to give the maximum flux at the sample for a certain resolution.

The results and comparison with other instruments are shown below

$E_i$	IN5 (new) $n \text{ cm}^{-2} \text{ s}^{-1}$	IN6 $n \text{ cm}^{-2} \text{ s}^{-1}$	LET(ESS 5MW) $n \text{ cm}^{-2} \text{ s}^{-1}$
2.27	$>10^5$ (2%res)	-----	$4.9 \times 10^6$ (2%res)
4.86	-----	$8.9 \times 10^4$ (3.5%res)	$6 \times 10^6$ (2%res)
20.45	-----	-----	$9.5 \times 10^5$ (2%res)

### An MCS on the Long Pulsed Source

It is clear from the above discussion that a broader neutron pulse provides flux enhancements as long as the length of the spectrometer and resolution constraints are such that the whole or a substantial portion of the pulse width can be viewed by the detectors. For a low-resolution, high intensity spectrometer, the long pulsed source offers some advantages. The use of a long flight path provides more space for installing large detector arrays and makes the removal of the prompt neutron pulse more straightforward. Pulse rate multiplication techniques could also be employed effectively to increase effective data rates.

### Summary

- A multi-chopper spectrometer viewing a coupled H moderator on the 50Hz target of the ESS provides performance that surpasses existing similar instrument by two orders of magnitude.
- A multi-chopper spectrometer on the 16.6Hz long pulse target station will provide a high intensity, low resolution spectrometer which would also dramatically out-perform existing instruments.

***A multi-chopper spectrometer at 50Hz target provides performance surpassing existing similar instrument by two orders of magnitude. At 16.6 Hz target a MCS would dramatically out-perform existing instruments***

Chopper development is important to fully realise the potential of both these instruments.

### Acknowledgements

We have drawn extensively from pervious ESS studies<sup>iii</sup> and benefited greatly from conversations with colleagues at several of Europe's neutron centres.

<sup>i</sup> M.Russina et al, ICANS XV Proc. (2001)

<sup>ii</sup> R.E.Lechner, Physica B 276-278 (2000) 67-68 (and references therein)

<sup>iii</sup> U.Steigenberger (ed.), 'Contributions to the ESS Instrument Working Group on Single Crystal Spectroscopy', ESS 98-74-T (1998).

# Indirect Geometry Spectrometers

**P. Allenspach<sup>1</sup>, K.H. Andersen<sup>2</sup>, D. Colognesi<sup>2</sup>, B. Fåk<sup>2</sup>, O. Kirstein<sup>3</sup>, M. Zoppi<sup>4</sup>**

<sup>1</sup>Paul Scherrer Institut, 5232 Villigen, Switzerland

<sup>2</sup>ISIS Facility, Rutherford Appleton Laboratory, Chilton, Didcot, OX11 0QX, United Kingdom

<sup>3</sup>Forschungszentrum Jülich, 52425 Jülich, Germany

<sup>4</sup>Consiglio Nazionale delle Ricerche, Firenze, Italy

We looked at six instruments, covering a very wide range of science and energy scales:

- Backscattering
  - 0.8  $\mu\text{eV}$  – direct-backscattering Si 111
  - 1.5  $\mu\text{eV}$  – near-backscattering Si 111
  - 17  $\mu\text{eV}$  – near-backscattering PG 002
- Constant-**Q** (PRISMA)
- Vibrational Spectroscopy (TOSCA)
- Resonance High-Energy (eV spectroscopy)

The backscattering instruments cover quasielastic and inelastic measurements over a range of resolutions. The use of pulse-shaping choppers is considered in some detail, assuming that the pulse-shaping chopper needs to be outside the bulk shielding of the target station. The resultant loss of dynamic range is found to be unimportant for the Si ( $\sim 1 \mu\text{eV}$ ) machines, but very significant for the 17  $\mu\text{eV}$  (graphite) machine. The 0.8  $\mu\text{eV}$  machine is best served by a cold coupled moderator with a pulse-shaping chopper on the 50Hz target. This combination is also optimal for the 1.5  $\mu\text{eV}$  machine. Though the cold poisoned moderator without pulse-shaping performs just as well for quasielastic measurements, the use of a coupled moderator and a pulse-shaping chopper allows a more flexible tuning of the resolution, particularly for inelastic measurements. The graphite machine can be served by a range of moderators, giving different combinations of flux and dynamic range. The best option is probably the decoupled cold moderator on the 50Hz target. The Si machines outperform present reactor-based instruments by at least an order of magnitude in both flux and dynamic range simultaneously. The graphite machine outperforms IRIS by a factor of 200.

The constant-**Q** machine offers to cover a large fraction of experiments presently performed on triple-axis instruments. It uses an array of analyser arms to construct an energy scan at constant **Q** from a single measurement. The preferred moderator is the decoupled hydrogen moderator on the 50Hz target. Evaluation of the instrument is not sufficiently advanced to make quantitative comparisons with existing instruments.

The vibrational spectroscopy instrument is very similar to the present TOSCA instrument at ISIS. It measures the vibrational density of states over a wide range of energy transfers in a single measurement. The preferred moderator is decoupled hydrogen or poisoned water. The improvement in the source flux between ISIS and ESS is the major gain factor over TOSCA.

The eV spectroscopy instrument measures atomic momentum distributions by neutron Compton scattering. This instrument requires a poisoned moderator; thermal or cold on the 50Hz target.

Given the choice between the three proposed ESS targets, all six instruments identify the 50Hz short-pulse target as their first choice. 2 instruments choose the 10Hz short-pulse target as the second option. 2 instruments choose the long-pulse target as the second option.

## Backscattering Instruments

Three such instruments are examined.

- 1) 0.8  $\mu\text{eV}$  direct-backscattering machine using Si 111. Optimised for the best combination of resolution and counting rate for quasielastic measurements.
- 2) 1.5  $\mu\text{eV}$  near-backscattering machine using Si 111. Optimised for the best combination of resolution and counting rate inelastic measurements.
- 3) 17  $\mu\text{eV}$  near-backscattering machine using PG 002.

The 0.8  $\mu\text{eV}$  machine uses Si crystals arranged in direct backscattering (DBS) which means that the detectors are placed directly behind the sample (seen from the analysers). The secondary spectrometer resolution of this machine could be improved to 0.3-0.4  $\mu\text{eV}$  by using polished Si crystals and/or long secondary flight paths (3m or more). This instrument uses unpolished Si crystals at a distance of 2m from the sample to give a compact machine with a high counting rate and a resolution function without Lorentzian tails. It is optimised for quasielastic measurements, as performed at present on instruments such as IN16 and HFBS at NIST.

The 1.5  $\mu\text{eV}$  machine also uses unpolished Si crystals at 2m, but the detectors are arranged in near-backscattering (NBS), i.e. around and below the sample, so that direct line-of-sight from the sample to the detectors is eliminated. The penalty is a degradation in resolution, compared to DBS, but an improvement in background and potential "spurious". In a DBS instrument, elastic and quasielastic scattering from the sample directly into the detectors is eliminated using a "timing chopper". However, sharp inelastic events may still contaminate the data. NBS is thus a good choice for a truly inelastic machine.

The 17  $\mu\text{eV}$  machine uses pyrolytic graphite (PG) crystals in near-backscattering, at a distance of 1m from the sample, and cooled to about 10 K to reduce thermal diffuse scattering. It is very similar to IRIS at ISIS.

The DBS Si machine has a secondary spectrometer resolution of 0.56  $\mu\text{eV}$  FWHM. A timing chopper is used to discriminate against neutrons scattering directly into the detectors from the sample. This has the net effect of reducing the flux on the sample by a factor of two, which is taken into account in the flux numbers given here. The NBS Si machine has a secondary spectrometer resolution of 1.06  $\mu\text{eV}$  FWHM and no timing chopper. The graphite machine has a secondary spectrometer resolution of 12  $\mu\text{eV}$ . The secondary spectrometer resolution line shape is Gaussian for all three instruments.

The instruments are optimised to match the primary and secondary instrumental energy resolutions, i.e. the DBS Si machine is optimised for a total energy resolution of  $2 \times 0.56 \mu\text{eV} = 0.80 \mu\text{eV}$  and the NBS Si and graphite instruments have a total resolution of 1.50  $\mu\text{eV}$  and 17.0  $\mu\text{eV}$ , respectively.

The resolution calculation includes the time-width from the moderator speed distribution, time-width (if applicable) from a pulse chopper, chopper path length uncertainty due to guide

***The 0.8 meV Si backscattering instrument covers quasielastic measurements, in the same way as present-day reactor-based backscattering instruments.***

***The 1.5 meV Si instrument covers inelastic measurements.***

***The graphite instrument provides a resolution of 17 meV for both quasielastic and inelastic measurements.***

***The instruments are optimised by matching the primary and secondary resolution.***

pulse-shaping chopper, path-length uncertainty due to guide geometry and sample size. The resolution contributions are modelled as realistically as possible: The moderator shape is from the parameterisation circulated by the moderator working group. The pulse-shaping chopper contribution (if applicable) is triangular and the path-length uncertainties in the guide are calculated by Monte Carlo. The flux is calculated by numerical integration over the sampled region of the moderator time-speed distribution, combined with a Monte Carlo calculation of the guide transmission. The guide is straight with a cross-section of 60mm x70mm (W×H) and  $m=2$  supermirror coating. At the end, an  $m=4$  supermirror converging guide focuses the beam down to a sample size of 20mm x30mm (cylindrical). No systematic optimisation of the guide geometry has been performed. Increased gain factors can be obtained by using ballistic guides and improved-reflectivity supermirrors.

Instruments without pulse-shaping choppers rely on the intrinsic time-width of the moderator neutron distribution to give the desired energy resolution. Resolution is improved by moving away from the moderator. The table below summarises the essential instrument parameters for such instruments.

**Resolution and flux are calculated by a combination of numerical integration and Monte Carlo.**

**Conventional backscattering instruments: no pulse-shaping choppers.**

mod	Dt ms	$L_i$ m	$\hbar\omega$ range 50Hz / 10Hz meV	F ( $I_0$ ) 50Hz / 10Hz $10^7$ n/cm <sup>2</sup> /s/Å
0.8 $\mu$ eV DBS Si machine				
1	27	235	-0.01 $\rightarrow$ 0.19 / 0.14	0.8 / 0.2
2	43	335	-0.01 $\rightarrow$ 0.14 / 0.86	1.6 / 0.3
4	59	440	-0.01 $\rightarrow$ 0.09 / 0.61	8.0 / 1.6
5	95	680	-0.01 $\rightarrow$ 0.06 / 0.36	15.6 / 3.1
1.5 $\mu$ eV NBS Si machine				
1	27	108	-0.01 $\rightarrow$ 0.47 / 6.05	1.8 / 0.4
2	43	155	-0.01 $\rightarrow$ 0.31 / 2.76	3.5 / 0.7
4	59	205	-0.01 $\rightarrow$ 0.23 / 1.73	16.8 / 3.4
5	95	315	-0.01 $\rightarrow$ 0.15 / 0.94	31.8 / 6.5
17 $\mu$ eV graphite machine				
4	60	14.4	-0.39 $\rightarrow$ 7.97 / -1.70 $\rightarrow$ 7.97	17 / 3
5	96	22.4	-0.10 $\rightarrow$ 3.53 / -1.57 $\rightarrow$ 6.97	33 / 7
6	229	71	-0.10 $\rightarrow$ 0.50 / -0.55 $\rightarrow$ 5.87	111 / 23

**Flux and dynamic range of conventional backscattering instruments:**

**0.8 meV machines are unfeasibly long.**

**1.5 meV machines are just about feasible**

**17 meV machines can be served by a range of moderators**

The moderator numbers refer to those specified by the moderator working group (1-3 thermal, 4-6 cold). The value of  $\Delta t$  given in the table is the FWHM of the moderator time-distribution at the elastic wavelength  $\lambda_0$  (6.27 Å for Si 111 and 6.70 Å for PG 002).  $L_i$  is the moderator-sample distance.  $\hbar\omega$  range is the useable range of energy transfers which is determined by a combination of repetition rate, instrument length, contamination from the first higher order reflection (Si 333 or PG 004, respectively), sweep time over the guide of the bandwidth (frame-overlap) chopper running at the source frequency and the requirement that the elastic peak must be included. The last column shows the time-averaged flux at the elastic wavelength.

Some of the flight paths for the Si instruments are very long and probably unfeasible. In principle, there is no technical

**The dynamic range is given by the need to eliminate frame overlap and higher-order contamination**

and probably unfeasible. In principle, there is no technical problem in building very long guides; the limiting factor is the cost. The cost of  $m=2$  supermirror guides is approx. 10 k\$/m for a typical guide cross-section, giving a price tag of 2 M\$ for a 200m guide. If we set the feasibility limit at around 200m, that leaves perhaps one instrument for the DBS Si instrument and three instruments for the NBS Si instruments.

Pulse-shaping choppers offer the possibility of improving resolution in a more flexible way than simply lengthening the instrument. A fast chopper is placed as close as possible to a coupled moderator. In principle, the enhanced peak flux from the coupled moderator can be combined with a much narrower time structure, given by the chopper speed. In practice, fast choppers cannot be placed arbitrarily close to the moderator for safety and maintenance reasons. Moving the pulse-shaping chopper away from the moderator translates into a reduced dynamic range. In these calculations, the pulse-shaping chopper is placed at a distance  $L_{\text{chop}}$  of 6.3 m from the moderator, which is the closest that can presently be achieved at ISIS. Either a Fermi or disk chopper can be used. At present the shortest burst time achievable with a disk chopper is about 15  $\mu\text{s}$  (FWHM) using a narrowed guide at the chopper position (NEAT, HMI). A Fermi chopper can achieve pulses as narrow as 2  $\mu\text{s}$  (ISIS). In these calculations, a triangular transmission function is used with a peak transmission of 100% without reference to the type of chopper. The table below gives  $\Delta t$  as the FWHM of this peak. To maximise the flux, the instrument length and chopper burst time are scanned together keeping the total resolution constant (at 0.8, 1.5 or 17  $\mu\text{eV}$ ). For the Si instruments, the flux on the sample was found to increase with instrument length beyond feasibility. We use 200m as the longest feasible guide length. This also coincides roughly with the length at which the dynamic range given by the instrument at 50 Hz matches the dynamic range given by the moderator-chopper distance. For the graphite machine, the length given in the table below corresponds to that of maximum flux at the elastic wavelength.

**Instruments much longer than 200 m are classed as unfeasible.**

**Pulse-shaping: a fast chopper close to the moderator defines the time-width of the pulse.**

**Placing the pulse-shaping chopper outside the bulk shielding significantly reduces the dynamic range.**

**Flux is maximised by scanning instrument length and chopper burst time together at constant resolution.**

**200 m is kept as the maximum feasible length.**

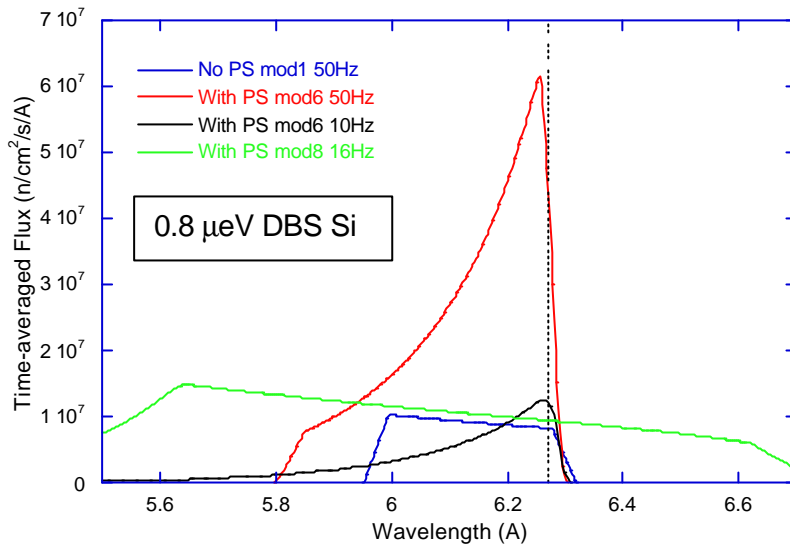
mod	f Hz	Dt ms	$L_i$ m	$\hbar w$ range meV	F ( $I_0$ ) $10^7 \text{ n/cm}^2/\text{s}/\text{\AA}$
0.8 $\mu\text{eV}$ DBS Si machine					
6	50	32	200	-0.02 $\rightarrow$ 0.27	6.2
6	10	32	200	-0.02 $\rightarrow$ 0.35	1.3
8	16	31	200	-0.21 $\rightarrow$ 0.73	1.0
1.5 $\mu\text{eV}$ NBS Si machine					
6	50	76	200	-0.05 $\rightarrow$ 0.23	27.5
6	10	76	200	-0.05 $\rightarrow$ 0.34	5.4
8	16	73	200	-0.21 $\rightarrow$ 0.73	4.4
17 $\mu\text{eV}$ graphite machine					
6	50	300	59.5	-0.15 $\rightarrow$ 0.26	50
6	10	300	59.5	-0.15 $\rightarrow$ 0.26	10
8	16	600	114	-0.30 $\rightarrow$ 0.88	32

**Flux and dynamic range of backscattering instruments with a pulse-shaping chopper**

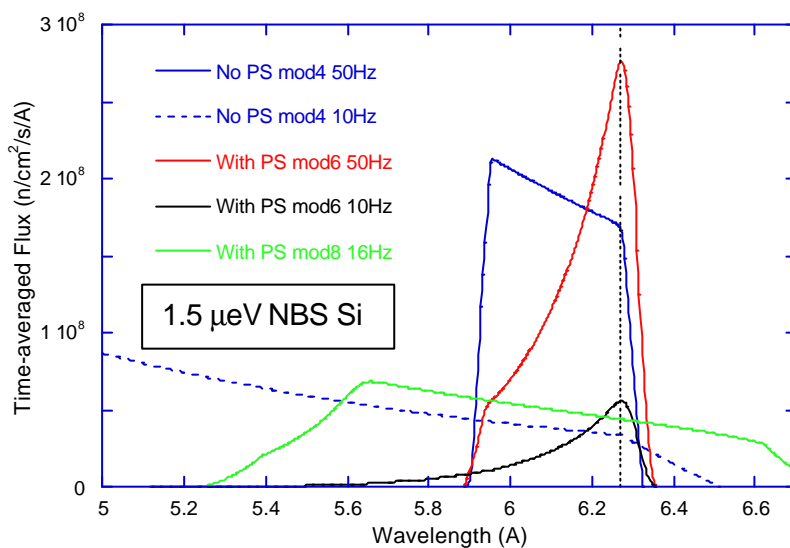
**0.8 and 1.5 meV instruments are 200 m long.**

**Long-pulse instruments have twice the dynamic range**

**17 meV instruments are shorter but with the same dynamic range.**



**The 0.8 meV instrument is best served using a pulse-shaping chopper.**



**The 1.5 meV instrument does equally well with and without a pulse-shaping chopper.**

**Fig. 1:** Flux versus wavelength for the Si backscattering machines. The elastic wavelength is indicated by the black dotted line. PS stands for pulse-shaping.

The highest flux on the 0.8  $\mu\text{eV}$  DBS instrument is achieved using a pulse-shaping (PS) chopper on the coupled cold moderator (mod6) at 50Hz. For the 1.5  $\mu\text{eV}$  NBS instrument, the 205m long conventional (no PS) instrument viewing the poisoned cold moderator (4) has a similar flux to the pulse-shaping instrument on the coupled moderator. The preference is for the pulse-shaping instrument, as it gives the flexibility to more closely match primary and secondary resolutions when measuring at large energy transfers. It also allows the option of increasing the flux by relaxing the resolution. For example, at an energy transfer of 10 meV, the conventional machine has a non-tuneable resolution of 6.3  $\mu\text{eV}$ , while the pulse-shaping machine can be tuned to give a resolution of between 3 and about 30  $\mu\text{eV}$ , with approximately the same flux at the same resolution. For both Si machines, the flux can be increased by about an order of magnitude by relaxing the resolution by an order of magnitude. There is also a small advantage for the long-pulse target: The long-pulse instruments can gain about twice as much flux as the instruments on the short-pulse target by relaxing resolution.

**For the Si machines, a pulse-shaping chopper is the best option: it provides far higher flux for the 0.8 meV machine and tuneable resolution for both machines.**

**For the 1.5 meV machine, this means that primary and secondary resolutions can be more closely matched when measuring at large energy transfers.**

The dynamic range of the pulse-shaping instruments is up to three orders of magnitude greater than the resolution width and is thus more than adequate for quasielastic scattering and also for inelastic measurements after a survey measurement has been done elsewhere. For both instruments, the long-pulse target offers an increase in dynamic range by about a factor of two with a decrease in flux by a factor of 2-3. The 10Hz target is of no interest, combining the reduced dynamic range of the 50Hz pulse-shaping machines with the reduced flux of the long-pulse target.

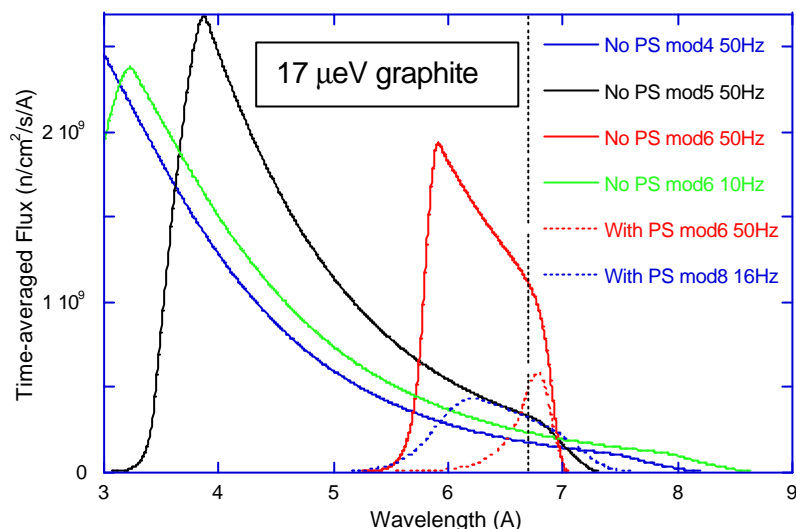


**Fig. 2.** Flux versus wavelength for the graphite backscattering machine. The elastic wavelength is indicated by the black dotted line. PS stands for pulse-shaping.

A wide range of combinations of flux and dynamic range is available for the graphite machine. The conventional decoupled-moderator (mod5) instrument on the 50 Hz target (shown in black) gives a high flux with a dynamic range of 3.5 meV, representing a conventional compromise between flux and dynamic range. This is the reference graphite instrument, similar to IRIS at ISIS. The dynamic range of the pulse-shaping instruments (shown as dotted lines) is seen to be drastically reduced compared to the conventional instruments; down to about 0.4 meV with a similar flux as the reference instrument. The long-pulse instrument also has the same flux as the reference instrument at the elastic wavelength and a dynamic range of about 1 meV. Both pulse-shaping instruments are clearly uncompetitive compared to the 50Hz coupled-moderator instrument without pulse-shaping (shown in red) which provides a much higher flux at the elastic wavelength and a similar dynamic range.

The flux on the graphite pulse-shaping instruments cannot be increased much by relaxing resolution, as the opening time of the pulse-shaping chopper is already comparable to the intrinsic moderator time width. On the short-pulse target, there is no flux gain to be made, while on the long-pulse target the flux can be increased by about a factor of two by relaxing the resolution by a factor of two.

We compare the performance of the Si instruments with IN16 at the ILL and the High Flux Backscattering Spectrometer (HFBS) at NIST.

***The 50Hz target offers the highest flux with a good dynamic range. The long-pulse target provides twice the dynamic range with half the flux. The 10Hz target is not competitive.***

***For the graphite instrument, pulse-shaping choppers are not competitive with conventional machines.***

***A wide range of combination of flux and dynamic range is available for conventional graphite machines.***

***The reference graphite instrument views the decoupled hydrogen moderator.***

***On the pulse-shaping graphite instruments, only marginal flux increases can be gained by relaxing resolution.***

The energy resolution on IN16 is 0.9  $\mu\text{eV}$  (FWHM) giving a flux on the sample of  $1 \times 10^5$   $\text{n/cm}^2/\text{s}$  over a dynamic range of  $-15 \rightarrow 15$   $\mu\text{eV}$ . The best energy resolution on HFBS is 0.80  $\mu\text{eV}$  (FWHM) giving a flux on the sample of  $1.4 \times 10^5$   $\text{n/cm}^2/\text{s}$  over a dynamic range of  $-11 \rightarrow 11$   $\mu\text{eV}$ . Integrating over the corresponding wavelength ranges for the ESS 50Hz coupled-moderator instrument with pulse-shaping, gives a flux of  $2.5 \times 10^6$   $\text{n/cm}^2/\text{s}$  and  $2 \times 10^6$   $\text{n/cm}^2/\text{s}$ , respectively, for these two dynamic ranges. The flux is 25 times higher than IN16 and 14 times higher than HFBS. In addition, for both these instruments, the dynamic range of the ESS instrument is an order of magnitude greater.

***The 0.8 meV instrument has 20 times higher flux at the elastic wavelength than the present best (HFBS and IN16) and an order of magnitude greater dynamic range.***

Comparing with the 1.5  $\mu\text{eV}$  instrument is not as straightforward, as there is no truly inelastic instrument of this type in existence. For a flux comparison, we use the broadest energy resolution available on HFBS, which is 1.01  $\mu\text{eV}$  (FWHM) giving a flux on the sample of  $1.4 \times 10^5$   $\text{n/cm}^2/\text{s}$  over a dynamic range of  $-36 \rightarrow 36$   $\mu\text{eV}$ . Integrating over the corresponding wavelength range for the ESS 50Hz coupled-moderator instrument with pulse-shaping, gives a flux of  $2.5 \times 10^7$   $\text{n/cm}^2/\text{s}$ , which is more than 2 orders of magnitude higher. The resolution of the ESS instrument is about 50% broader, while the dynamic range is an order of magnitude greater.

***The 1.5 meV instrument has more than 100 times higher flux than the closest existing instrument.***

The two existing instruments in Europe which come closest to the graphite machine are IRIS at ISIS and IN13 at the ILL. IN13 has an energy resolution of 8  $\mu\text{eV}$  and a dynamic range from  $-0.12$  to 0.3 meV. It has a Q-range about twice as wide as this instrument. The monochromatic flux on IN13 is  $2 \times 10^4$   $\text{n/cm}^2/\text{s}$ . The ESS 50Hz reference instrument is calculated to give a flux of  $33 \times 10^7$   $\text{n/cm}^2/\text{s}/\text{\AA}$  at  $\lambda = 6.7$   $\text{\AA}$ . Integrating over the resolution width ( $\Delta E = 0.017$  meV gives  $\Delta \lambda = 0.031$   $\text{\AA}$ ) gives a "monochromatic" flux of  $1.0 \times 10^7$   $\text{n/cm}^2/\text{s}$ , nearly three orders of magnitude higher than IN13.

***The graphite instrument has 500 times higher flux than IN13 and 150 times higher flux than IRIS.***

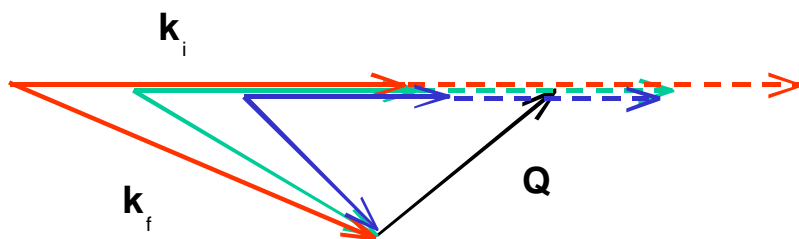
IRIS is very similar to the reference graphite instrument. It has an energy resolution of 17.5  $\mu\text{eV}$  using cooled PG 002 crystals and sits at a distance of 36.5m from the ISIS decoupled  $\text{H}_2$  moderator which has a similar time-structure to the ESS decoupled  $\text{H}_2$  moderator (for  $\lambda=6.7\text{\AA}$ , ISIS  $\Delta t=110\mu\text{s}$  and ESS  $\Delta t=96\mu\text{s}$ ). The measured white beam flux on IRIS is  $5.0 \times 10^7$   $\text{n/cm}^2/\text{s}$ . This translates into a flux of about  $1.3 \times 10^7$   $\text{n/cm}^2/\text{s}$  for the integrated wavelength range from 4.6  $\text{\AA}$  to 6.9  $\text{\AA}$ . Over the same wavelength range, the ESS instrument gives a flux of  $1.8 \times 10^9$   $\text{n/cm}^2/\text{s}$ , more than two orders of magnitude higher. This is to be expected as the instruments are basically identical except for the source which gives a factor of 30 increase in flux and the supermirror guide which can give another factor of 4 compared to the IRIS nickel guide.

## Constant-Q Instrument

Energy scans at constant wave vector  $\mathbf{Q}$  in a single crystal can be obtained in a single measurement using an indirect geometry spectrometer with a multi-analyser array, where

***A multi-analyser-arm instrument can perform a***

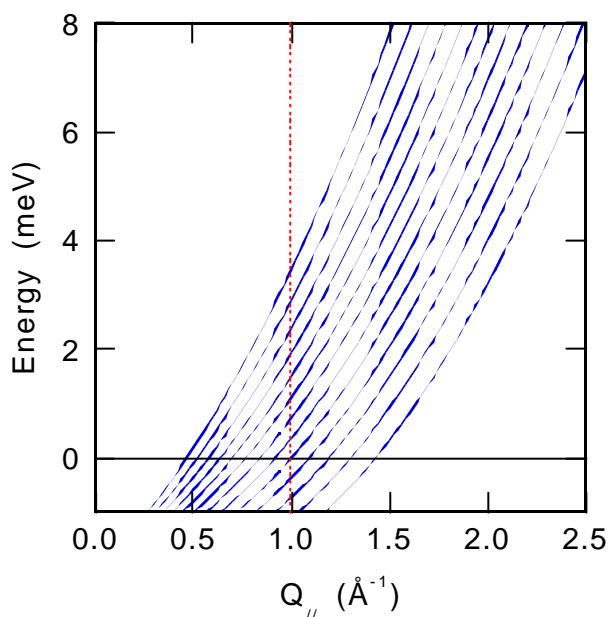
geometry spectrometer with a multianalyser array, where analyser arms at different scattering angles have different final energies. Each detector scans the energy along the direction of the incoming wave vector, i.e. along  $Q_{\parallel}$ . Each arm can be made to have the same  $Q_{\perp}$ , by adjusting  $k_f$  to the scattering angle  $\phi$  according to  $k_f = Q_{\perp}/\sin\phi$ , as illustrated:



**large fraction of triple-axis-type measurements.**

**The analysing energy of each arm is set so that a scan at constant  $Q$  can be constructed from a single measurement.**

By rebinning the detectors, a series of constant  $Q$  scans for different  $Q_{\parallel}$  and the same  $Q_{\perp}$  is then obtained:



A prototype spectrometer (PRISMA) has been in routine operation at ISIS for several years.

In order to be competitive with respect to triple-axis spectrometers and direct geometry chopper spectrometers, the energy resolution and dynamical range should match those types of spectrometers. The only suitable option seems to be to use the (002) reflection of pyrolytic graphite analysers, which gives an upper limit of the final energy of approximately 32 meV (due to space restrictions and deteriorating resolution), while the lowest useful final energy for measuring dispersive excitations in single crystals is approximately 2 meV. To avoid collisions between analyser arms, either a RITA-type arrangement of analysers and a position-sensitive detector or a vertical scattering geometry on the analyser side are envisaged.

In order to construct a reasonable constant- $Q$  scan without scanning the analyser angles, it is estimated that at least 20 analyser arms are needed with at most  $1^\circ$  separation.

This is a new type of instrument, which offers the exciting possibility of covering a large fraction of TAS-type measurements at a pulsed source. The resolution and flux are

**Graphite crystals are used for energy analysis and the most promising scattering geometry for the analysers may well be vertical.**

**At least 20 analyser arms are needed with at most  $1^\circ$  separation.**

**The resolution is less tuneable than on a triple-axis instrument.**

significantly less tuneable, as they are largely dictated by non-adjustable parameters, such as the position in  $(\mathbf{Q}, \omega)$ -space being measured and to a lesser extent, the moderator characteristics and instrument length.

The highest useful incident energy is limited to four times the final energy by second-order reflections of the analysers. This defines the dynamical range of the spectrometer. The energy resolution for *elastic* energy transfer can be approximated as

$$\Delta E / E = 2\sqrt{(\Delta t/t)^2 + (\cot \mathbf{q} \Delta \mathbf{q})^2} \quad (1)$$

where  $\Delta\theta$  will be of the order of one degree, as collimators should be avoided due to space restrictions. In order to be competitive with a TAS equipped with collimators, the  $\Delta t/t$  term is only allowed to increase the total  $\Delta E/E$  by 10-20%. This has the auxiliary advantage of giving a nearly Gaussian resolution function, important for line shape analysis. For elastic scattering, the restriction on  $\Delta t$  given by Eq. (1) is only important at low final energies, where the  $\Delta\theta$  term is small. However, as the energy transfer increases, the term  $\Delta t/t$  increases in importance. For a final energy of 2 meV, we find from Eq. (1) that the longest acceptable  $\Delta t$  (in microseconds) for elastic scattering is

$$\Delta t = 5.1 L_i \quad (2)$$

where  $L_i$  is the incident flight path (in meters). As usual, longer pulse widths can be accepted by increasing the length of the primary spectrometer.

Due to frame overlap, the length of the primary spectrometer is limited by the pulse repetition rate. For a final energy of 2 meV (the limiting case), allowing for a large dynamical range, the longest distances will be approximately 12, 25, 38, and 63 m, for pulse repetition rates of 50, 25, 16.7, and 10Hz, respectively.

We have calculated the time-averaged flux at the sample position for these four different distances using the moderators that can fulfil the resolution requirement Eq. (2). A straight  $m=3$  supermirror guide starting at 1.7m from the moderator surface is included. The last 4m consists of an  $m=4$  focusing supermirror guide. At the low-energy end, the best solution appears to be a 17Hz 38m source with a coupled liquid hydrogen moderator (6) while the high-energy end is better served by a 25Hz 25m source, with a coupled ambient water moderator. Since the energy resolution due to the crystal analyzers deteriorates rapidly with increasing final energy, it appears best to optimize the spectrometer for cold neutrons. Given the choice between 10Hz and 50Hz target stations, the preference for this instrument is for the 50Hz target station with a decoupled hydrogen moderator. The long-pulse option with a pulse-shaping chopper at 6.3m and an instrument length of 160m using a coupled liquid hydrogen moderator is also interesting concerning flux, but the band width is reduced to only 1.2 Å. The flux gain would then in many cases be outweighed by the increase in measuring time, as several measurements using different incident energy ranges are required. The full optimization for strongly inelastic scattering remains to be done.

***axis instrument.***

***Liquid H<sub>2</sub> is probably the best option.***

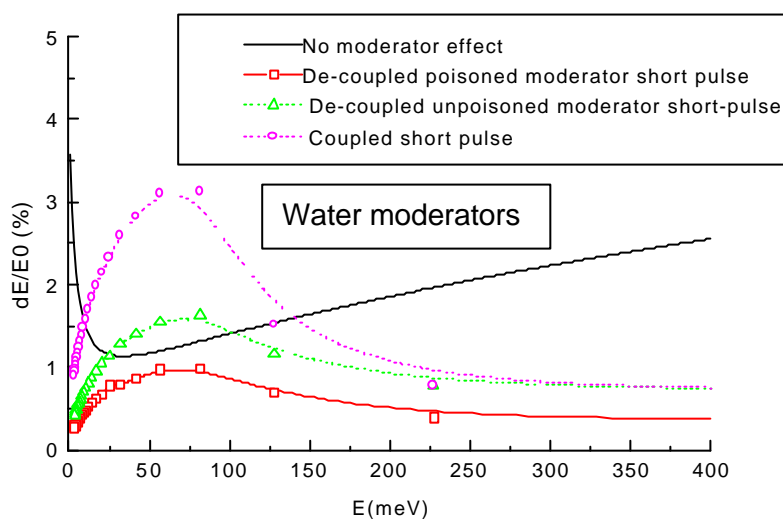
***The 50Hz target is preferred with the 10Hz target as the second option.***

***The long-pulse target is probably not useful.***

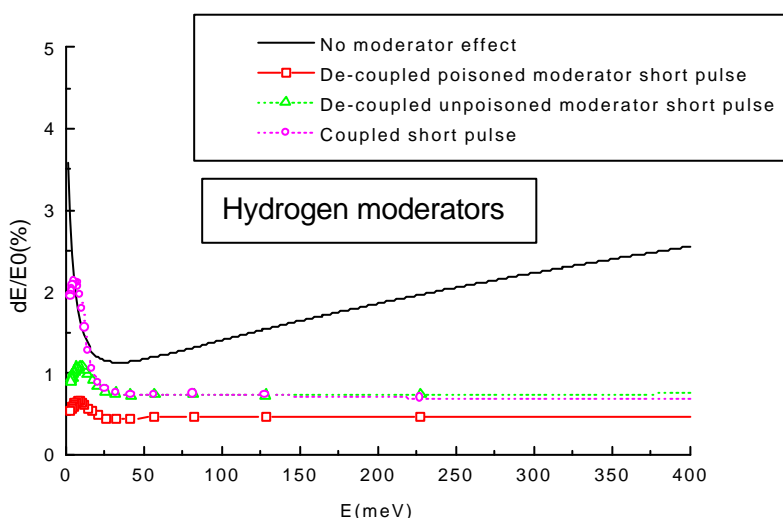
## Vibrational Spectroscopy Spectrometer

This is an instrument specialised for the measurement of the vibrational density of states, very similar to the TOSCA spectrometer at ISIS. It uses graphite 002 analysers with a fixed take-off angle, covering as large a fraction of the available solid angle as possible. Cooled Be filters are used to eliminate higher-order contamination. The instrument needs to cover a range of energy transfers from 0 to 1000 meV in a single measurement, which corresponds to a wavelength range of 0.2 to 5.0 Å. The two figures below show the instrumental energy resolution for the water and hydrogen moderators respectively.

**An instrument for measuring the vibrational density of states, similar to Raman and infrared light scattering.**



**Of the water moderators, only the poisoned moderator can match the secondary spectrometer resolution.**



**The decoupled hydrogen moderator can do even better.**

The solid line shows the secondary spectrometer resolution for a TOSCA-type instrument. From these figures, the best moderators are poisoned water and decoupled hydrogen, with the decoupled hydrogen moderator giving an increased flux at longer wavelengths. The long-pulse target cannot be used, as without pulse-shaping the resolution is too poor and with pulse-shaping the dynamic range is too restricted.

**The preferred moderators are the poisoned water and decoupled hydrogen.**

**The long-pulse target is ruled out.**

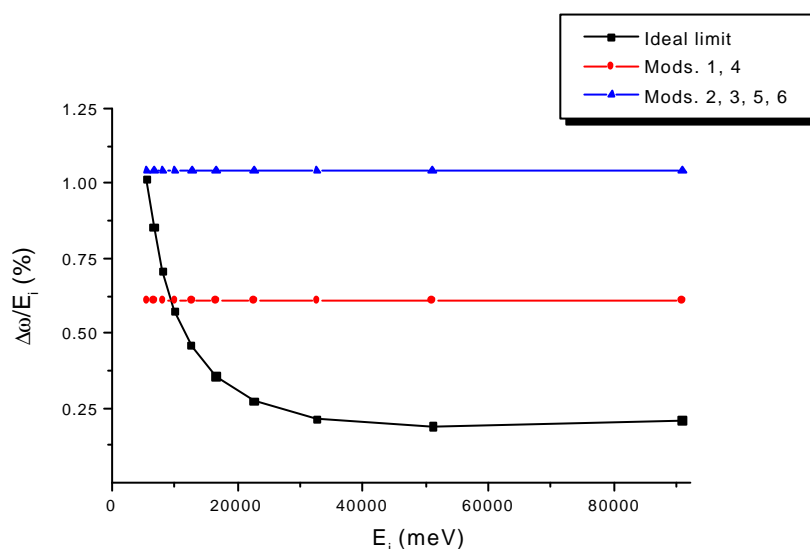
For this type of instrument, the 50Hz target offers the highest flux. The 10Hz target is also of interest for a longer, high-resolution version with the same dynamic range.

**The preferred target station is 50Hz with the 10Hz target as an interesting second option.**

## Resonance High-Energy Spectrometer

This instrument uses the resonant neutron absorption of  $^{238}\text{U}$  at 6.67 eV as energy analyser. It is similar to the eVS spectrometer at ISIS. Neutron Compton scattering is used to measure the momentum distribution, mainly of light atoms, e.g. H, D, He or C. The typical incoming energy range is 5 to 64 eV, corresponding to wavelengths between 0.04 and 0.11 Å, in the non-Maxwellian part of the neutron spectrum.

The energy resolution for the different moderators is shown below:



**Neutron Compton scattering: measuring atomic momentum distributions.**

**Very high energies: non-Maxwellian part of spectrum.**

**Far from Maxwellian => moderator temperature is unimportant**

**Coupling is unimportant**

**Only moderator size matters: poisoned moderator is best.**

The black line shows the secondary spectrometer resolution for a realistic instrument geometry. We can easily see that the choice of a suitable moderator is restricted to either number 1 or 4 only, if the machine has to be pushed close to its theoretical energy-resolution limit.

To match the secondary spectrometer resolution, the time-width of the neutron pulse needs to be significantly less than 1 μs, which is not achievable with present-day choppers. This rules out the use of the long-pulse target.

The ideal repetition rate is of the order of 1kHz, which makes our choice of the 50Hz target an easy one.

**The optimal moderator is poisoned water or hydrogen.**

**The 50Hz target station is preferred.**



# Neutron Spin-Echo Instruments

**M. Monkenbusch<sup>1</sup>, B. Farago<sup>2</sup> and C. Pappas<sup>3</sup>**

<sup>1</sup>IFF, Forschungszentrum Jülich, 52425 Jülich, Germany

<sup>2</sup>Institut Laue Langevin, BP 156, 38042 Grenoble Cedex 9, France

<sup>3</sup>Hahn-Meitner-Institut, Glienicker Str. 100, 14109 Berlin, Germany

Neutron Spin Echo (NSE) spectroscopy decouples energy resolution from beam characteristics like monochromatisation or collimation and combines the highest energy resolution from all inelastic neutron scattering techniques with the high intensity advantage of a beam which is only 10-20% monochromatic. As a consequence of that, when it comes to pulsed neutron sources, the most relevant parameter is the integrated neutron flux and pulse width characteristics have only minor importance on the NSE performance. The recent break-through experiment at IN15 demonstrated the feasibility of NSE at pulsed sources. NSE is a Fourier method and yields the intermediate scattering function  $S(Q,t)$  directly. High resolution means high values of  $t$ . This may be achieved by using long wavelength (as for any TOF instrument the resolution depends on  $\lambda^3$ ) and by employing large field integrals. Since at a reactor it uses 10-20% broad bands of neutrons from a velocity selector, however, the possible intensity gain due to the pulse structure is limited in an analogous way as that for a SANS machine. Therefore it needs the combination of cold neutrons with a broad wavelength band, which implies that the optimal choice would be a low repetition rate, full power target with a coupled cold moderator. This calls for the 16Hz long pulse option, which combines the highest integrated neutron flux with a low repetition rate. When it comes to choosing between the two short pulse options, it becomes clear that NSE can only benefit from the higher integrated neutron flux of the 50Hz source and the second choice would be the one with a cold coupled moderator at 50Hz. A dilute 10Hz target would then be the worst choice.

## Introduction

Neutron Spin Echo (NSE) reaches the highest energy resolution from all neutron spectroscopic techniques by decoupling the value of the minimal neutron velocity changes that may be detected from the width of the velocity distribution of the incoming neutrons [1]. This is achieved by using the neutron spin as a kind of stop-watch carried by each neutron individually. Inelastic scattering leads to a difference in spin precession of neutrons flying through a precession path before the sample and a symmetric path after the sample, and this affects the final beam polarisation, which is converted to an intensity signal by an analyser in front of the detector. In the original generic IN11 spectrometer type the precession paths are magnetic field regions generated by a pair of solenoids (Fig.1).

**Neutron spin precession in magnetic fields measures velocity changes individually.**

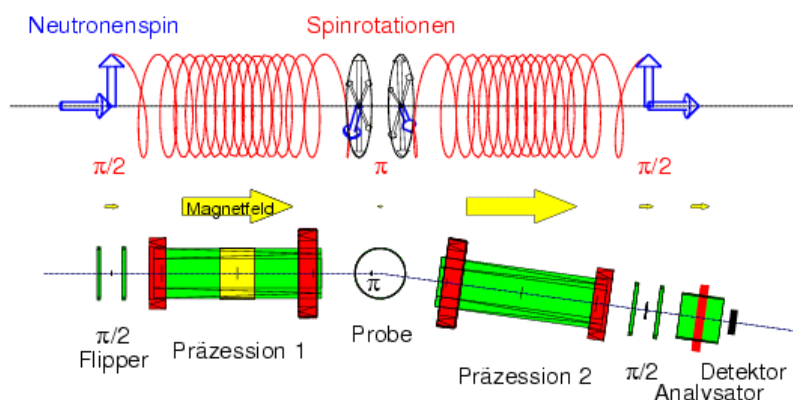


Fig. 1: NSE principle.

NSE spectroscopy yields directly the Fourier-transform  $S(Q,t)$  of the scattering function rather than  $S(Q,\omega)$ .

For quasi-elastic scattering ( $\omega=0$ ) the detected intensity is given by the relation:

$$I(Q) = \eta \left( S(Q) + \delta \int \cos(\mathbf{w} \cdot \mathbf{g} \cdot J) S(Q, \mathbf{w}) d\mathbf{w} \right) \quad (1)$$

where  $\eta$  and  $\delta$  are instrument constants for sensitivity and polarisation efficiency respectively and  $J = \int |B| dl$  is the magnetic field integral in

each precession region. The Fourier time is given by:  $t = \gamma \lambda^3 J$  with  $\gamma = 1.86 \times 10^{20} \text{ s}/(\text{Tm}^4)$ , i.e.  $t = 186 \text{ ns}$  for  $J=1 \text{ Tm}$  and  $\lambda=1 \text{ nm}$ . As a Fourier method –with respect to the energy spectrum–, NSE suffers from the known properties of all Fourier methods and small spectral contributions are buried under the noise caused by the total scattering intensity  $S(Q)$ . However, the method is ideally suited for the investigation of quasi-elastic scattering and relaxation type motions, which dominate  $S(Q)$  and are best analysed in the time domain, where a detailed line shape analysis is of crucial importance and resolution “deconvolution” consists of a simple division.

The relevant parameter for the NSE resolution is the maximum value of the Fourier time,  $t = t_{\max}$ , at which a useful measurement can be performed. As pointed out above, this “resolution” parameter depends only on  $\lambda^3$  and on the magnetic field integral. The Fourier time does NOT depend on the bandwidth of the incoming neutrons and for this reason all existing NSE spectrometers use a 10-20% FWHM monochromatic beam for an improved data acquisition rate. All these spectrometers operate at steady sources. From the above it becomes clear that when it comes to the operation at a spallation source, the Fourier time will NOT depend on the pulse width, which determines the width of the wavelength band “seen” at some instant by a detector

**NSE is a Fourier method**

**Fourier Time =  $t$   
 $\mu \text{I}^3 \times B \times \text{pathlength}$**

**Resolution does not depend on pulse width!**

the width of the wavelength band “seen” at some instant by a detector element.

A reasonably accurate determination of the polarisation change due to inelastic scattering requires a large number of counts (>several  $10^4$ ) and for this reason the method calls for the highest incoming flux and the most efficient solid angle detection.

**Intensity is crucial!**

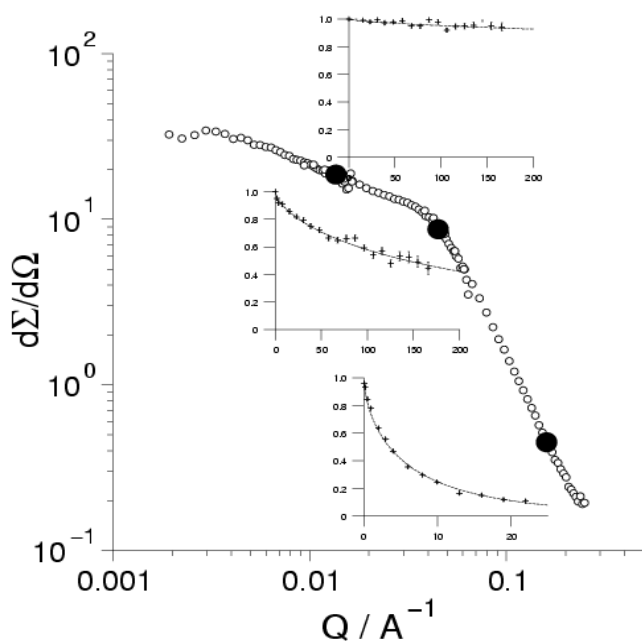
**(Q, w /t) – Range**

As far the dynamics in the small angle scattering (SANS) region is concerned (soft-condensed matter systems, ferromagnetic critical dynamics etc) NSE offers a  $\omega$ -resolution, which is reasonably well adapted to the dynamics investigated. Other problems like glass dynamics and magnetic fluctuations are also in the scope of NSE spectroscopy. As pointed out above, the NSE resolution is rather to be expressed in terms of the maximum achievable Fourier-time,  $t_{max}$ . In order to allow for unified comparisons this Fourier time can be converted to an energy transfer:  $\Delta\omega = 1/t_{max}$ . In the low Q (SANS) regime the current state-of-the-art is still limited by the longest Fourier-time rather than by the proper Q-resolution of the instruments, since typically the relaxation rates behave proportional to  $Q^{2..4}$ .

**Resolution is  $t_{max}$**

**For comparison:**

$$Dw = 1/t_{max}$$



**Longer Fourier times  $t_{max}$  needed for low Q !**

**Fig. 2** NSE relaxation curves corresponding to different locations on the SANS intensity of a bicontinuous microemulsion. Note the considerable slowing down at low Q reaching the state-of-the art limit (IN15) already at  $Q=0.15 \text{ nm}^{-1}$  as displayed by the inserts showing  $S(Q,t)/S(Q)$  versus  $t$  in ns obtained at IN15,IN15,FZJ-NSE.

An unambiguous determination of small decays in relaxation curves at  $t_{max}$ , like the one seen in the upper part of Fig.2, requires a low statistical error (i.e. high intensity) and a high stability of the spectrometer, particularly when it comes to decay rates  $\Gamma(Q)$  which are much smaller than  $1/t_{max}$  ( $\Gamma(Q) < 1/t_{max}$ ). The  $\lambda^3$ -dependence of Fourier times  $t$  together with  $Q \sim 1/\lambda$  helps to cope with this general physical trend.

**....and intensity !**

In the NSE-SANS regime the Q-resolution is usually of minor importance. The situation is somewhat different in the large Q-regime, when it comes to investigating the dynamics at or around structure peaks, e.g. in a glass-forming polymer. Here Q-resolutions better than

the 10-20%, imposed by the typical wavelength distribution of reactor based instruments, are often needed. In exceptional cases as oriented lamellar phases (microemulsions, block-copolymers) or macrocrystals of colloids a Q-resolution better than 10% would also be beneficial in the SANS regime.

As it will be pointed out below, a welcome feature of the pulsed structure of spallation sources is the improved monochromatisation of the beam detected at any instant by the detectors, which would lead to an improved Q-resolution with respect to the one of reactor based NSE instruments.

The design goals for novel NSE spectrometers at the ESS would be to overpass the existing instruments both in resolution, Q-range and luminosity. The maximum Fourier time in the SANS region should reach the  $10^{-6}$  s domain, which up to now was only covered by dynamic light scattering techniques.

**ESS+development→**

$t_{max} = 1000 \text{ ns}$

**1:1000000**

**$0.07 \text{ nm}^{-1} < Q < 40 \text{ nm}^{-1}$**

### Best-in-class Instruments

Currently 6 high resolution instruments of the generic IN11 type exist in the world (IN11<sub>ILL</sub> [1], IN15<sub>ILL</sub> [2], FZJ-NSE<sub>FZ-Jülich</sub> [3] = NIST-NSE<sub>NIST,USA</sub>, C2-2-NSE<sub>Tokai,Japan</sub>, MESS<sub>LLB</sub>). A large detection solid angle of 30° has been realised in the IN11 add-on IN11-C [4] with a severe drawback in resolution. A novel instrument class, realised by the SPAN spectrometer at HMI-Berlin, allows for simultaneous measurements in a very wide solid angle reaching 0.27 strad with a resolution, which should be made comparable to that of high resolution instruments like IN11 [5]. The zero-field NSE technique has been realised at the LLB in Saclay (G1bis) [6] and an improved version (RESEDA) of this instrument will be operated at the new Munich reactor FRM-II.

**IN11**

**IN15**

**FZJ-NSE**

**NIST-NSE**

**C2-2-Tokai**

**MESS**

**IN11C**

**SPAN**

**G1bis**

**RESEDA**

“Normal” and resonance NSE add-ons to triple axis (TAS) spectrometers have been installed or are being developed [7, 8]. These spectrometers use the TAS method to filter out all contributions to S(Q) except the inelastic one that should be investigated and allow for measuring intrinsic linewidths of elementary excitations like phonons with an energy resolution in the range of 1 μeV. The NSE technique is also used/proposed to detect other than velocity changes coded into the precession angle like direction changes for Ultralow-(S)ANS [9]. Furthermore, a modified NSE method can be used in high resolution diffraction [9]. These more general applications of Larmor precession to neutron instrumentation should better be discussed in the context of the hosting instruments, i.e. TAS, SANS and single crystal diffractometers than in the frame of NSE spectrometers.

**Triple-axis add-ons**

**Diffraction add-ons**

**→ hosting instruments**

IN11, the first NSE spectrometer ever built [1] has a high neutron flux on the sample. The incoming wavelength of IN11 can be varied from 0.4 up to 1.2 nm leading to large dynamic (1:20000) and Q-ranges (from 0.1 up to 27 nm<sup>-1</sup>). The total signal of three single detectors is used for the detection of neutrons.

**IN11: 1:20000 dyn.**

**Range**

**Q ≤ 27nm<sup>-1</sup>**

A substantial improvement in NSE spectroscopy was marked by the IN15 spectrometer [2]. The long incident wavelengths (0.8 λ 2.4 nm) of this spectrometer allow for reaching long Fourier times up to 350 ns. The dynamic range of IN15 is ~1:13500 and the Q-range spans from 0.01 up to 1.5 nm<sup>-1</sup>. Detection is done by an area detector, which covers a solid angle of ~ 5 · 10<sup>-3</sup> strad. IN15 was also conceived with a TOF option and is the test rig for NSE at spallation sources.

**IN15: t<sub>max</sub> = 350ns**

The FZJ-NSE [3] is the latest development of the IN11-type instruments. It uses novel magnetic field compensation techniques and computed setup for increased stability. The spectrometer can be

**FZJ-NSE:**

**compensation,**

**no “tuning”**

and computed setup for increased stability. The spectrometer can be easily operated at large scattering angles and it is equipped with a multidetector similar to that of IN15. The maximum magnetic field integral is about twice that of IN15. The maximum Fourier time, however, is limited by the corrections needed to cover the total solid angle of the detector and by the restrictions of beam delivery from a multilayer bandpass mirror ( $\lambda \sim 0.8$  nm).

Combination of new techniques for magnetic field corrections with the use of a broad wavelength band including long wavelengths, improvement of the corrections for large solid angle operation and use of superconducting main solenoids for very large magnetic field integrals and long Fourier times will lead to the next generation instrument of IN11 type. Such a spectrometer will combine the virtues of the above state-of-the-art instruments and further extend them.

Another development option, besides extending the maximum Fourier time, consists into increasing the detector solid angle over which NSE measurements can be performed simultaneously and thus increase the NSE counting rate. The NSE homogeneity requirements for IN11 generic instruments, where magnetic fields are created by long solenoids give however an upper limit for the detector solid angle. The novel magnetic field configuration of the spectrometer SPAN at BENSNC allows for significantly increasing the detector solid angle. The novelty consists in the precession field, which has a real cylindrical symmetry and all scattering angles, typically from  $-150^\circ$  to  $150^\circ$ , are accessible at the same time. The coils and power supplies of SPAN lead to a reduced energy resolution, amounting  $\sim 1/3$  that of IN11. The high symmetry and homogeneity of the magnetic field configuration however allows for much higher resolution and the real limit of the set-up should be beyond 2-3 times the actual one [5]. SPAN is characterised by a very broad wavelength band from 0.25 up to 1.0 nm leading to large dynamic (1:30000) and Q-ranges (from 0.2 up to  $48 \text{ nm}^{-1}$ ). Neutrons are detected by three groups of detectors and at the present stage the overall opening of detectors equipped with analysers reaches  $30^\circ$  and a solid angle of 0.02 strad.

The resonance NSE technique (NRSE) has virtually equal requirements for the delivered beam (i.e. target and moderator characteristics) as NSE. Therefore it should not be considered separately. However, the highest Fourier times –at viable intensity– and the highest detector solid angles are reached by NSE spectrometers. We will therefore compare state-of-the-art and best-in-class properties of current and future instruments only in terms of NSE spectrometers.

The first successful tests at IN15 [10] showed that it is technically possible to combine NSE and TOF and that this combination brings considerable advantages: a high flexibility in choosing the Q resolution and a wider simultaneously covered NSE dynamic range. After this significant breakthrough, NSE can be implemented at pulsed neutron sources at its present state of the art. Intensity gains or losses with respect to existing spectrometers are then determined by the luminosity of the source and the wavelength band covered by a measurement. Furthermore, in the frame of ESS, novel instrumentation concepts should be developed, that would open possibilities beyond the current limits of NSE spectroscopy. A development of the SPAN-generic design to combine energy resolution comparable to that of IN11 with a maximum solid angle is part of the long time scale ILL Millennium program. Similar development should also take place in the frame of ESS. Extending the Fourier times and resolution beyond the actual limits, set by IN15,

**Needs:**

- **Long wavelengths**
- **Broad band / frame**
- **Field integrals > 1Tr**
- **Large solid angles**

→ **generic IN11 type**

→ **SPAN type**

→ **NRSE**

→ **NSE at pulsed sources**

should open new possibilities in the (Q,t)-window. This development is of crucial importance for soft-condensed matter and biological systems and the first NSE instrument at ESS should be a highest-as-possible resolution machine.

### Target Station and Moderator

For the choice of target station (i.e. repetition frequency, pulse width and average power) and moderator (i.e. spectral distribution and pulse width) the following criteria apply for NSE spectrometers:

- High intensity, is important for all measurements but it is crucial at long wavelengths
- The width of the pulse should lead to less than 10% relative wavelength uncertainty at the detector for an improved Q-resolution, with respect to reactor based instruments
- The bandwidth of useable neutrons within one frame should be as large as possible.

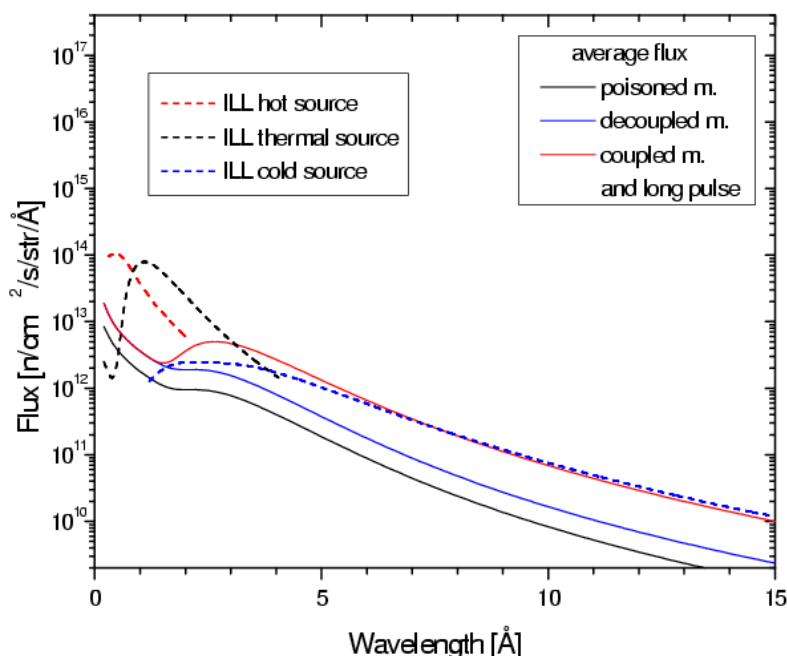
→ **coupled cold moderator**

→ **long pulse (2ms) OK!**

→ **repetition rate < 20Hz**

→ **5MW average power !**

The first criterion calls for a cold coupled moderator. Fig.3 (taken from the ESS-moderator picture gallery) shows that the average flux from a cold moderator at a 5MW target is virtually equivalent to that of the ILL cold source, independently of repetition frequency and pulse length.



**Average cold flux:  
<ESS> = <ILL>**

**Fig. 3:** spectral flux expected for different ESS-moderators in comparison with that of the ILL.

Any further gains (beyond ILL) should come from the effective simultaneous use of a larger wavelength band than that of a steady source instrument. The absolute width  $\Delta\lambda = \lambda_{\max} - \lambda_{\min}$  of the wavelength band arriving at a detector positioned at a distance L from the moderator depends only on L and on the repetition frequency of the source  $\nu$ :

**Bandwidth/frame → gain**

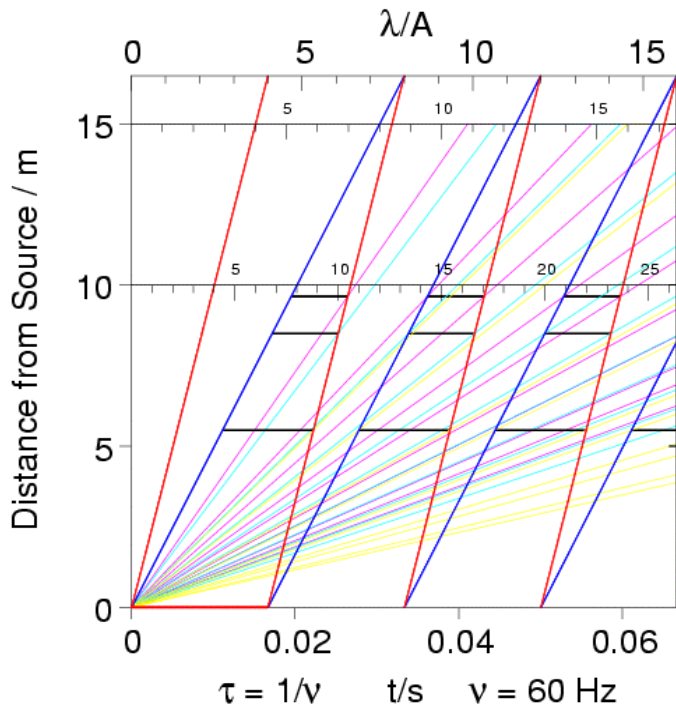
**Bandwidth/frame ~ 1/L**

$$\Delta \mathbf{l} = (h / m_n) / (\nu L) = (3.96 \times 10^{-7} \text{ m}^2 / \text{s}) / (\nu L) \quad (2)$$

Analogously, wavelength uncertainty  $\delta\lambda$  depends only on the pulse width of the source  $\Delta\tau$  and on the distance L:

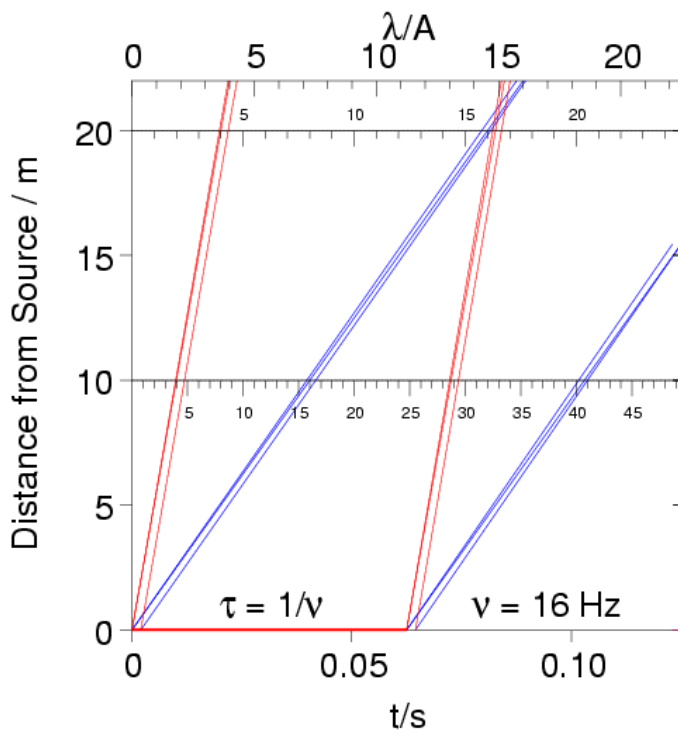
$$\delta \mathbf{l} = (h / m_n) \Delta \mathbf{t} / L = (3.96 \times 10^{-7} \text{ m}^2 / \text{s}) \Delta \mathbf{t} / L \quad (3)$$

The resulting wavelength widths for different situations may be read off from Figures 4 and 5.



**50(60)Hz**  
**→ 3+choppers needed**

**Fig. 4:** Path-time diagram for a fast repetition frequency target, min. 3 choppers are needed to prevent wavelength mixing from different pulses. The bandwidth at L=17m is about  $\Delta\lambda=0.4$  nm.



**16Hz**  
**→ 1 chopper (at 6m)**

**Fig. 5:** Path-time diagram illustrating the situation expected at the long pulse target. The wavelength uncertainty due to the pulse width is about 0.04 nm and the free bandwidth exceeds 1nm at L=20m allowing for constructions with even larger moderator-detector distances. One frame overlap chopper at about 5m is sufficient.

An unbiased gain factor may be obtained by comparing the time needed to perform a pulsed source experiment with a wavelength band from  $\lambda_{\min}$  to  $\lambda_{\max}$  with that for a corresponding sequence of experiments using different wavelength bands each with the same relative width  $w$ , given by the velocity selector, at a reactor as illustrated by Fig. 6.

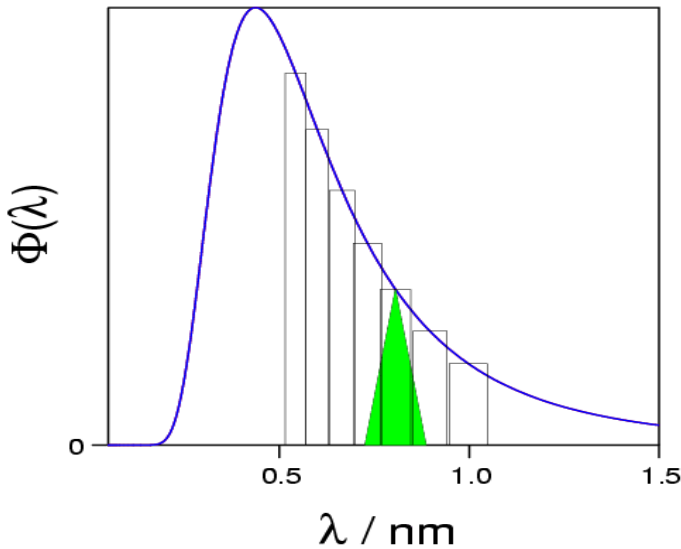


**Fig. 6:** Matching selector bandwidth experiments (green triangle) to a time-of-flight sequence encountered in a spallation experiment.

The resulting gain factor is:

$$g_0 = (\Phi_{ESS} / \Phi_{ILL}) \ln(I_{max} / I_{min}) / w \quad (4)$$

The flux ratio is assumed to be 1 for the 50Hz target and the long pulse target (see Fig. 1), whereas the 10Hz target with its “diluted” pulse sequence is assigned a flux ratio of 0.2. Furthermore we assume the reference velocity selector width to be 10%, i.e.  $w=0.1$ . It should be noted that for a wide wavelength span the distribution of intensity does not perfectly comply with the experimental needs because the counting time is necessarily equal for all sub-bands. Fortunately many SANS samples exhibit increasing intensity with lowering Q (i.e. at longer wavelengths for the same scattering angle) which may partly compensate the spectral intensity drop at long wavelengths. In addition the  $\lambda^3$  proportionality of the Fourier time fits to the dynamical slowing down with some power of Q. Nevertheless, a gain factor  $g_0$  derived from large wavelength ratios (>2-3) will probably be an overestimation.

For the same distance from the source, a 50Hz target will reduce the waveband width  $\Delta\lambda$  by a factor of 3 with respect to the 16Hz option, which is the choice par excellence for NSE. This will lead to a consequent reduction of the gain factor. In order to partly counterbalance this drawback the 50Hz target will force to a very compressed design heading at a source-detector distance of  $L < 18m$ , which is about the minimum conceivable. This will yield to a free wavelength-band of 0.44 nm with a plain gain factor of 7.4 if the range between  $0.4 \text{ nm} < \lambda < 0.84 \text{ nm}$  is considered, and this factor reduces to 2.7 in the more interesting range (as far as large Fourier times are concerned) between  $1.4 \text{ nm} < \lambda < 1.84 \text{ nm}$ .

On the other hand the 16Hz long pulse source would allow for building longer instruments, which would also improve the background. The band width at 20m from the source would be  $\Delta\lambda = 1.2 \text{ nm}$  and the gain factor would reach almost 14 in the range  $0.4 \text{ nm} < \lambda < 1.6 \text{ nm}$  and would reduce to 6.9 in the range  $1.2 \text{ nm} < \lambda < 2.4 \text{ nm}$ . For the same distance between the source and the detector, the 16Hz long pulse option delivers a gain factor typically twice as high as that of the 50Hz.

**Gain factor  $g_0$**   
 $\sim \ln(I_{min}/I_{max})/w$

**$w$  = selector width at reactor**

**50Hz: gain = 2.7-7.4**

**10Hz: gain = 14 x 0.2 = 2.8**

**16Hz Long-Pulse: gain = 14 !**

**$\ln(4)/0.1 = 13.9$**

**$g_0 > 10$  may be questionable**

**50Hz  $\rightarrow L < 18m$  needed**

## Technical Issues

NSE instruments at pulsed spallation sources will look very similar to those at continuous sources. There will be some extra pressure – depending on the repetition rate- to reduce the length if possible. Data collection has to cope with the assignment of incoming neutrons to varying Fourier times  $t$  and  $Q$  values according to the  $\lambda$  determined from the time-of-flight. Only the flippers and the phase coil (and possibly some current sheets, which would correct for gravitational effects on the paths) should be wavelength dependent in a way that requires broadband operation. The recent results obtained at IN15 showed that current ramping synchronised to the pulse frequency as indicated in Fig. 7 is sufficient for combining NSE and TOF [10] and well defined echo-signals were observed over the totality of a large wavelength frame from  $\lambda=0.6$  nm up to 1.8 nm.

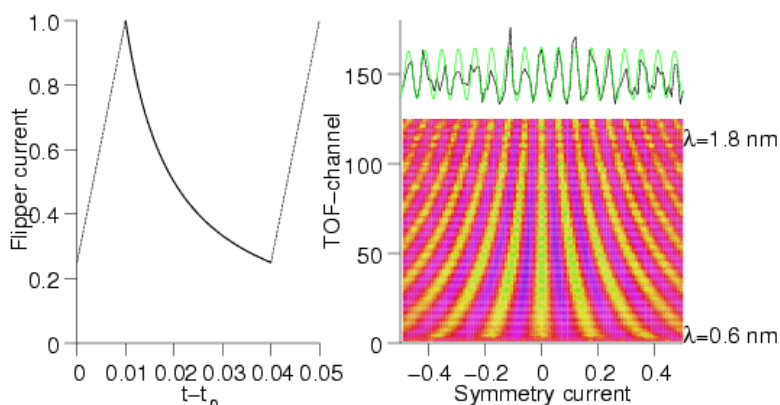


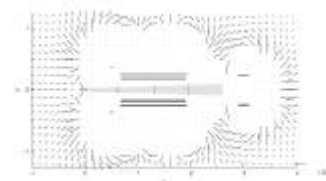
**Fig. 7:** Dynamical flipper ramping allows for broadband operation.

***Dynamical flipper operation by ramped currents is tested***

The narrow space for the instruments imposed by the requirement to keep  $L$  short and the necessity of massive shielding is not compatible with extended stray fields. Magnetisation of iron shields must be avoided, which calls for well compensated “stray-field-free” designs for the instruments positioned close to the source, which should be of IN11 type. A high resolution SANS - NSE spectrometer, which would benefit the most from broad band operation should be placed typically at a (detector)-distance of 18-20m from the source. Such a spectrometer should be relatively compact and should mainly operate in the SANS range. For that reason it should easily placed in the “crowded” region next to the shielding of the source.

For NSE measurements at high  $Q$  a SPAN-type spectrometer with improved energy resolution would be needed. Such a spectrometer should be placed at a larger distance from the source, typically at 40m. This large distance is dictated by the space requirements (diameter of 8-9m) of the spectrometer and should also allow for reducing magnetic cross talk with other instruments. From the equations above it is clear that at 40m from the source the wavelength band will be restricted by a factor of two with respect to that delivered at 20m, which will consequently reduce the gain factors. With the 16Hz long pulse source the gain factor amounts to 9.2 for  $0.4 \text{ nm} < \lambda < 1.0 \text{ nm}$  and 4.7 for  $1.0 \text{ nm} < \lambda < 1.6 \text{ nm}$ , i.e. a factor 1.5 less than the gains obtained at 20 m from the source. When it comes to the 50 Hz target the wavelength band spans only  $2 \text{ \AA}$  and the gain factors amount to 4 for  $0.4 \text{ nm} < \lambda < 6 \text{ nm}$  and 2.2 for  $0.8 \text{ nm} < \lambda < 1.0 \text{ nm}$ , i.e. roughly a factor 23 less than at 18m from the source. However, the large solid angle (up to 0.27 strad) over which simultaneous NSE measurements will be possible will largely

***No stray field design will be required***



***SPAN design  
L = 40m***

***16Hz Long-Pulse:  
gain = 9.2***

***50Hz  
gain = 4!***

which simultaneous NSE measurements will be possible will largely compensate the drawback in gain factors. The long distance would also lead to an improved monochromatisation and Q-resolution, which would be a welcome feature of this configuration. Indeed no wide angle NSE spectrometer with good Q-resolution exists at the moment although some NSE experiments at high scattering angles require good Q-resolution.

Finally, compared to the existing instruments additional gains should be expected due to the application of advanced neutron optics like improved neutron guides and optimised analyser/polariser -techniques. Especially the necessarily shorter distances of guide and free flight sections will yield to intensity gains compared to existing installations. Despite the fact that these are “soft” gains they will still contribute to the real achieved gains.

***Additional “soft” gains may contribute a factor of 10***

## References

- [1] F. Mezei (Ed.), “Neutron Spin Echo Proceedings”, Lecture Notes in Physics 128 , Springer, Berlin (1979)
- [2] P. Schleger, G. Ehlers, A. Kollmar, B. Alefeld, J. F. Barthelemy, H. Casalta, B. Farago, P. Giraud, C. Hayes, C. Lartigue, F. Mezei and D. Richter, Physica B, 266 (1999) 49-55
- [3] M. Monkenbusch, R. Schätzler and D. Richter, Nucl. Instr. and Methods A399, 301 (1997)
- [4] B. Farago, Physica B, 241-243 (1998) 113
- [5] C. Pappas, F. Mezei and G. Ehlers, B. Farago, C. Pappas and F. Mezei, ILL Millenium Workshop, 6-7 April 2001, Grenoble France
- [6] M. Köppe , M. Bleuel , R. Gähler, R. Golub , P. Hank , T. Keller , S. Longeville, U. Rauch , J. Wuttke Physica B 266 (1999) 75
- [7] TASSE (NSE-TAS combination) C.M.E. Zeyen, J. Phys. Chem. Solids 60 (1999) 1573
- [8] T. Keller, R. Golub, F. Mezei, and R. Gähler, Physica B 241-243 (1998) 101
- [9] M.Th.Rekveltdt, T.Keller, W.H.Kraan, Physica B 297 (2001)18
- [10] B. Farago et al., ILL Annual Report 1999.

# Single Crystal Diffraction and Protein Crystallography Instruments

**C.C. Wilson<sup>1</sup>, W. Jauch<sup>2</sup>, G.J. McIntyre<sup>3</sup>, D.A.A.Myles<sup>4</sup>, J. Peters<sup>2</sup>**

<sup>1</sup>ISIS Facility, Rutherford Appleton Laboratory, Chilton, Didcot, Oxfordshire OX11 0QX, United Kingdom

<sup>2</sup>Hahn Meitner Institut, Glienicker Str 100, 14109 Berlin, Germany

<sup>3</sup>Institut Laue Langevin, BP 156, 38042 Grenoble Cedex 9, France

<sup>4</sup>EMBL, BP 181, 38042 Grenoble Cedex 9, France

Qualitative and quantitative assessments have been made of the performance of generic single crystal instruments for the source options available at the ESS, via detailed flux/reflection intensity/resolution calculations. The nature of single crystal diffraction measurements, particularly those involving hydrogen atoms, make it difficult to produce a single figure-of-merit relating performance between different sources, particularly as optimisation of instrumentation at existing sources is proceeding rapidly. Nonetheless, the huge increase in flux of pulsed neutrons at the ESS will lead to qualitative new opportunities in instrument performance, with a factor 40 increased brightness in the sharp pulse, and time-averaged flux equal to that of the most intense reactor sources.

We have assessed the requirements for single crystal neutron diffraction in a range of areas covering chemistry, physics, materials science and biology, and related these requirements to the likely available facilities on ESS.

This has been carried out within the framework of the following generic instrument types:

- Chemical Crystallography
- High Resolution Macromolecular Crystallography/Protein Crystallography
- High Resolution (short d & low  $\Delta Q/Q$ ) and Diffuse Scattering
- Low Resolution Biological Crystallography
- "Single Reflection" Measurements

Clearly instrumentation for single crystal diffraction normally requires good resolution (in all three dimensions of reciprocal space, normally covered in two spatial and one time-of-flight dimensions in detector space) which means that in every case we favour the short pulse option. Clearly most of our generic instruments will be optimally located on the 50Hz target, with one optimally placed on the 10Hz target. The 16.6Hz long pulse target is only a marginal option for our instrument types.

We have not attempted to design instruments as such, but rather define the framework into which single crystal instruments would fit with respect to the ESS source parameters. Nonetheless we can reinforce several messages regarding instrument design. The resolution of a diffractometer on a short pulse time-of-flight source is dependent on the flight path (instrument length) and on the detector characteristics. Gaining resolution by extending the length of instruments has implications for frame overlap and can favour the adoption of a low repetition rate target (the 10Hz target) to maintain bandwidth, an important feature in time-of-flight single-crystal diffraction. The alternative involves discrete or continuous rephasing of the frame, which may be unfavourable in many situations. This is true, for example, in rapid time-resolved studies where the whole snapshot of reciprocal

space is ideally obtained in a single shot as the diffraction pattern may be evolving rapidly, and also in measurements of the whole diffraction pattern, where quantitative interpretation of the pattern can be helped by having it measured continuously. Our assumptions on single crystal instrumentation are also based on the availability of efficient, large-area, position-sensitive detectors, and we assume that large area coverage ( $\geq 2\pi$ ) can be obtained if necessary. We assume a reasonable degree of detector development to allow individual modules of say 200mm x200mm, 60% efficiency at 1Å, and 1-1.5mm pixel resolution to be available, and that these can be combined to form a quasi-continuous detector array. We also assume the full range of standard neutron sample environment can be made available in the presence of these detector arrays and that polarisation analysis of white beams will be addressed.

We have based our considerations on the target-moderator options available at present. However, it is clear that for several of the instruments, and certainly for the macromolecular crystallography applications, provision of an intermediate temperature, 130K, moderator would lead to further significant gains (3-5 in flux) and we urge re-examination of this possibility. We also note that in the case of at least the biological instruments, additional optimisation of medium-long wavelength flux on a low power target, due to enhanced target-moderator configurations in such a low power scenario, may cause the 10Hz option to become more favourable.

## Introduction

Our choice of a generic suite of single crystal instruments is based on original discussions of instrumentation at ESS [1]. Our assessments of the performance of these instruments have been based on detailed flux/reflection intensity/resolution calculations which have been carried out in the past, notably involving one of our group (Jauch). These comprehensive assessments have included:

- the original SNQ report in 1984 [2], from which we note the Jauch and Dachs paper on single crystal diffraction [3] and also a paper from Mogens Lehmann (ILL) on low resolution crystallography [4];
- the 1996 Jauch paper on single crystal diffraction at long pulse spallation sources [5];
- the original ESS large unit cell study - Working Group convened by Mogens Lehmann, and including Jauch & Wilson along with Clive Wilkinson (EMBL) and Lennart Sjölin (Stockholm). The report of this group was issued as ILL Report ILL97/JA19T [6].

We start from the pulse length requirements dictated by the problem dependent parameters  $d_{\min}$  ( $\equiv Q_{\max}$ ) and  $a$  (the cell edge).

	$D_{\min}(\text{Å})$	$a(\text{Å})$	$d_{\min}^2/a(\text{Å})$
Chemical cryst.	0.4	30	0.0053
Physical cryst.	0.2	15	0.0026
High resolution bio.	1.2	100	0.0144
	1.5	200	0.0113
	2.4	200	0.0288
Low resolution bio.	6	300	0.12

Leading to the following basic requirements

	$L(\text{m})$	$dt(\text{ms})$	Moderator
Chemical cryst.	15	30	thermal poisoned
Physical cryst.	15	10	thermal poisoned
High resolution bio.	40	110	cold coupled
Low resolution bio.		very large	cold coupled

In terms of flux we note the need to optimise the "effective flux" on the sample  $\phi(\lambda)\lambda^2$  (proportional to the measured intensity), in the wavelength range of interest.

## Chemical Crystallography

Standard chemical crystallography is a "high resolution" technique, typically requiring the measurement of  $d$ -spacings to as low as 0.35-0.4Å. This also requires good  $Q$ -space resolution to allow for peaks to be separated and therefore integrated accurately. A short pulse is therefore best, around 30  $\mu\text{s}$  pulse length.

**Assessments based on analyses of predicted reflection intensities in single-crystal instruments.**

**For single-crystal diffraction, the parameter  $d_{\min}^2/a$  defines the pulse length requirements and hence constrains the source-moderator choice.**

**ESS can revolutionise neutron chemical crystallography, offering more parametric measurements and the study of very small crystals.**

To maximise the flux in the region of interest a thermal poisoned moderator would be chosen (with the option of intermediate 130K poisoned moderator), with high flux at 1 Å or lower but also retaining significant flux in the region up to and beyond 2-3 Å. Sharp pulses are required for good Q-space resolution to high Q, so a decoupled moderator.

This instrument type can have a medium path length (15m) on a 50Hz source, where the band-width will be adequate.

We note also here that such an instrument could also serve for the measurement of magnetisation densities from flipping ratios if an efficient white-beam spin polariser is available.

*Such an instrument type on ESS will be world-leading, and will offer the opportunity for qualitatively new science to be opened up, for example, in parametric measurements and in the use of very small crystals.*

### High Resolution Macromolecular Crystallography (Protein Crystallography)

***ESS can make high resolution neutron protein crystallography more routine, increasing the impact of neutrons in this important and expanding area.***

The definition of high resolution here implies measurements to a d-spacing of typically 1.5-1.8 Å, on unit cell edges of up to 150-200 Å. However, it is now well established that some hydrogen/deuterium positions in proteins can also be established reliably at lower resolution if necessary, say  $d_{\min}$  of 2.4 Å, which greatly facilitates the experiment. Once again there is the need to resolve peaks well to allow for adequate integration implying a short pulse source.

A cold, coupled moderator (see below for a discussion of the background implications) is the most obvious choice for this instrument, with a length of 40m chosen to regain some of the resolution lost by coupling. The question can be asked as to why a cold and not a thermal moderator in the high resolution macromolecular field? The optimum wavelength range is 1.8-3 Å and the effective flux conditions are not dissimilar for both temperatures:

$\lambda$	$f(\lambda)\lambda^2$ (cold)	$f(\lambda)\lambda^2$ (thermal)
1.8Å	9	$27 \times 10^{12} \text{Å}^3/\text{s}/\text{cm}^2/\text{sr}$
3Å	42	10

In the desired wavelength range the cold moderator, however, has a much better line shape. At 2 Å,  $dt$  is 40 μs for the cold moderator but 85 μs for the thermal moderator. Furthermore,  $dt/\lambda$  is constant between 2 and 3 Å for the cold moderator. With such short pulses even a 15m flight path may also be acceptable.

However, the choice of moderator is not quite so straightforward, since in this case a medium cold moderator (130K) is undoubtedly best, with optimal flux (or more particularly the

"effective flux",  $\phi(\lambda)\lambda^2$ ) in the 2-5 Å region, offering a factor 3-5 improvement over the cold or ambient options. If the instrument is relatively long, then coupling (or "partial" coupling) to a pulse width of, say, 100 μs would be acceptable (though see the Aside below).

As noted in the original Lehmann Working Group report [6], a 40m instrument on a 50Hz source gives a restricted bandwidth ( $\Delta\lambda=2$  Å), so a reduced repetition-rate target is a possibility for this instrument, particularly if low power moderator options can enhance the flux in the important region.

*This instrument on ESS promises to be world-leading, even in comparison with the dramatic developments on e.g. LADI at the ILL (the reduction in background due to the time-of-flight Laue method being very important here). This is particularly true if a 130K moderator is available.*

#### **Aside – peak width and background**

Coupling (or "partially" coupling) to a pulse length of up to 100 or even 200 μs offers increased flux, but the reduced resolution has consequences not only for peak separation but also for the background from "chemical" samples. The broader pulses lead to significant build up of background under Bragg peaks (incoherent scattering plus long reflection tails which becomes increasingly less ideal as the pulse is broadened/resolution lessened). Hence, it is not just sheer flux but signal/background which is important in determining the instrument performance.

Quantitatively, both peak height P and P/B ratio are important. For large unit cells the signal is generally lower than the background so that

$$\sigma(P)/P = [2/(P \times P/B)]^{1/2} \quad (1)$$

and the sheer flux is also very important.

In addition to the signal/background ratio, if peaks overlap very severely then there can be problems in separating the peak from the background. Even full-profile methods such as Rietveld refinements of powder data can suffer from this problem, and in cases (i) and (ii) under consideration here we have the added complication that much of our "background" is coming from hydrogen incoherent scattering; the cross-section of this is wavelength-dependent. The consequence is that even if good peak modelling/intensity extraction software is available, the underlying physics of the scattering in the sample can make the situation more complicated.

***While sheer flux is important, the control of background levels is also important in single-crystal diffraction, particularly from hydrogen-containing materials. The time-of-flight Laue technique has advantages here, in "stretching" the background throughout the data collection frame.***

## High Resolution Diffraction

Here we consider very high Q measurements, to d-spacing of 0.2 Å or less, primarily for “physics” measurements, e.g. anharmonicity. Frequently this must also be accompanied by another high resolution aspect – high  $\Delta Q/Q$  resolution to allow the examination, for example, of incommensurate or satellite reflections or of diffuse scattering close to Bragg peaks (e.g. critical scattering). This instrument type clearly requires a short pulse source and a pulse width of around 10-15  $\mu\text{s}$ .

The need for very high epithermal flux places us on an ambient, thermal, moderator, which with the need for very sharp pulses to maintain very high resolution will be decoupled and poisoned.

The instrument would be envisaged to be of medium length (15m) on the 50Hz source; there is no problem with bandwidth.

*This instrument type would be world-leading, and accessing very high Q values is potentially unique on a pulsed source.*

***The ability of short pulse spallation sources to offer very high flux of short wavelength neutrons gives the opportunity for very high resolution single-crystal applications in physics.***

## Diffuse Scattering

During the discussions in our working group a diffuse scattering instrument type became separate from the high resolution instrument. This instrument type refers to diffuse scattering which is not necessarily close to Bragg peaks. It must, however, maintain good Q resolution and hence requires a short pulse source, with a pulse width of around 50  $\mu\text{s}$ .

The instrument, since it examines often weak non-Bragg peak scattering, requires good intensity at both high and low Q, and should couple this with extremely low (ideally “zero”) background. In addition the instrument set-up must be well understood and reproducible to allow accurate corrections.

Related to this, it is clear that band width is also important, to allow reliable collection of a continuous diffraction pattern over all of reciprocal space/Q values for whole pattern modelling, for example using probability density function and related techniques – like those carried out by the Disordered Materials community.

Such diffuse scattering measurements would be ideally carried out on a medium-length instrument on a low repetition rate source (e.g. 10Hz) as wide simultaneous band-width is needed. It would of course be possible in principle to slew choppers continuously to cover the full necessary Q-range but why do this if a good flux instrument sitting on a 10Hz source can yield a sufficiently wide band in a single shot with the ability to be normalised accurately and consistently? The moderator would have to be decoupled for high resolution, but

***The ability of time-of-flight Laue diffraction to measure fully resolved, continuous 3D volumes of reciprocal space offers unique opportunities in the measurement and interpretation of diffuse scattering.***

the need for good flux over the whole Q-range means that a medium-cold or cold moderator would be most appropriate.

*This instrument type would be world-leading on ESS, with the potential for fully 3D resolved measurements of reciprocal space volumes unique on a pulsed source.*

### **Low Resolution Biological Crystallography**

For low resolution biological crystallography (typically to a d-spacing of 6-8 Å on a 200-500 Å cell edge) we require a high flux of long wavelength neutrons. A long pulse source is an option here, while if a short pulse option is chosen, we would clearly require a cold, coupled moderator. However, we must always be wary of the problems of pile-up of incoherent background (see (ii) above). Resolution is not a major issue here and so this instrument can probably be of medium length, on a 50Hz source.

Such an instrument would open up new areas of biology, for example in the study of membrane protein and protein-nucleic acid complexes, if fully optimised. Capacity is also important here – in the biological sciences area we must offer more instrumentation to meet the needs and demands of this large and expanding community. Structural biology is now focusing upon understanding interactions of complex systems and we should be looking to pursue this important area on ESS even if the instrument gains over reactor possibilities are rather lower than some others.

*Our preliminary conclusion is that this instrument type on the ESS would offer significant gains on the leading existing steady state instrumentation, with an optimised moderator.*

### **“Single Reflection” Measurements**

This type of measurement is an extremely important component of, for example, the programme on D10 at the ILL. We have therefore benchmarked this instrument type.

The aim is to follow a single peak (or very limited selection of reflections) as a function of some external variable (e.g. temperature, pressure, magnetic field),. Q-space resolution is also often important to follow the development of, for example, critical scattering, twinning, or incommensurate propagation vectors.

Thus the requirements are for a very high point by point flux over a limited wavelength range, clearly opening up the long pulse option, but noting that high Q-space resolution may also be required.

However, there is also the need to have also a more standard

***Low resolution biological neutron crystallography offers access to new areas of study such as membrane protein and protein-nucleic acid complexes. ESS will offer a highly competitive alternative instrumentation option to the best reactor facilities in this important area.***

***An optimised single-crystal instrumentation suite on ESS will offer the ability to track rapidly individual reflection intensities as they change under the influence of changing external environment.***

“chemical crystallography” capability on the same instrument to characterise important sample characteristics (such as extinction etc. under the same data collection conditions as those in which the single peak changes are followed. This can still be achieved in the bng pulse case, but is less obviously favourable.

We note that some of the single peak measurements can of course be done on a 15m instrument with the poisoned thermal moderator, but will often involve complex sample environment.

*Such an instrument type can be competitive with the best steady-state options, given the same time-averaged flux.*

## References

- [1] A.D. Taylor (1992). Instrumentation and Techniques for the European Spallation Source, RAL Report, RAL-92-040.
- [2] R. Scherm & H. Stiller (1984). Proceedings of the Workshop on Neutron Scattering Instrumentation for SNQ. Maria Laach, Jülich document 1954.
- [3] W. Jauch & H. Dachs (1984) in Ref [2], p. 31; W. Jauch (1993). Trans. Am. Cryst. Assoc., **29**, 55.
- [4] M.S. Lehmann (1984) in Ref [2], p. 53.
- [5] W. Jauch (1996). In LPSS Workshop, ed. F. Mezei et al, HMI Berlin.
- [6] W Jauch, M S Lehmann, L Sjölin, C Wilkinson & C C Wilson (1997). ESS: Report from working group on large unit cell crystallography. ILL internal report, ILL97/JA19T.

# Powder Diffraction Instruments

**P.G. Radaelli<sup>1</sup>, S. Hull<sup>1</sup>, H.J. Bleif<sup>2</sup> and A. M. Balagurov<sup>3</sup>**

<sup>1</sup>ISIS Facility, Rutherford Appleton Laboratory, Chilton, Didcot, Oxfordshire OX11 0QX, United Kingdom

<sup>2</sup>Hahn Meitner Institut, Glienicker Str 100, 14109 Berlin, Germany

<sup>3</sup>Frank Laboratory for Neutron Physics, JINR, 14980 Dubna, Moscow Reg. Russia

We have completed a preliminary analysis of the target/moderator options of the powder diffraction programme at the ESS. This includes a series of analytical simulations of steady-state and time-of-flight instruments, and is aimed at addressing the following questions:

1. What is the perspective gain factor at the ESS with respect to existing steady-state and time-of-flight instrumentation?
2. What is the likely choice of target for the different applications?
3. What is the likely choice of moderator for the different applications?
4. What priorities for further moderator developments can be identified?

Answer to Question 1.: at the ESS we can expect a source-related gain factor varying between 10 and 80 with respect to present-day state-of-the-art instruments. The bigger gains, which can be further increased ( $\times 2$ ) by beam-optics optimisation, are for the longer wavelengths, while the gains at shorter wavelengths are limited by the lack of a truly sharp cold moderator.

Answer to Question 2.: all the ESS powder diffractometers should have the 50Hz target as first choice. Locating some or all the instruments on the 10Hz short-pulse target will result in a significant but not catastrophic loss in flexibility. Of course, this statement holds true only assuming that there is no peak flux gain in optimising the 10Hz target over the 50Hz target. The best instruments to be assigned to the 16.6Hz long-pulse target are a variable-resolution cold-neutron diffractometer. A Fourier diffractometer can also be considered.

Answer to Question 3.: coupled moderators are not ideal for powder diffraction, primarily because of the long "tails". From this provisional assessment, the following moderator choices have emerged:

De-coupled poisoned H<sub>2</sub> moderator for high-resolution applications.

De-coupled unpoisoned H<sub>2</sub> moderator for medium-resolution magnetic and low-Q diffraction.

De-coupled unpoisoned H<sub>2</sub>O moderator for medium-resolution crystallography.

Answer to Question 4.: a truly sharp cold moderator, similar to the ISIS liquid CH<sub>4</sub> moderator, is dearly missed. Some more work should be done to identify a possible alternative.

## Introduction

By all accounts, the outlook for powder diffraction at the new high-power sources in Europe and elsewhere is extraordinarily bright. Powder diffractometers at present pulsed sources are already competitive with steady-state machines, and one can expect further gains of 1-2 orders of magnitude at the ESS. Nevertheless, one can already identify two main challenges for powder diffraction at future high-power pulsed sources. First of all, there is a general desire to broaden the scope of time-of-flight powder diffraction into traditional steady-state strongholds, such as magnetic diffraction. This is in line with the stated philosophy of turning ESS into a “super-ILL” as well as a “super-ISIS”. Secondly, we will have to adapt to a target-moderator landscape bearing little resemblance with the one we have been used to at ISIS and other pulsed sources. This document is a preliminary attempt to address these issues. We have purposely chosen to use rather simple simulation tools, so that a sizeable number of options could be tested. We have also included suggestions for further work to be undertaken in the powder diffraction task group and in the moderator/target group.

***Introduction: Future prospects of powder diffraction at intense pulsed sources.***

## Preliminary considerations

### *Performances of a powder diffractometer*

Powder diffraction is in many ways an ideal technique to be applied at pulsed sources. In fact, powder diffraction fulfils the two main criteria for pulse source efficiency: it can make effective use of a broad wavelength band and it benefits from high resolution. In the next few paragraphs we will elaborate on this statement, and set out the fundamental formulas to evaluate the performances of a time-of-flight diffractometer and to compare it with a steady-state diffractometer.

The main difference between steady-state and pulsed sources is that, for the latter, the neutron emission is concentrated in short bursts. In other words, the *peak power* of pulsed sources is much higher than their *average power*. One is primarily interested in maximising the time-averaged flux on the sample. In fact, the average count rate for a diffractometer

$$P \propto \dot{O} \cdot \dot{U}_{\text{det}} \cdot \mathbf{e}_{\text{det}} \cdot V_{\text{eff}}, \quad (1)$$

is proportional to the time-averaged flux on the sample, the detector solid angle and the “effective” (absorption-corrected) sample volume.

Under certain circumstances, however, the source parameter that ultimately determines the instrument count rate is in fact the *peak power*. For a diffractometer, this is verified when the following two conditions are simultaneously met:

1. The pulse width is a significant component of the resolution function.
2. The time frame (i.e., the range of time-of-flights in which “useful” neutrons are collected) is equal to the reciprocal of the source repetition rate. We will see later that this condition dictates the wavelength band to be employed by the

***Performances of a powder diffractometer.***

***The average count rate is the product of the flux at the sample, the detector solid angle and efficiency and the sample volume (Equation 1).***

tion dictates the wavelength band to be employed by the diffractometer.

If condition 2. Is verified, it is possible to show that the average flux on the sample for a pulsed-source diffractometer is given by

$$\bar{O} = R \cdot \langle B_{peak}(\mathbf{I}) \cdot \mathbf{e}(\mathbf{I}) \cdot \Omega_{source}(\mathbf{I}) \rangle, \quad (2)$$

where  $B_{peak}(\mathbf{I})$  is the peak *brilliance* (neutrons-sec<sup>-1</sup> cm<sup>-2</sup> ·sterad<sup>-1</sup> %BW<sup>-1</sup>),  $R$  is the dispersive ( $\Delta\tau/\tau$ ) component of the resolution (here assumed to be constant),  $\mathbf{e}(\mathbf{I})$  is the optical system efficiency and  $\Omega_{source}(\mathbf{I})$  is the viewing solid angle of the source (moderator or guide; in the latter case the solid angle is wavelength-dependent). The average is over the wavelengths used by the instrument. Equation (2) has to be compared with the equivalent formula for a steady-state source,

$$\dot{O} = R \cdot B_{peak}(\mathbf{I}) \cdot \mathbf{e}(\mathbf{I}) \cdot \Omega_{source}(\mathbf{I}), \quad (3)$$

where, now,  $R=DI/I$ . The comparison between equations (2) and (3), taking into account equation (1) as well, elicits a few considerations:

- Time-of-flight and constant-wavelength machines achieve high count rates in different ways. Reactor-based instruments tend to maximise the source solid angle, by exploiting focussing monochromators, whereas diffractometers at pulsed sources tend to have much larger detector solid angles.
- Since ISIS and the ILL have comparable peak brilliances, and all the other factors in Equation (1) balance out in the first approximation, comparable machines at the two sources should have comparable performances. For the two high-resolution machines D2B and HRPD, which have overlapping domains of application, this has been empirically demonstrated through the experience of many users. The same is not true for high-flux machines, which are optimised for rather different uses at the two sources.

#### *The wavelength bandwidth of a time-of-flight diffractometer*

As already mentioned, the wavelength band is a critically important parameter defining the performances of a time-of-flight diffractometer. Its maximum value is defined by the need to avoid *frame overlap*, which is the superposition of neutrons coming from different pulses onto the same frame:

$$\Delta \mathbf{I}_{Max}(\text{\AA}) = \frac{3957}{\mathbf{n}_{source} \cdot L_{tot}(m)}, \quad (4)$$

where  $\mathbf{n}_{source}$  is the repetition rate of the source and  $L_{tot}$  is the total flight-path.

It is important to distinguish between this *single-frame* bandwidth and the effective bandwidth, which can be much larger if multi-frame data acquisition is employed (see below) In modern time of flight diffractometers, this single frame wave

**Equation (1) can be re-written in terms of the source brilliance and the instrument dispersive resolution for TOF (Equation 2) and CW instruments (Equation 3)**

**TOF and CW instrument achieve high count rates by different means the effectiveness of which varies as a function of Q.**

**The single-frame wavelength bandwidth is a key parameter in understanding the performances of a TOF diffractometer.**

modern time-of-flight diffractometers, this single-frame wavelength band is usually set by means of a system of choppers. It is immediately apparent from (4) that long instruments at fast sources have a narrow bandwidth. When this is perceived to be a disadvantage, another chopper can be added to reduce the source frequency by suppressing some of the pulses. Another approach is that of making repeated measurements with different wavelength ranges. This is known as *multi-frame* data collection.

#### Resolution of a time-of-flight diffractometer

In addition to the usual geometrical terms, the pulse width usually gives an important contribution to the instrumental resolution, especially in back scattering. The actual shape of the pulse and its dependence on wavelengths are complex functions, dictated by the physical processes occurring within the moderator [1] (Fig. 1). Quite often, it is assumed that  $Dt$  is directly proportional to  $I$ , which would be equivalent to approximate the curve in Figure 1 with a straight line with zero intercept, and, in this case, approximate slope of  $S \sim 1 \cdot 10^{-5}$  sec/Å. The pulse-width component of the resolution function can then be approximated by

$$R_{pulse} \approx \frac{3956}{L_{tot}(m)} \cdot \Sigma \quad (5)$$

Combining (4) with (5) we obtain:

$$\Delta I_{Max}(\text{Å}) = \frac{R_{pulse}}{n_{source} \cdot \Sigma}, \quad (6)$$

which defines the relationship between bandwidth, resolution, repetition rate and pulse width.

**The “dispersive” resolution of a TOF diffractometer is proportional to the pulse width and, the total flight-path.**

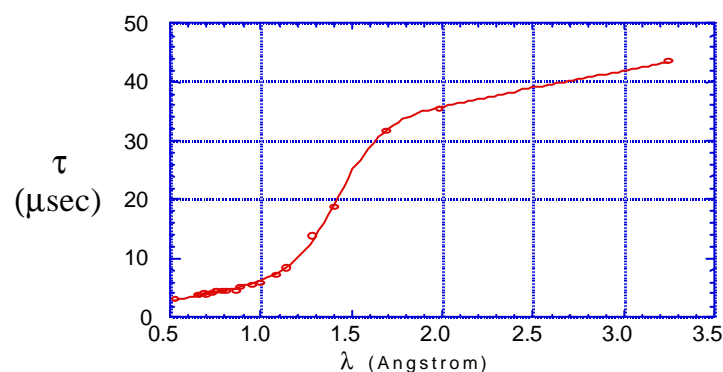


**Fig. 1:** Exponential decay constant for the ISIS liquid-methane moderator, measured on GEM.

#### Setting the optimum bandwidth

At the end of the seventies, when the first time-of-flight diffractometers were being conceived for pulsed sources such as Zing-P', IPNS, and, later, ISIS, a number of options were considered in principle. However, at the end, the design philosophy was dictated by considerations of mostly practical nature:

- The need to avoid as much as possible expensive neutron guides favoured relatively short instruments ( $L_{tot} \sim 10\text{-}15\text{m}$ ), naturally leading to wide single-frame bandwidths. This dictated the use of “sharp” (decoupled/poisoned) water or cold (liquid or solid) methane moderators. 50 or 60Hz repetition rate was standard.
- The original methods of time-of-flight data reduction (electronic focussing) and analysis (single-histogram Rietveld refinement) also favoured broad bandwidths, which allowed relatively large wavelength-dispersive histograms to be produced.
- For the high-resolution machine HRPD, the single-frame bandwidth was kept reasonably large by reducing the source repetition rate.

***First and second-generation instruments are typically broad-bandwidth, wavelength-dispersive machines. New technologies have enabled new configurations to be explored.***

It is clear that most of the considerations underpinning the design philosophy of first-generation diffractometers are now superseded by developments in neutron optics and by the massive increase of computing power available to the instrument scientists and the users. For example, multi-histogram analysis of time-of-flight data from different detector banks, once performed only in exceptional circumstances, is now applied routinely, automatically and, to a certain extent, transparently, on instruments such as GEM [2]. In the near future, and certainly well before the advent of the ESS, new data collection techniques, such as commensurate or incommensurate chopper “slewing” will enable narrow-bandwidth instruments to perform extended data collections as short as a few frames. Consequently, the single-frame bandwidth is rapidly losing importance as a defining parameter for diffractometers design. Also, new data computer-intensive focussing methods can be implemented, when this represents an advantage.

## **Comparison with existing instrument/sources**

In this section, we will attempt to make a quantitative comparison between existing state-of-the-art instrumentation at steady-state and pulsed sources and at the ESS. It is important to remark that, in doing this, we will not introduce any element of novelty in the instrumentation itself, but we will only consider the enhanced performances of the source.

***An initial comparison between ESS, ISIS and the ILL is made, to estimate the perspective gains.***

### *Choosing the instruments for the comparison*

It seems appropriate to base the comparison on the most recent instrumentation installed at existing sources. For both ILL and ISIS, the latest powder diffractometers are both high-intensity, medium-resolution machines, D20 and GEM, respectively. D20 became operational in 1997, while GEM saw its first neutrons in late 1999. As already remarked, these medium-resolution machines have quite different characteristics, which reflect the differences in scientific interests of the ILL and ISIS powder diffraction communities. In the most commonly used configuration, D20 has a resolution  $\Delta d/d \approx 0.01$ , and achieve a high count rate mainly through high flux on the sample. These characteristics are ideal for studying

magnetic diffraction and the macroscopic parameters (lattice parameters, phase fractions, peak intensities, etc.) of time-resolved chemical or physical phenomena. On the contrary, GEM has a much better resolution  $\Delta d/d \approx 0.002$ , and a much lower incident flux, which is compensated by a very large detector solid angle. This is ideal to study both macroscopic and microscopic parameters (atomic coordinates, Debye-Waller factors, occupancies, etc.) with a very high time resolution. Because of these differences, the comparison between these instruments has to be taken *cum grano salis*. As for the ESS, we have taken an instrument with the same characteristics of GEM (flight-path, detector system, moderator size) and tested it on four different *de-coupled* moderators (cold-poisoned, cold-unpoisoned, thermal poisoned, thermal-unpoisoned). Clearly, using a coupled moderator at 17m primary flight-path is not a viable option, and we have not considered it here.

### Defining the parameters for the comparison

We will present comparisons between two different parameters. The first one is the *effective flux*  $f_{eff}$ , which enables one to calculate the integrated intensity  $I_{hkl}$  of a given Bragg peak, expressed in neutrons per second:

**We define effective flux and effective peak height as comparison parameters.**

$$I_{hkl} [n/sec] = \ddot{O}_{eff} \times \frac{V_{sample} \cdot f}{v_{u.c.}} \times m_{hkl} |F_{hkl}|^2, \quad (7)$$

where  $V_{sample}$  is the sample volume in  $cm^3$ ,  $v_{u.c.}$  is the unit cell volume in Angstroms,  $f$  is the packing fraction of the powder,  $m_{hkl}$  is the reflection multiplicity and  $|F_{hkl}|^2$  is the square of the structure factors expressed in Barns. Note that  $f_{eff}$  contains all the appropriate geometrical and wavelength-dependent terms, which are different for steady-state and pulsed diffractometry. Perhaps a better indicator of relative performances for instruments with different resolution (see below) is the *effective peak height*  $H_{eff}$ , which is given by the effective flux divided by the peak width (FWHM) in Angstroms.

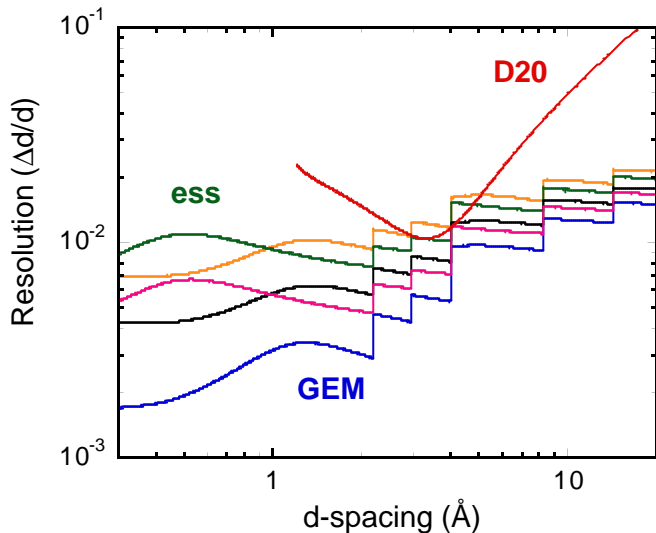
Table I: Instrument characteristics for the comparative simulations of steady-state and time-of-flight diffractometers at present sources and at the ESS.

	Monochromator /Moderator	Flux/Incident spectrum	Flight-paths $L^1/L^2$	Detector system	Efficiency
D20	HOPG 42° take-off, 2.4 Å	$3.7 \times 10^7$ n/cm <sup>2</sup> /sec <sup>†</sup>	-	<sup>3</sup> He microstrip system, 1600 elements.	90%
GEM	ISIS CH <sub>4</sub> poisoned	From V-rod measurements	17m/1.3-2.3m	6 banks of SZn scintillators, 8000 elements, $W_{det} = 3.5$ sterad	50% @ 1 Å
ESS-1	H <sub>2</sub> decoupled poisoned	From ESS-Instr.-4.12.00	17m/1.3-2.3m	6 banks of SZn scintillators, 8000 elements, $W_{det} = 3.5$ sterad	50% @ 1 Å
ESS-2	H <sub>2</sub> decoupled unpoisoned	From ESS-Instr.-4.12.00	17m/1.3-2.3m	6 banks of SZn scintillators, 8000 elements, $W_{det} = 3.5$ sterad	50% @ 1 Å
ESS-3	H <sub>2</sub> O decoupled poisoned	From ESS-Instr.-4.12.00	17m/1.3-2.3m	6 banks of SZn scintillators, 8000 elements, $W_{det} = 3.5$ sterad	50% @ 1 Å
ESS-4	H <sub>2</sub> O decoupled unpoisoned	From ESS-Instr.-4.12.00	17m/1.3-2.3m	6 banks of SZn scintillators, 8000 elements, $W_{det} = 3.5$ sterad	50% @ 1 Å

<sup>†</sup> Source: ILL-D20 web page.

$$H_{eff} = \frac{\ddot{O}_{eff}}{W[\text{\AA}]} \quad (8)$$

The instrument parameters used for the simulations are summarised in Table I. The resolution curves for the six instruments are plotted in Figure 2.



**For similar flight-paths, ESS instruments have much higher flux (in excess of the canonical  $\sim 30$ ) but at the expense of a loss of resolution.**

**Fig. 2:** Resolution functions of GEM (blue), D20 (red) and GEM-like instruments at ESS on the four decoupled moderators: H<sub>2</sub>-poisoned (black), H<sub>2</sub>-unpoisoned (orange), H<sub>2</sub>O-poisoned (light gray) and H<sub>2</sub>O-unpoisoned (dark gray).

The first thing to notice is the quite considerable loss of resolution of the ESS instruments with respect to GEM, the primary flight-path being equal. This is due, on one hand, to the poorer peak-shape characteristics of the ESS-H<sub>2</sub> moderators with respect to the ISIS-CH<sub>4</sub> moderator, and to the fact that the switch-over between slowing-down and thermalisation occurs at much shorter wavelengths for H<sub>2</sub>O than for either H<sub>2</sub> or CH<sub>4</sub>. It is noteworthy that the resolution functions of the ESS instruments are still below that of D20 in the high-flux configuration used here.

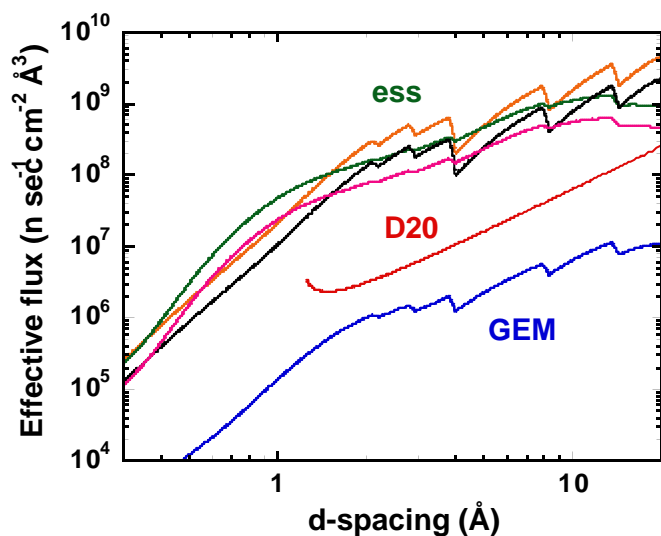


**Fig. 3:** Effective flux parameter  $f_{eff}$  (see text) for GEM (blue), D20 (red) and GEM-like instruments at ESS on the four decoupled moderators: H<sub>2</sub>-poisoned (black), H<sub>2</sub>-unpoisoned (orange), H<sub>2</sub>O-poisoned (light gray) and H<sub>2</sub>O-unpoisoned (dark gray).

Nevertheless, a realistic analogue of GEM at the ESS will have to be moved farther away from the moderator, at or beyond 40m (more on this later). Part of the loss in source solid angle  $W_{source}$  can be compensated by the large surface area of the ESS moderators (120mm  $\times$  120mm: here, we have used the canonical ISIS value of 100mm  $\times$  100mm).

Even larger moderators (e.g., 140mm  $\times$  140mm) would be worth considering, if technically feasible, since the loss of resolution is likely to be a problem common to other instruments.

- The effective flux and effective peak height parameters,  $f_{eff}$  and  $H_{eff}$ , for the same set of instruments are plotted in Fig. 3 and 4, respectively.  $f_{eff}$  is the relevant parameter when the sample contribution to the resolution function dominates the instrumental term, or when one is interested in determining integrated intensities from data with poor statistics.  $H_{eff}$  is the parameter used in most data collection strategies (which generally look at signal-to-noise ratios) for samples that are well matched to the instrument. Even if all Bragg peaks are resolved, an increase of the peak width at constant  $H_{eff}$  will somewhat improve the statistics on the structure factors but will worsen the accuracy on lattice parameters and propagation vectors. Obviously, a decrease of the peak width is an advantage for partially overlapping peaks. It is clear from the data that we can expect an improvement of over two orders of magnitude in both  $f_{eff}$  and  $H_{eff}$  at long d spacing with respect to GEM. The improvement over D20 is over an order of magnitude for  $f_{eff}$  and two orders of magnitude for  $H_{eff}$ .

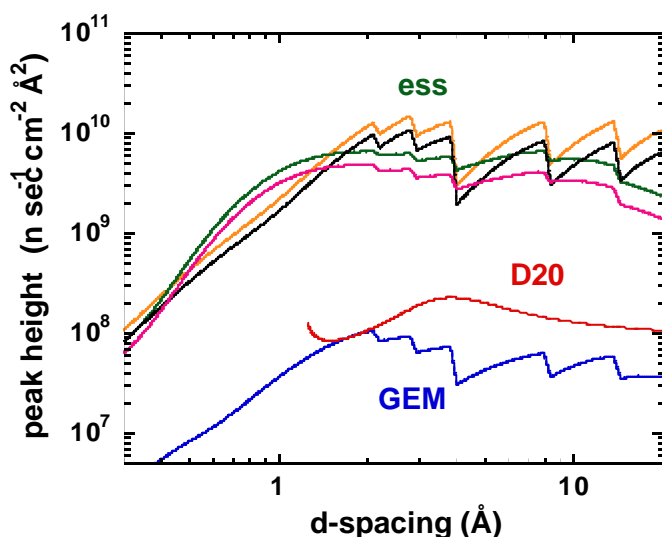


**Fig. 4:** Effective peak height parameter  $H_{eff}$  (see text) for GEM (blue), D20 (red) and GEM-like instruments at ESS on the four decoupled moderators: H<sub>2</sub>-poisoned (black), H<sub>2</sub>-unpoisoned (orange), H<sub>2</sub>O-poisoned (light gray) and H<sub>2</sub>O-unpoisoned (dark gray).

### The proposed ESS instrument suite

The original suite of ESS instruments [3] included 6 powder diffractometers (see Table II). Two of them were located on the 50Hz target and four on the 10Hz target. 5 out of 6 diffrac-

***The original ESS powder instrument suite needs to be revised in the light both of the emerging needs of***



## The choice of the target/moderator package: Instrument simulations

### *Instrument parameters*

In defining the choice of the target/moderator package, one has to take into account three fundamental parameters:

1. The combination of moderator type and primary flight path, which defines the ultimate resolution of the diffractometer.
2. The source/chopper setting, which defines the average value of the wavelength and its single-frame range.
3. The detector configuration and the data collection strategy, which defines the Q-range of the measurement and the Q-dependent resolution function, as well as the fragmentation of the data set.

In this preliminary analysis of the problem, we have considered in detail points 1. and 2., making the assumption that data collected at all scattering angles will be of use. We have chosen to consider an instrument with a peak resolution  $Dd/d \sim 2 \cdot 10^{-3}$ . As already discussed, this resolution can be reached by at least two different viable choices of the moderator and primary flight-path.

### *Methods*

We have compared two medium-resolution ESS instruments with comparable resolution  $Dd/d \sim 2 \cdot 10^{-3}$ : a 40m machine looking at a poisoned  $H_2$  or  $H_2O$  moderator and an 80m machine looking at an unpoisoned  $H_2$  or  $H_2O$  moderator. As a reference, we have also calculated the performances of a 17m ISIS machine looking at a poisoned  $CH_4$  moderator, also having a similar resolution. The detector system we have chosen is the same in all cases: a continuous detector with a secondary flight path of 2m and a constant elevation angle of  $\pm 22.5^\circ$  on either side of the equatorial plane, for a total solid angle of  $\Omega$ . All the calculations were performed analytically, using the moderator parameters given in the document ESS-Instr.-4.12.00. The following beam line parameters were adopted:

- For the 17m ISIS instrument, the sample has a direct view of a  $100\text{mm} \times 100\text{mm}$   $CH_4$  moderator, without any guide.
- For the 40m ESS instrument on the poisoned moderators, the first 20m of the flight tube, which has the same dimensions as the moderator ( $120\text{mm} \times 120\text{mm}$ ), is coated in Ni ( $\mu_c = 0.00173 \text{ rad/\AA}$ ) on all 4 sides, while the rest of the flight tube is coated with an absorber.
- For the 80m ESS instrument on the unpoisoned moderators, the first 76.6m of the flight tube, which is straight and has dimensions  $20\text{mm} \times 40\text{mm}$ , are coated with Ni on all 4 sides.

It is noteworthy that the maximum vertical divergence of the 80m machine is doubled with respect to the other two. Therefore, we can expect a factor of two gain in effective flux.

***Parameters and methods for the comparison between instrument are laid out.***

The 40m instrument could be equally optimised by adding a guide section coated on the top and bottom sides. This option was not considered here, as it introduces an additional complication in the simulation.

A simple analytical expression, based on the calculation of the number of “bounces” at a given divergence angle, was used to calculate the guide transmission. Since the difference in instrument resolution between the different configurations is quite small, we have chosen to compare the values of  $f_{eff}$ . The ESS curves have been normalised to the ISIS curve, to yield a wavelength-dependent “gain factor”. The ISIS 17m instrument was operating at 50Hz, with a wavelength band of 4.05 Å. All the parameters used in the simulation are summarised in Table III.

### Wide-band operation

The gain factors of the two ESS instruments operating in wide-band mode (25 Hz for the 40m machine and 10Hz for the 80m one) are shown in Figure 5 for both H<sub>2</sub> and H<sub>2</sub>O moderators. For the cold moderators, one can immediately observe that the gain for the 40m ESS diffractometer over the 17m ISIS one is a factor of 50 at long d-spacings, while the gain is less than a factor of 10 below 0.5 Å. As already observed, the fundamental reason for this is the poorer resolution of the H<sub>2</sub> poisoned moderator with respect to the ISIS CH<sub>4</sub> one, which forces to double the flight-path and, consequently, to have a 4-times smaller direct view of the moderator. The 80m instrument is better by another factor of 3.6 at long wavelengths. Of this, a factor of 2 is due to the optimised optics. A good part of the rest is due to the higher peak flux from the unpoisoned moderator.

**With the current ESS moderator suite, access to epithermal neutrons is problematic even for medium-resolution machines.**

Table III: Instrument characteristics for the comparative simulations of different target/moderator choices at the ESS.

	Monochromator /Moderator	Flight-paths L <sub>1</sub> /L <sub>2</sub>	Beam optics system	Operating Frequencies
ISIS-17m	ISIS CH <sub>4</sub> poisoned	17m/2m	Direct view of 100×100 mm <sup>2</sup> moderator.	50 Hz
ESS-40m-H <sub>2</sub>	H <sub>2</sub> decoupled poisoned	40m/2m	20 m of 120×120 mm <sup>2</sup> Ni guide.	25 Hz 50 Hz
ESS-40-H <sub>2</sub> O	H <sub>2</sub> O decoupled poisoned	40m/2m	20 m of 120×120 mm <sup>2</sup> Ni guide	25 Hz
ESS-80-H <sub>2</sub>	H <sub>2</sub> decoupled unpoisoned	80m/2m	76.6 m of 20×40 mm <sup>2</sup> Ni guide	10 Hz 25 Hz 50 Hz
ESS-80-H <sub>2</sub> O	H <sub>2</sub> O decoupled unpoisoned	80m/2m	76.6 m of 20×40 mm <sup>2</sup> Ni guide	10 Hz

However, the short-wavelength performances are significantly deteriorated. This would suggest that the 40m machine is better suited for high-Q crystallographic applications, while the 80m diffractometer is better for magnetism. The gain curves are somewhat more balanced for the water moderators. An H<sub>2</sub>O moderator could perhaps be adopted for the 40m machine, if the scientific programme calls for predominantly crystallographic work (this choice was done at the SNS for the 80m POW-GEN3). Further changes could be introduced by adopting a more efficient optical system (e.g., a <sup>58</sup>Ni guide or even a ballistic guide).

### Frequency-dependent gains

Figure 6 shows the effect of varying the operating frequency (and hence the single-frame bandwidth) for the 40m diffractometers.

By all accounts, high-frequency operation is particularly appealing when one is only interested in d-spacing above 1 Å. In this case, a gain of a factor of two over the wide-band operation is attainable. At 80m, there is no longer any gain from going from 25 to 50Hz. This happens because we are effectively in the angle-dispersive limit, where the wavelength spread contributes little to the Q-range. Of course, this will no longer be true if one looks at a narrow angular range, for instance, in back scattering, to achieve high resolution. In this approach, one can still trade Q-range for flux.

**High-frequency, narrow-bandwidth operation would produce sizeable gains for some experiments.**

### Perspectives at a long-pulse target

The long 2.5 msec pulse from the proposed long-pulse target is not suitable as such for powder diffraction use, and needs to be reshaped. This is done by means of a disc chopper placed at a distance  $L_{chop}$  from the moderator. It is easy to deduce the following relationship between  $L_{chop}$ , the pulse length  $t$  and the band width:

$$\Delta I (\text{\AA}) = \frac{3956}{L_{chop}} \cdot t, \quad (9)$$

**Given the parameters of the long-pulse target, and the restrictions in the upstream disk chopper position, a diffractometer at the long-pulse target must have a flight-path in excess of 180 m. The flux is reduced with respect to other moderators, but the variable resolution and triangular peak shape make this machine appealing.**

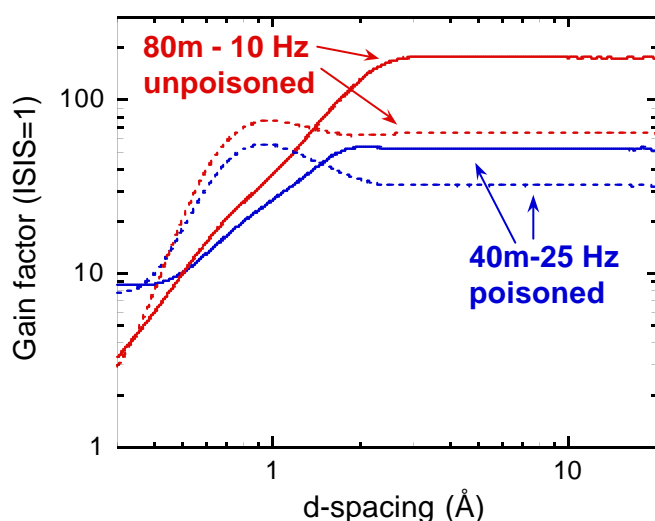


**Fig. 5:** Effective flux gain factors over an equivalent ISIS machine for two ESS medium-resolution diffractometers: a 40m machine looking at a poisoned H<sub>2</sub> moderator (blue continuous line) and a poisoned H<sub>2</sub>O moderator (blue dotted line) and for an 80m machine looking at an unpoisoned H<sub>2</sub> moderator (red continuous line) and an unpoisoned H<sub>2</sub>O moderator (red dotted line).

Taking  $L_{chop} = 6\text{m}$  (slightly less than the standard ISIS value of 6.5m), and  $t = 2.0\text{ msec}$  (we here consider only the intense part of the pulse) one calculates a band width of 1.28 Å. From equation (4), one can then calculate the primary flight path at which the resulting histogram is filled, which is also the condition for optimum use of the peak brilliance.

$$L_{tot} = \frac{L_{chop}}{\mathbf{n} \cdot \mathbf{t}}, \quad (10)$$

from which one deduces a flight path of 181m at 16.6Hz. The most favourable application for such a source/moderator combination would be for a cold-neutron, variable-resolution diffractometer [4], with excellent peak resolution and perfectly triangular peak shape. At long wavelengths, the long-pulse target peak-brilliance compares more favourably with the short-pulse targets. Also, at long wavelengths, the chopper system is better optimised (for chopper-shaped pulses, for any given bandwidth, there is a penalty factor  $\sim \frac{I_{min}}{I_{max}}$  on the peak

brilliance). Possible applications are for the study of extended magnetic defects and for complex structure solution. Nevertheless, the peak brilliance loss is a factor of two at best over the short-pulse target for the wavelengths of interest, and it is hard to argue for this machine as a first choice.

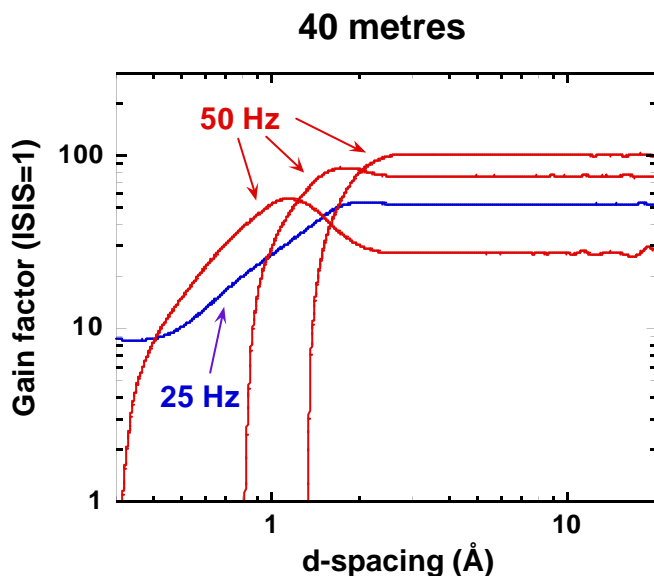


**Fig. 6:** Effective flux gain factors as a function of the operating frequency over an equivalent ISIS machine for the 40m ESS medium-resolution diffractometer. The blue curve is for 25Hz operation, while the red curves are for 50Hz with wavelength bands centred at 1.5, 2.5 and 3.5 Å.

A possible alternative would be a high-resolution Fourier diffractometer [5], of the type that successfully operated for a long time at the IBR-2 pulsed reactor in Dubna. Fourier diffractometers can be much shorter than conventional machines having the same resolution. Therefore, a gain of a factor of 10 in wavelength-integrated peak brilliance is to be expected because the wider wavelength range compatible with frame overlap and the absence of beam attenuation from the guide. On the other hand, the peak height is reduced by a factor of 2 with respect to a conventional disk chopper, because the Fourier chopper has only 50% transmission in the “full open” state. Furthermore, the high-resolution to low-resolution peak height ratio is always less than one. The maximum theoretical value for this ratio is 0.75, but its real value depends on the quality of the Fourier chopper manufacture and the TOF/geometrical contributions in the resolution function, and, in the

***A possible alternative to the disk-chopper machine is a Fourier diffractometer. The main advantage of the latter is the lower cost for comparable performances. The main disadvantage is the presence of a correlation background.***

practice, is in the range 0.2-0.4. The overall gain of the Fourier technique in terms of *peak height* is therefore between 1 and 4. State-of-the-art electronics and computing technique should make the Fourier data reduction and analysis much more facile than in the past, although. Also on the positive side for Fourier diffraction is the projected instrument cost, since the cost of the sophisticated Fourier electronics is largely offset by the absence of a long neutron guide. On the negative side is the presence of an intense correlation background, which would hamper the observation of weak peaks next to stronger reflections. This effect is particularly severe in the case of the proposed ESS long-pulse source, since the 2.5 msec pulse width is 7 times larger than for the Dubna reactor. Another option to be considered for this type of machine is a coupled moderator, which would have a higher peak brilliance and a narrower peak width.

## Final considerations

### *Preliminary assessments*

- Given the choice, the 50Hz target is always better than the 10Hz one. However, locating a number of instruments on the 10Hz target would only result in a minor loss in flexibility.
- The poisoned de-coupled H<sub>2</sub>O and unpoisoned de-coupled H<sub>2</sub> moderators are the likely first choices for structural and magnetic work, respectively. At high resolution, the poisoned H<sub>2</sub> moderator is ideal for both fields.
- We dearly miss a truly sharp cold moderator, especially for crystallography requiring high and low Q at the same time.
- The long-pulse target is not a priority for powder diffraction. However, if it is built, a cold variable-resolution diffractometer and a Fourier diffractometer should be considered as the most promising choices.

### *General considerations*

If the choice of abandoning the 10Hz target is made, this would result in an enormous pressure onto the 50Hz target. Most likely, of the instruments originally assigned to the 10Hz target, only 50% or less will have the long-pulse target as their first choice. In particular, the 50Hz target would be the first choice for all the powder (and, probably, single-crystal) diffractometers. Even assuming that some of the instrument originally on the 50Hz would shift to the long-pulse target, this is likely to create a problem. In a sense, this is unavoidable, if one's goal is to widen the scientific breath of ESS from being a "super-ISIS" to combining this with a "super-ILL" role. However, the powder diffraction community should be swift in looking after its interests (which, in this scenario, will be threatened) as well as the needs of the broader community.

***Attention should be paid to the overall availability of beam port suitable for powder diffraction. Choice of a long-pulse target will have a profound influence on the overall balance.***

## References

- [1] S. Ikeda and J. M. Carpenter, Nucl. Instr. and Methods in Phys. Res. A **239** (1985) 536-544.
- [2] W.G. Williams, R.M. Ibberson, P.Day and J.E. Enderby, Physica B **241-243** (1998) 234-236.
- [3] The Europeand Spallation Source Study – Volume III: The ESS Technical Study, ESS-96-53-M, November 1996.
- [4] J.A. Stride, D. Wechsler, F. Mezei and H.-J. Bleif, “Powder Diffraction on a Long Pulse Spallation Source, Nucl. Instr. and Methods in Phys. Res. in Press.
- [5] V.L. Aksenov, A.M. Balagurov and V.A. Trounov, J. Neutron Research Vol. **6** (1997) 135-148.



# Materials Science and Engineering Instruments

**M.R. Daymond<sup>1</sup>, P.J. Withers<sup>2</sup> and E. Lehmann<sup>3</sup>**

<sup>1</sup>ISIS Facility, Rutherford Appleton Lab., Chilton, Didcot, Oxon., OX11 0QX, UK

<sup>2</sup>Manchester Materials Science Centre, The University of Manchester and UMIST, Grosvenor Street, Manchester, M1 7HS, UK

<sup>3</sup>Paul Scherrer Institut, Villigen, CH-5232, Switzerland

This document considers instrumentation requirements for Engineering Diffractometers and for a Radiography/Tomography station at the ESS. Substantial gains are possible in performance for an Engineering Diffractometer for Strain Measurement at the ESS, compared with either existing reactor or pulsed sources. In the case of an optimally designed engineering strain scanner the overriding requirement of the instrument is the accurate measurement of a lattice parameter,  $d_{hkl}$ , at a known location within the material under study. The instrument is thus essentially a powder diffractometer, modified to meet these specific requirements. Secondary issues include the requirement for considerable space and flexible setup around the instrument to allow for large samples and complicated sample environments.

Gain over existing instrumentation is of the order of 30-60 over instrumentation presently under construction at ISIS and ILL, and from 50-600 over presently operational instrumentation, depending on type of experiment.

The Engineering diffractometer would require a high resolution moderator (decoupled / poisoned). It is felt that neither the proposed H<sub>2</sub> or H<sub>2</sub>O moderator options so far presented fully met the needs of a strain measurement diffractometer, and that the possibility of obtaining higher resolutions using methane or hybrid moderators should be investigated. Further gains in performance could then be achieved.

Such an instrument would ideally be situated on the 50Hz short pulse (SP) target. It would lose considerable flexibility and some performance in operating on the 10Hz SP target described. An instrument could be built on the long pulse target, running in a 'reactor mode' with a monochromator, but there would be a reduction in range and performance. Gains for an ESS traditional radiography instrument compared with siting a traditional radiography instrument at ILL are negligible. However Bragg edge radiography would allow totally new types of science which are unfeasible on a reactor source.

## Introduction - Engineering Diffractometer:

Not long after the publication of the Bragg equation in 1912 the potential of diffraction based techniques for the measurement of lattice strain ( $\epsilon_{hkl}$ ) was appreciated [1]. The measurement of stress with neutrons has grown in importance over the last decade, with the European academic community taking a lead in this development. This has led to the construction of dedicated stress measurement diffractometers at many neutron facilities. Industrial interest and usage has grown similarly as it has become clear that the technique has matured. This is evidenced by an ISO international standard, developed under the Versailles Project on Advanced Materials and Standards (VAMAS) Technical Working Area 20, for stress measurement using neutrons [2] which is presently in draft form, with initial issue expected in 2001/2.

Two broad classes of experiment make use of these techniques, on a wide range of structural materials. Firstly, measurement of changes in lattice separation as a function of position within an actual component provide maps of the stresses remaining after production, joining or use. Such residual stresses affect fatigue resistance, fracture toughness and strength of materials, and hence influence safety, component lifetime, costs and speed of the design cycle. The second class of experiments studies the effect of stress, temperature and other environmental variables on the deformation of materials, thus providing a fundamental understanding of the mechanics of materials. Both types of experiments provide information for process modelling, and materials development.

Irrespective of the source or method, accurate strain or stress measurement thus relies upon the accurate location of diffraction peaks, in order to determine the lattice parameter. Secondly, in many experiments, this must be carried out at a precisely known position within the sample. Finally, many engineering materials must operate at considerable stresses or temperatures, and the modern engineering diffractometer must have the capability of applying realistic environmental variables to samples *in situ*. This is likely to become more important in the future as the drive to optimise processing parameters requires the investigation of material production routes (e.g. rolling) *in situ*.

**Strong European academic community**

**Growing industrial usage**

**Draft ISO / CEN standards submitted.**

## Instrument Optimisation - Engineering Diffractometer:

In the case of an optimally designed engineering strain scanner the overriding requirement of the instrument is the accurate measurement of a lattice parameter,  $d_{hkl}$ , at a known location within the material under study. To enable different instruments to be compared it is reasonable to define a FOM such that an increase of a factor of two in the source illuminating an instrument results in a factor of two increase in the FOM. It is also necessary to take into account the uncertainty of the result obtained. Hence the most useful high-level definition of a FOM for a strain measuring instrument will be '*the inverse of the time taken to measure a d-spacing to a given uncertainty*'.

d-spacings are obtained from the observed diffraction patterns by a 'least-squares' fitting procedure, and it has been shown by Sivia [3] that in the situation of an isolated Gaussian peak the time (t) taken to measure (with an uncertainty of  $\sigma$ ) the position of a peak is:

$$t \propto w^2 / I \sigma^2 \quad (1)$$

where  $w$  is the width of the peak, and  $I$  the (integrated) intensity within the peak recorded in unit time. Hence the FOM required for an instrument concerned solely with measuring the peak position may be written :

$$\text{FOM} = I \sigma^2 / w^2 \quad (2)$$

if the peaks were Gaussian in shape and well separated. The correctness of equation 2 when an *arbitrary* not necessarily symmetric peak shape is fitted by the least squares method is derived in [4]. The veracity of this result has also been demonstrated empirically, using experimental data from a number of sources and on a number of different materials [5].

It is further possible to include the effect of background in the optimisation [6]:

$$\text{FOM} \approx I \sigma^2 / (w^2 (1 + 2 B/P)) \quad (3)$$

where  $P$  is the peak height, and  $B$  the background signal.

A number of assumptions can be made to make full use of this expression in instrument design. These include matching of instrument resolution terms, an expression for the number of diffracting peaks in a given wavelength window (which is material dependent), intensity losses with distance, and a simple form for the incident intensity spectrum. Carrying out this calculation [4] produces the FOM shown in Figure 1 as a function of primary flight path. This clearly demonstrates the requirement for a 40-60m flight path instrument, somewhat of a departure from the philosophy of existing engineering instruments. However, it should be noted that the calculation above does not include contributions from sample resolution. When this constraint and a 50Hz running option is

**Background can be included in the Figure of Merit.**

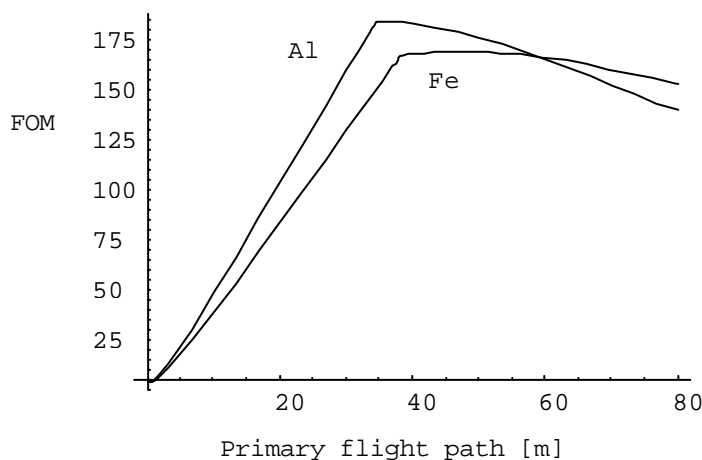


**Fig.1:** Figure of Merit as a function of primary flight path for 25Hz source [4], ignoring sample broadening contribution, for aluminium and iron.

included in [4], the optimum instrument instead has a primary flightpath ~50m, with the added requirement of tuneable resolution, i.e. the option to gain flux by coarsening the horizontal resolution. A number of scenarios can be imagined for achieving this flexibility, for instance by allowing the final sections of flight path to switch between guide and absorber [7].

The explosion of interest and demand for neutron strain measurement diffractometers has led to the construction of several new dedicated and optimised instruments at this time (early 2001). While specific design details follow from Monte Carlo modelling of the complete instrument with its particular source, all the 2<sup>nd</sup> generation strain diffractometers presently under construction or in the design phase make use of these ideas to a greater or lesser degree (at LANSCE, ISIS, ILL and SNS). The ESS instrument will be highly competitive with these instruments, not only because of the massively improved source, but also because of the further lessons which will be learnt over the next two to three years as these new instruments are commissioned.

### **Instrument Design - Engineering Diffractometer:**

Based on the arguments above, the optimum instrument requires

- a variable resolution, from medium to high,
- a moderately large detector array centred on  $\vartheta = 90^\circ$  with resolution matched to the best case intrinsic resolution
- backscattering and transmission detectors
- a variable gauge volume and
- at least 1-2m<sup>3</sup> space for large components and sample environments.

These requirements can only be properly achieved with a dedicated instrument, i.e. a shared powder diffractometer beamline will require unacceptable compromises for both engineering and powder diffraction communities. The optimised instrument would have a 50m flight path, with frame definition choppers at 6 and 9m, and curved with a 5km radius from 10m to 37m. Guide (m=3+) extends from within the primary shutter (~4m) to 48.5m (i.e. within 1.5m of the sample position). The top and bottom of the guide will always be in place [8], but the sides of the guide will be switchable for absorbing material from 38m to 48.5m. This allows horizontal divergence (and hence instrument resolution) to be improved, at the expense of neutron flux, 'tuning' the instrument resolution to match the sample resolution in order to maximise performance, as judged by the FOM (Eq. 3). Achievable resolution in the 90° detector banks would be  $\Delta d/d \sim 2 \times 10^{-3}$  to  $7 \times 10^{-3}$ . The wavelength window would be ~1.5Å at 50Hz, corresponding to a lattice parameter window of ~1Å in the 90° detectors.

Based on the criteria of Eq. 3, the instrument will perform ~30 times better than best in class instruments presently under construction, and 50-300 times compared to existing instruments. By including backscattering and transmission detectors, and extending the main detector banks, extra strain components will be obtained for some types of experiments allowing rapid mapping of strain tensors. While only providing improvements in some types of

#### ***Main components of the instrument***

- ***Large 90° detector array***
- ***Tuneable resolution***
- ***Variable gauge volume***
- ***Backscattering and transmission detectors***
- ***Large, flexible sample space***

#### ***Parameters of the instrument***

- ***50m curved flight path***
- ***Frame definition choppers***
- ***Swappable m=3 guide / absorber for end section***

#### ***Performance of the instrument***

- ***Resolution  $\Delta d/d \sim 2 \times 10^{-3}$***
- ***d-spacing window ~1Å at 90° and 50Hz***
- ***FOM x30 compared to best in class under construction***
- ***FOM x 90 for some experiments***

experiment, this would improve performance by a further factor of 2 to 3.

On the 50Hz source, the flexibility exists to run the instrument at 50, 25 and 16.6Hz – all options which would be used depending on the material and type of experiment. If moved to the 10Hz source, this flexibility would be lost, without any concurrent gain in flux (such as would be achievable on the planned ISIS 10Hz target). While the instrument (moved to a ~80m primary flight path) could be built on the 10Hz target, it would suffer around a 1/3 performance for the majority of experiments compared with siting on the 50Hz target. The long pulse (LP) target could be used, running with a monochromator, but would provide poor performance for this instrument.

The instrument requires a high resolution moderator, hence a thermal, decoupled / poisoned moderator is appropriate. It is felt that neither the  $H_2$  or  $H_2O$  moderator options so far proposed fully meet the needs of a strain measurement diffractometer; the best case moderator provides a pulse nearly twice as wide as achievable with the ISIS  $CH_4$  moderator. Hence the possibility of obtaining higher resolutions using methane or hybrid moderators should be investigated for ESS. Further gains in performance could be achieved under this scenario.

### **Technical feasibility - Engineering Diffractometer:**

The instrument is highly feasible. The novel feature is the requirement for a tuneable resolution diffractometer, however the engineering requirements for accurate switching of guide/absorber sections is certainly achievable.

Further gains can be envisaged from future improvement in performance of high  $m$  guides, improvements in detector efficiency and use of in-shutter guides. It is likely that experience gained in the commissioning of the 2<sup>nd</sup> generation instruments presently under construction will influence the detailed design of this instrument, though not the main features of the design.

Finally, considerable opportunities and improvement in throughput and achievable science, will be available with improvements in experimental setup (use of coordinate measurement machines), advanced sample environments and development of integrated software.

### **Radiography / Tomography station:**

The primary requirements for traditional radiography are for high thermal or cold neutron flux, with a reasonably parallel beam. However, there is the considerable potential advantage while doing radiography on the 50Hz SP target of carrying out Bragg edge discrimination during radiography measurements, allowing simultaneous identification of the material present.

Gains for an ESS traditional radiography instrument compared with siting a traditional radiography instrument at ILL are negligible. However Bragg edge radiography would allow totally new types of science which are unfeasible on a reactor source. Gains compared to an ISIS Bragg edge radiography instrument would be 30.

*Preferred target is 50Hz short pulse.*

*10Hz target is possible, with loss of performance. Long pulse target not suitable.*

*Requires sharp thermal moderator.*

*Options such as methane or hybrid moderators should be investigated.*

*Instrument is feasible with present technology.*

*New type of science possible at ESS source.*

*50Hz SP or LP target and high flux moderator useable for traditional radiography*

*50Hz SP target and moderate resolution moderator required for Bragg edge radiography*

For traditional radiography, either 50Hz SP or LP targets would be appropriate, using an intensity optimized moderator (cold or thermal). For Bragg edge radiography, the 50Hz SP target is required, using a moderate resolution moderator.

### Introduction - Radiography / Tomography station:

Neutrons have been used as a tool for non-destructive evaluation of materials and components for many years. The quality of the images obtained and the sample properties which can be measured depend strongly on the quality of the neutron source and the detector performance and efficiency. One of the main applications of neutron radiographs is the study of materials distribution in macroscopic samples. Due to the neutron cross section of hydrogen it can be measured very precisely, to some mg per g. Thus the study of time and space dependent moisture distribution has been studied in civil engineering, biology and hydraulic engineering. Further, hydrogen in materials is of much more widespread interest, for instance in the investigation of adhesive joints or the precipitation of hydrides.

The high depth penetration of neutrons even in heavy materials makes it highly relevant to industrial applications, in particular the monitoring of internal defects in components. It is these two areas, monitoring of hydrogen in materials, and viewing of defects in components that neutron radiography has been most utilised.

An added benefit is provided when carrying out radiography at a pulsed neutron source. In crystalline solids the coherent neutron scattering cross section varies abruptly at the 'Bragg edge' (Fig. 2). Since the spacings of the Bragg edges are characteristic of a diffraction pattern of the material, one can imagine making measurements at energies above and below major Bragg edges, providing radiographs in which material show up with different scattering intensities, thus helping to selectively identify the

***Use of information from Bragg edges, combined with traditional radiography, would provide a unique facility, exploring new areas of science.***

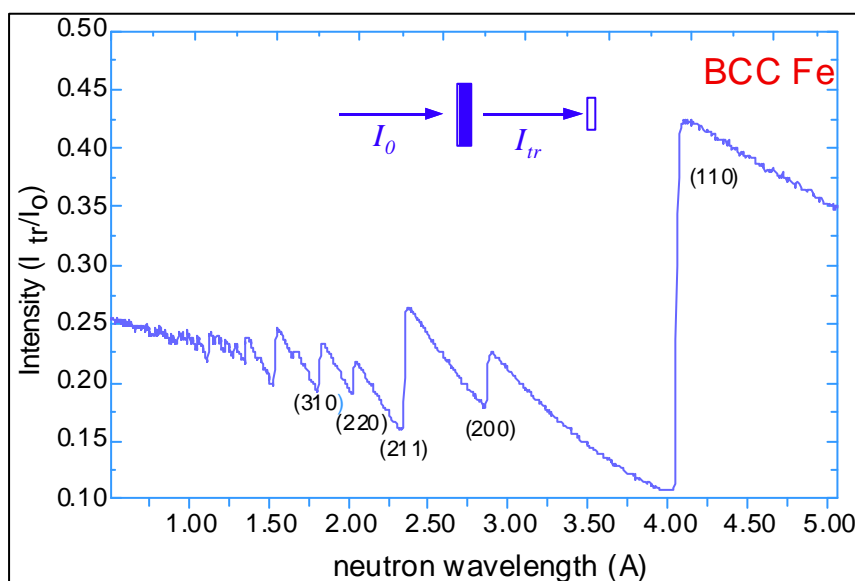


**Fig. 2:** Spectrum of transmitted intensity through bcc iron, showing clear Bragg edge spectrum.

distribution of particular phases. Further, if a true Bragg edge diffraction pattern could be collected with both the fine spatial and time resolution required, true 3D maps could be produced of both phase and stress.

### **Instrument Design - Radiography / Tomography station:**

A detailed design study of this instrument has not been carried out, however the following aspects are noted:

- Depending on the type of experiment, the spatial resolution (pixel size) required for radiography varies between 0.02mm and 0.2mm, with typically requested sizes of 0.05mm to 0.1mm. Active areas of 20mm x20mm to 250mm x250mm are used, again dependent on the type of science.
- The instrument characteristics, most importantly beam divergence, must match these requirements. It is possible to achieve the required divergence either by extending the flight path, or through the use of soller type collimation.
- Many detector systems are sensitive to fast neutrons and gamma rays. The use of a t0 chopper or curved guides followed by soller collimation needs to be considered.
- The instrument requires space for manipulation and rotation of samples, variable sample-detector distance and variable incident beam size/divergence.
- Traditional radiography requires only high total flux (in either the thermal or cold neutron range, dependent on type of science). Hence the 50Hz SP or LP targets are both acceptable, using high flux moderators. The gain in performance compared with constructing such an instrument at the ILL however, is small.
- Bragg edge radiography has been proved in concept, but to become truly feasible and useful it will require detector developments.

Phase specific radiography / tomography would provide a unique facility at the ESS. This technique is not presently possible, and to be truly useful requires the high pulsed fluxes which will be achieved at the ESS. At least moderate resolution in the pulse shape would be required; the decoupled hydrogen moderator is a good choice. The instrument would require a short flight path combined with soller collimators, to allow both a large wavelength window and the highly parallel beam required for high spatial resolution.

### **Technical feasibility- Radiography / Tomography:**

The instrument is highly feasible in its simplest form. To take advantage of the pulsed nature of the source, detector developments are required.

In the past few years a number of detector developments have been made, providing high sensitivity detectors with good dynamic range and linearity, in the fields of imaging plates and scintillator screen-CCD cameras. These detectors are limited in their readout

#### ***Traditional radiography***

- ***15 – 50m flight path***
- ***50Hz SP or LP targets***
- ***High flux thermal or cold moderators***

#### ***Bragg edge radiography***

- ***New science***
- ***15m flight path***
- ***Soller collimation***
- ***50Hz SP target***
- ***Moderate resolution thermal moderator***

***Traditional radiography / tomography is technically feasible now.***

***Bragg edge radiography /tomography requires detector development, thought to be achievable in 5 year time frame.***

speed and are sensitive to gamma radiation. However, it is newly emerging technologies which hold great promise; amorphous silicon arrays and micro-strip gas counters.

With rapid readouts and fast data acquisition, the step from neutron radiography to neutron tomography becomes feasible, allowing a 3D reconstruction of the object, providing far greater spatial sensitivity. The software and techniques for combining multiple radiographs to produce tomographs are well established from work in the x-ray community.

### References:

- [1] H. H. Lester and R. M. Aborn, *Army Ordnance* **120**, 200 (1925).
- [2] G. A. Webster ed., VAMAS Report No. 38, (2000).
- [3] D. S. Sivia, *Data Analysis - A Bayesian Tutorial* (Oxford University Press, 1996).
- [4] M. W. Johnson and M. R. Daymond, submitted *J. Appl. Cryst.* (2001).
- [5] L. Edwards, M. E. Fitzpatrick, M. R. Daymond, *et al.*, in *Int. Conf. on Residual Stress VI*, Oxford, (2000).
- [6] M. R. Daymond and M. W. Johnson, in *ICANS-XV*, Tsukuba, Japan, (2000).
- [7] X.-L. Wang, SNS Report no. IS-1.1.8.2-6035-RE-A-00, (2000).
- [8] M. W. Johnson, L. Edwards, and P. J. Withers, *Physica B: Condensed Matter* **234-236**, 1141 (1997).

# Reflectometry instruments

H. Fritzsche<sup>1</sup>, C. Fermon<sup>2</sup>

<sup>1</sup>Hahn-Meitner-Institut, Glienicker Str. 100, 14109 Berlin, Germany

<sup>2</sup>Laboratoire Léon Brillouin, C. E. A. Saclay, 91191 Gif sur Yvette, France

We investigated the performance of a reflectometer for non-magnetic samples in a  $q$ -range from 0.01 to 0.5  $\text{\AA}^{-1}$  at a reactor source and a spallation source for a set of wavelength resolutions ranging from 1% to 8%. We considered an ambient water and liquid hydrogen moderator with different characteristics (coupled, decoupled poisoned, decoupled unpoisoned) at the three different target stations, which are currently under discussion for the planned ESS. The performed simulations show that the performance of a reflectometer is roughly proportional to the power of the source. Therefore the coupled cold moderator together with the most powerful target station (5MW short pulse or 5MW long pulse) is the best choice for reflectometry. The 50Hz short pulse spallation source (SPSS) is the first choice for high resolution and the 16.6Hz long pulse spallation source (LPSS) is the first choice for high intensity. The performance gain is about 100 compared to a reflectometer at ISIS. This is due to the higher power (factor 33) and the usage of a coupled moderator (at least a factor of 3) and about a factor of 15 compared to ILL for high intensity.

In order to have optimized parameters for all reflectometry experiments we recommend to build two reflectometers: a high-resolution reflectometer at the 50Hz SPSS and a high-intensity reflectometer at the LPSS.

## Basic instrument design criteria

The reflectometer is designed to measure small angle reflectivities down to  $10^{-8}$  in a  $q$ -range up to 0.5  $\text{\AA}^{-1}$  for solid and liquid samples.

There are two basic parameters which have to be determined for the design of a reflectometer: the length of the instrument and the usable wavelength band.

The fundamental relation between neutron velocity  $v$ , wavelength  $\lambda$ , time of flight  $T$  and distance  $D$  between source and detector is:

$$v = \frac{D}{T} = \frac{h}{m \lambda} \quad (1).$$

The resolution  $r$  is defined as:

$$r = \frac{\Delta \lambda}{\lambda} = \frac{t}{T} \quad (2)$$

with the pulse length  $t$ , which is just the uncertainty  $\Delta T$  of the time of flight  $T$ .

If one wants to have a definite resolution, the distance be-

**reflectivities down to  $10^{-8}$**

**$q$ -range up to 0.5  $\text{\AA}^{-1}$**

tween source and detector should be:

$$D = \frac{Th}{m\mathbf{l}} = \frac{th}{rm\mathbf{l}} = \frac{h}{m} \frac{t}{r\mathbf{l}} \quad (3)$$

For an optimum data acquisition time  $dT$ , i.e.  $dT=1/f$ , the optimum acceptable wavelength band  $\delta\lambda_{opt}$  is given by:

$$d\mathbf{l}_{opt} = \frac{h}{mD} (dT - t) = \frac{h}{mD} \left( \frac{1}{f} - t \right) \quad (4)$$

For a wavelength of  $\lambda = 3 \text{ \AA}$  and a resolution of 3% an instrument length of 88 m is needed for the LPSS, whereas 12m are enough at the SPSS. The usable wavelength band is 2.6  $\text{\AA}$  for the LPSS, 6.5  $\text{\AA}$  for the 50Hz SPSS and 33  $\text{\AA}$  for the 10Hz SPSS. From equations (3) and (4) the basic design criteria for a reflectometer at a pulsed neutron source are quite obvious. Comparing the short pulse spallation source (SPSS) and the long pulse spallation source (LPSS) the instrument at the LPSS needs to be much longer to achieve the same wavelength resolution because of the longer pulse width. The reflectometer at the 50Hz and 10Hz SPSS needs the same length of the instrument but the usable wavelength band is inversely proportional to the source frequency and hence, the 10Hz source has a five times larger usable bandwidth. For the SPSS setup the frame definition is realized by putting supermirrors into the neutron beam, whereas for the LPSS setup a chopper system is used.

**length of instrument is proportional to the pulse length and inversely proportional to the wanted resolution**

**usable wavelength band is inversely proportional to repetition rate and pulse length**

## Moderator assessment

As can be concluded from the above section only the pulse width but not the exact pulse shape is important. Therefore the best moderator for neutron reflectometry is the one which delivers the highest flux, i.e. the coupled moderator. A point of discussion is whether an ambient water or a liquid hydrogen moderator is preferable. To answer that question one has to consider not only the incoming intensity but the reflected intensity as a function of scattering angle  $\theta$  and scattering vector  $q$ :

$$q = \frac{4p}{\mathbf{l}} \sin \theta \quad (5)$$

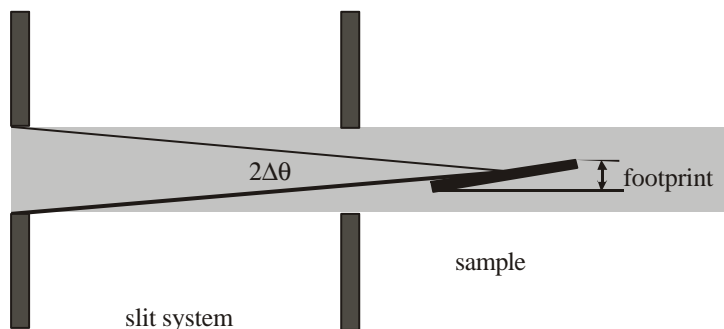


**Fig. 1:** Collimation in a reflectometer set-up.

As can be seen in Fig. 1 the reflected intensity  $R$  is proportional to the incoming intensity  $I_0$  times the opening of the first

slit (or the angular resolution  $\Delta\theta$ ) times the sample footprint which is proportional to the sample length  $L$  times  $\sin\theta$ . For a fixed  $q$ -value  $\sin(\theta)$  as well as  $\Delta\theta$  are proportional to  $\lambda$ . Therefore we get the following expression for the reflected intensity  $R_q$  at a fixed  $q$ -value:

$$R_q \propto I_0(\mathbf{l})\Delta\mathbf{q} \cdot L \sin \mathbf{q} \propto I_0(\mathbf{l}) \cdot \mathbf{l}^2 \quad (6) .$$

**reflected intensity is proportional to  $\mathbf{l}^2$**

In Fig. 2 the moderator flux multiplied by  $\lambda^2$  is displayed. Typically a bandwidth larger than  $3 \text{ \AA}$  is used at a spallation source. Hence, the liquid hydrogen coupled moderator is the best for neutron reflectometry as it provides the highest integrated flux.

**coupled cold moderator is best for reflectometry**

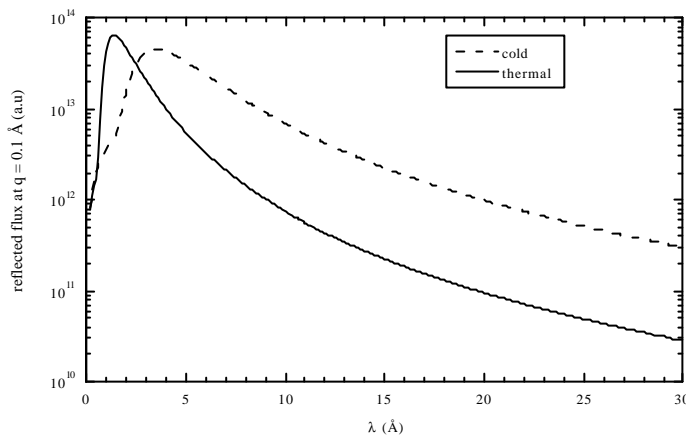


**Fig. 2::** Reflected neutron flux at a fixed  $q$ -value for a coupled ambient water moderator (solid line) and a coupled liquid hydrogen moderator (dashed line)

## Assessment of target stations

### a) 5MW at 50Hz versus 1MW at 10Hz

As discussed above the source parameters define the usable wavelength band. The lower the source frequency the larger the usable wavelength band and hence, the larger the total intensity. But because of the Maxwellian distribution only a band of few Angstroms give valuable information – the other wavelengths give only a minor contribution to the intensity. Therefore a scan at three different angles with a shorter wavelength band might be more effective than the data acquisition at a fixed angle of incidence using a large wavelength band. To quantify that consideration we performed MC-simulations with the software package VITESS [1] comparing a 5MW SPSS running at 50Hz with a 1MW SPSS at 10Hz. For the 10Hz target the sample was held at a fixed angle of  $2.6^\circ$ , whereas for the 50Hz target we took three different angles of incidence:  $0.5^\circ$ ,  $1^\circ$ , and  $2.6^\circ$ . In order to compare the flux at the same resolution we

- (i) changed the slit size to keep the angular resolution  $\Delta\theta/\theta$  constant

- (ii) performed a data binning proportional to the inverse of the time of flight or proportional to  $\lambda$ , respectively, to keep the wavelength resolution  $\Delta\lambda/\lambda$  constant.

Fig. 3 shows the reflected neutron flux from a D<sub>2</sub>O-surface. The reflectivity curve was simulated using the Parratt-formalism [2]. It can be clearly seen that the 50Hz source with three angles of incidence can cover the same q-range as the 10Hz source with a fixed angle of incidence. To calculate the performance we calculated the time which is needed to get the same statistics. The slit openings were adjusted for each scattering angle in order to have the same angular resolution at all q-values. For the 10Hz source it takes a factor of 4.4 longer to acquire the reflectivity curve with the same statistics. The q-dependence of the reflected intensity is displayed in Fig. 3. There is no influence of the resolution on the performance and the SPSS with 5MW at 50Hz performs 4.4 times better than a SPSS with 1MW at 10Hz.

**a 5MW source at 50Hz performs 4.4 times better than a 1MW source at 10Hz**

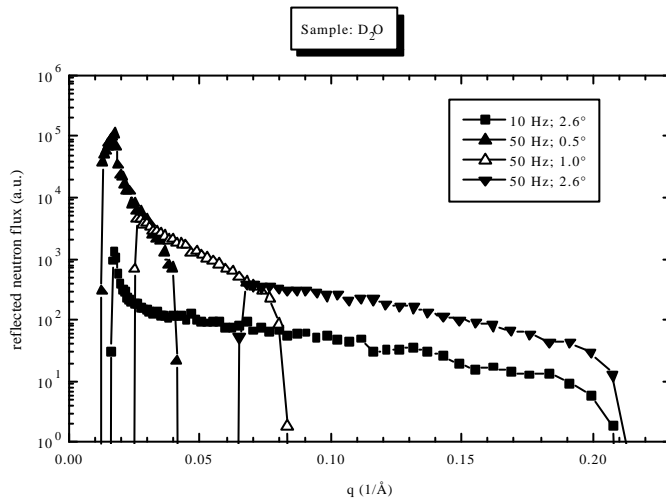


**Fig. 3:** Comparison of the reflected neutron flux from a 50 Hz SPSS and 10 Hz SPSS taking into account a D<sub>2</sub>O-surface as sample.

**b) SPSS versus LPSS**

Because of the smaller wavelength band used at the LPSS one needs more angles to measure the whole reflectivity curve. Instead of three different angles one needs five angles of incidence at a LPSS to cover the same q-range. The performance depends on the resolution. The SPSS performs better for high resolution whereas a LPSS performs better for high intensity or low resolution, respectively.

**high resolution:  
SPSS performs better.**

**low resolution:  
LPSS performs better.**

The simulations performed by C. Fermon are in reasonable agreement with the VITESS-simulations.

**a 5MW LPSS or a 5MW SPSS at 50Hz performs always better than a 1MW SPSS at 10Hz.**

The conclusion is that the performance of a reflectometer is roughly proportional to the moderator brightness as already stated in a detailed study of M. Fitzsimmons [3]. The estimated gain factors are listed in the instrument performance sheet. In order to have the best performance for high and low resolu-

tion we recommend to build a high-**resolution** reflectometer at the 50Hz SPSS and a high-**intensity** reflectometer at the 16.6Hz LPSS.

### Comparison to existing sources

A reflectometer at a 5MW 50Hz ESS-target station at the coupled cold moderator would perform about a factor of  $> 100$  better than the same reflectometer at ISIS. The flux gain because of the higher power is 33 and the flux gain because of the coupled moderator is at least 3. Simulation results show a factor 10-20 source intensity gain for the 5MW stations compared to ILL, somewhat depending on wavelength resolution.

***the source performance gain compared to ISIS is about 100***

### Technical issues

For both kinds of samples (solid and liquid) there is a need for an optimized reflectometer operating at high intensity as well as high resolution. Therefore, we recommend to build one reflectometer at the SPSS at 50Hz (high resolution) and one reflectometer at the LPSS (high intensity). Both reflectometers should provide polarized neutrons, either to investigate magnetic properties or to reduce the incoherent background of organic samples.

***high resolution reflectometer at the 50Hz SPSS***

***high intensity reflectometer at the LPSS***

As shown in the simulations experiments on liquid samples can gain a lot in performance when using different angles of incidence instead of using a broad wavelength band. The problems of calibration can be overcome as demonstrated e.g. at IPNS. A nice idea was presented for the new liquids reflectometer at SNS to realize the different angles of incidence by benefiting from the divergence of the neutron guide.

***both reflectometers with a polarized neutron option***

The 10Hz repetition offers the largest  $q$  range at a single angle of incidence, together with good wavelength resolution. This is advantageous for kinetic experiments. The same  $q$  range can be achieved at the 50Hz by using several angles of incidence. For kinetic experiments a fast switching between different angles (within a small fraction of a sec) needs to be realized.

### References

- [1] D. Wechsler, G. Zsigmond F. Streffer, and F. Mezei, Neutron News 11, 25 (2000).
- [2] L. G. Parratt, Phys. Rev. 95, 359 (1954)
- [3] M. R. Fitzsimmons, Nucl. Instr. and Meth. in Phys. Res. A 383, 549 (1996)

# SANS Instruments

**R.K.Heenan<sup>1</sup>, R.Cubitt<sup>2</sup>, K.Mortensen<sup>3</sup>, D.Schwahn<sup>4</sup>, A.Wiedenmann<sup>5</sup>, F.Mezei<sup>5</sup>.**

<sup>1</sup>ISIS Facility, Rutherford Appleton Laboratory, Chilton, Didcot, Oxfordshire OX11 0QX, United Kingdom

<sup>2</sup>Institute Laue Langevin, 6 Rue Jules Horowitz, BP 156, 38042 Grenoble, Cedex 9, France

<sup>3</sup>Risø National Laboratory, P.O. 49, 4000 Roskilde, Denmark

<sup>4</sup>IFF, Forschungszentrum Jülich, 52425 Jülich, Germany

<sup>5</sup>Hahn-Meitner-Institut, Glienicker Str. 100, 14109 Berlin, Germany

Small angle neutron scattering is a well established technique to examine structures on a distance scale of say 10 to 1000 Å. SANS was initially developed at fixed wavelength reactor sources and for detector-sample distances mainly between 1 and 20m. The advantages of pulsed source SANS using white beam, time-of-flight have not yet been widely appreciated, despite the presence of several good instruments on existing pulsed sources. For historical reasons these existing instruments have relatively short, fixed, flight paths. The key feature of SANS at the ESS is to be able to build flexible instruments with movable detectors that will allow an optimisation of Q range, count rate and Q resolution on an experiment by experiment basis. At lower pulse repetition rates time of flight allows a wide simultaneous Q range at a single setting of the instrument, suited to dynamic or anisotropic systems. At higher repetition rates considerably greater count rates may be achieved over a more limited Q range, with the detector being moved similar to present reactor instruments or perhaps the wavelength band changed in order to expand the Q range.

All three ESS neutron sources under discussion (50Hz, ~5MW; 10Hz ~1MW, and 16.6Hz long pulse ~5MW) would be suitable for SANS, and would in many aspects be superior to D22 at the ILL which is presently the best SANS instrument in the world. As illustrated below the 16.6Hz long pulse plus the 50Hz ~5Mw should be the best choice for the two target stations provided one also considers operation at sub-multiples of 50Hz for a wider simultaneous Q range.

Significant new experimental opportunities for SANS will arise with count rates up to an order of magnitude higher than presently available, wider simultaneous Q ranges and improved Q resolution.

It has been assumed in our discussions that a coupled hydrogen moderator on a 5MW ESS target has the same time averaged spectrum as the ILL cold source and that the effect of neutron guides and/or benders would be the same in each case.

**Future clarification of engineering details, such as the optimisation of neutron output for given target power and moderator layout might alter the outcome of the discussion here.**

## Key features of pulsed source SANS

Given similar time averaged moderator spectra, the ESS pulsed source has count rate gains of a few up to ~10 times D22 at the ILL the current world best. This may be achieved at lower pulse repetition rate by simultaneously using more of the spectrum OR at higher repetition rates with a smaller wavelength band and smaller Q range. These potential gains will provide new experimental opportunities for SANS.

Single "figure of merit" comparison of ESS SANS with reactor SANS is NOT possible – neutrons are used in different ways - conclusions depend on the system under study and the science involved. We present (Fig. 3 and 4) counts at a given Q for a notional "flat scatterer" rather than a simple "flux at sample at a given  $\lambda$ " as used on reactors. Since many scatterers fall off steeply with Q, the pulsed source puts relatively more counts where signals are weaker.

Some experiments need to optimise the instrument for highest flux in a given Q-range, other experiments might optimise for highest resolution ( $\delta Q/Q$ ), and others may optimise for maximum available Q-range, even using the low-flux limits. A flexible instrument, "looking like D22" with as a *minimum requirement* a ~1m square detector moving from say 2m to 20m in a vacuum tank, in order to optimise  $\lambda$  range, Q range, and geometric resolution to suit particular experiments, e.g. only neutrons  $\lambda > 4$  or 5 Å might be used with crystalline materials, above the Bragg cut-off, or when polarized neutrons are used. Dynamical studies require a large Q range in a single shot. Incident collimation will require choppers to select wavelengths and remove frame overlap (out to  $\lambda \sim 30$  Å) as well as the usual movable guide sections to change collimation length. The figures below illustrate two instrumental set-ups with the sample at 21m (relatively far out, which suits the long pulse) and a detector at two extremes, 23m and 36m ( $\lambda_{\text{max}} \sim 11$  Å at 10Hz).

If the use of a guide/bender and sufficiently good shielding allows operation at sub-multiples of 50Hz for wider simultaneous Q ranges, then the 16.6Hz long pulse and the 50Hz ~5MW sources might be the best scenario for the two target stations.

In many experiments a wide simultaneous Q range in a single measurement, by using a broad range of  $\lambda$  will be important. The wider Q range offered by the pulsed source will present new scientific opportunities for anisotropic scatterers, systems undergoing dynamic change and increasingly more complex multi-component samples. In such cases not having to move the detector improves the overall experiment quality. Data are well suited to model fitting or Fourier transform methods.

***Best in world count rates.***

***New opportunities for SANS experiments.***

***Simple comparison with reactor generally not possible.***

***Flexible instrumentation.***

***SANS possible on all proposed ESS sources.***

***Wide simultaneous Q range - suits complex experiments & data fitting.***

SANS instruments can be proposed to give improved Q resolution ( $\delta Q/Q$ ) over that given by a typical velocity selector on a reactor. This will improve data for "peaks" - in lamellar phases, membranes, flux line lattice etc., and "wiggles" - detailed investigation of interfacial structures etc. by contrast variation, many of which are resolution limited at current reactor sources.

***Improved Q resolution.***

A coupled cold moderator is preferred for highest flux. The longer time constants of coupled moderators do not unduly degrade Q resolution (except for very short flight paths at short  $\lambda$ ).

***Coupled cold moderator.***

A guide/bender is absolutely necessary to remove the instrument from a direct view of the moderator fast neutrons and prompt spike background, to give a  $\lambda_{\min} \sim 2 \text{ \AA}$  (or possibly towards  $1 \text{ \AA}$ , await results at SNS). Fig. 2 shows that the monitor prompt spike at ISIS is >20 times worse on CRISP, even after a  $T_0$  chopper, than on LOQ after a bender.

***Indirect view of moderator is essential.***

Careful attention has to be given to shielding & collimation for a sufficiently good signal/background. Improved flux is most often used to measure smaller scattering cross sections. Many SANS experiments are detector count rate limited; there is an essential need for larger, faster detectors, with good stability and 5 -10mm pixel size.

***Shielding for good signal/background is essential.***

***Faster, larger detectors needed.***

Individual run times will range from tens of seconds to hours. Rapid re-phasing of choppers to combine different data frames might be desirable at 50Hz.

***Rapid chopper re-phase may be useful.***

Generally the available Q range has to be "over specified" due to fall off inherent to pulse sources of the count rate at the extremes of the Q range. Accessible Q of  $0.001$  to  $1.0 \text{ \AA}^{-1}$  is required.

***"Over specify" the Q range.***

## ESS SANS - generic instruments

State of the art instruments would "look like D22 at the ILL", see Figure 1, with a large area detector of high-count rate capability, moving inside a heavily shielded vacuum tank. A 1m x1m multi-wire gas detector is the present best but development of larger and particularly faster detectors is important. The detector should be able to be offset from the beam axis to further enhance Q range when needed. There is no reason other than cost why even with present technologies a still larger detector area and vacuum tank could not be used. (Compare the success in other fields of MAPS and GEM at ISIS with up to 16m<sup>2</sup> of detector!) Having all detectors movable is a key feature, they are far easier to calibrate and normalise, as well as providing flexibility in SANS experiment design. Static "fixed banks at high Q" should be as far as possible avoided.

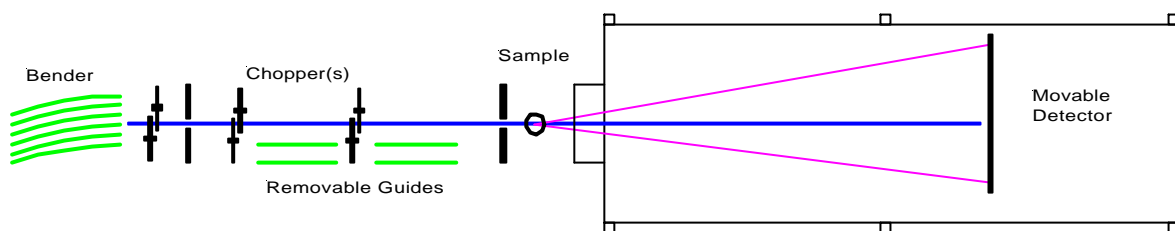


**Fig. 1:** Generic SANS instrument for ESS. Curved guide and/or bender removes beam from direct view of moderator. Large area detector ( at least 1m x1m) moves in vacuum tank, and may be offset sideways. Substantial beam line and vacuum tank shielding will be required.

The incident guide/bender and beam collimation should be designed to provide collimation to match the longest sample-detector distance, with removable guide sections to bring the effective source closer to the sample for shorter sample-detector positions to give the usual  $L_1 = L_2$ . The need to use a curved guide and/or bender to remove fast neutrons, which later moderate inside the instrument, cannot be overstated, and is illustrated in Figure 2. One or more double disc choppers (three at 50Hz) will be needed to define the  $\lambda$  band used from each pulse, to remove frame overlap, and to completely remove pulses to work at lower repetition rates. At long sample-detector distance inelastic scatter, separated by time-of-flight, could further restricts the  $\lambda$  range; neutrons accelerated at the sample arrive very rapidly at the detector, possibly swamping the weaker signal from the end of the previous pulse. Inclusion of short  $\lambda$ , below the Bragg cut-off ( $\sim 4 \text{ \AA}$ ) can cause problems from multiple Bragg scattering and requires care in the use of crystalline materials for beam windows.

A typical configuration might be 6/15/15, a 36m long beam line with 6m guide/bender to remove direct view of moderator, 15m of collimation (plus removable straight guide sections) and finally a 15m vacuum tank. The longer the overall length of the beam line the smaller the  $\lambda$  range available ( $\lambda (\text{\AA}) \sim 4T (\text{msec})/L (\text{m})$ ) but the better is the  $\delta\lambda/\lambda$  resolution, Given sufficient resources a further, shorter beam line (c.f. the old D17 at the ILL) might be attractive (at 50Hz, but not for the long-pulse). At a reactor SANS instrument per-

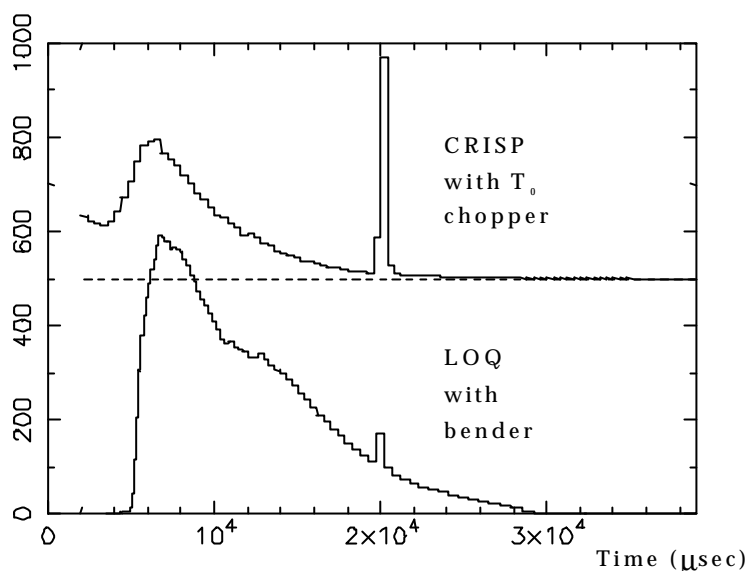


**Fig 2:** ISIS monitor spectra at 25Hz on CRISP reflectometer (displaced) & LOQ at ~10m. LOQ has bender and wavelength selecting chopper ( $\lambda \sim 2-10 \text{ \AA}$ ), CRISP has  $T_0$  chopper (10cm ?) and wavelength selecting chopper. Runs have same length and similar width bins at 20 msec, but scintillator detector types and beam sizes are different. CRISP is probably more efficient at short  $\lambda$  but has lost flux at long  $\lambda$  due to air paths. Despite  $T_0$  chopper CRISP spike makes monitor spectrum (and reflection measurements) impossible. "Prompt pulses" at 20 and 40 msec are *still* significant on LOQ, where note also aluminium Bragg dips due to beam line vacuum windows.

formance can be surmised from the neutron flux of a given wavelength arriving at the sample coupled with the sample-detector distance. On a pulsed source a range of wavelengths arriving at *different* radii on the detector may reach some given Q value, so that comparisons are not straightforward. Thus we compare scattering from a notional "flat scatterer" or some other scattering law as may be appropriate. Even such comparisons are difficult as count rate varies with the inverse fourth power of Q resolution ( $\delta Q/Q$ ) which itself varies inversely with wavelength  $\lambda$ . The Table and Figures below compare some "typical" SANS instrument configurations, which are not necessarily optimal for the individual source repetition rates, but do provide a basis for discussion.

## SANS at 16.6Hz long pulse, ~5MW

The 2msec long pulse time spread forces relatively long beam lines, with no short wavelengths used (which suits Bragg scatterers) in order to give wavelength resolution  $\Delta\lambda_{\text{whm}}/\lambda$  better than the usual ~10%. This broadening also affects incident beam monitor spectra prior to the sample, and alters the band-pass of disc choppers. The data in Figures 3b and 4b show that with suitable compromises in instrument design (long beam line with no short wavelengths) the Q resolution from the long-pulse remains as good as that from the short pulse.

Count rates from the long pulse source are clearly the best due to ~3 times as many neutrons per proton pulse. Overall Q range is about half that at 10Hz and gains at high Q are not so good as the

**Table 1.** Approximate Q ranges for short & long  $L_2$  SANS instrument case studies.

At 23m, $L_2 = 2m$ (19/2/2), 10mm sample	$T_P$ msec	Notes	Simultaneous I range* ( $\text{\AA}$ )	Q range <sup>§</sup> ( $\text{\AA}^{-1}$ )
50Hz, 5MW	20 msec		3.6 - 6.6	0.026 - 0.57
"	"		6.8 - 9.9	0.017 - 0.30
16.6Hz, 5MW	62.5 msec		4.6 - 12	0.014 - 0.45
"	"	Avoid prompt spike	4.6 - 9.9	0.017 - 0.45
10Hz, 1MW	100 msec		2 - 12	0.014 - 0.79
"	"	Avoiding Bragg	4.6 - 12	0.014 - 0.45
Reactor 10% fwhm			5	0.033 - 0.43
Reactor 10% fwhm			8	0.020 - 0.26
<b>At 36m, <math>L_2 = 15m</math> (6/15/15), 6mm sample</b>				
50Hz, 5MW	20 msec		4.6 - 6.6	0.0022 - 0.062
"	"		6.8 - 8.8	0.0016 - 0.042
16.6Hz, 5MW	62.5 msec	Avoid inelastic <sup>@</sup>	4.4 - 9.2	0.00155 - 0.066
10Hz, 1MW	100 msec		2 - 11	0.0013 - 0.145
"	"	Avoid Bragg	4.4 - 11	0.0013 - 0.066
Reactor 10% fwhm			5	0.0026 - 0.059
Reactor 10% fwhm			8	0.0017 - 0.038

\*Note  $\lambda$  range is restricted to  $>2 \text{\AA}$  (guide cut off) and  $\lambda < 12 \text{\AA}$  (sample transmission) and may be further restricted by time frame  $T_{II}$ , prompt pulses and inelastic scatter from hydrogenous samples.

§ Detector is assumed  $1m^2$ , centred on the beam, with isotropic scatterer, else divide  $Q_{max}$  by 2, or increase  $Q_{max}$  if detector is offset. Minimum detector radius  $\sim 2.5 \times$  penumbra.

@ Could use at other extreme, with reduced count rate,  $\lambda = 7.5 - 11.0 \text{\AA}$ , ( $Q = 0.0013 - 0.038 \text{\AA}^{-1}$ ), or some intermediate range between these.

peak flux of the spectrum is not available unless poor resolution can be tolerated. (Using say  $\lambda < 4 \text{\AA}$  the Q resolution curves would broaden assymmetrically to high Q.)

For the best  $\lambda$  range at 16.6Hz we have to count through a prompt spike of at present uncertain size, e.g. removing at least 9.9-10.5  $\text{\AA}$  at 23m, or 6.6-7.0  $\text{\AA}$  at 36m.

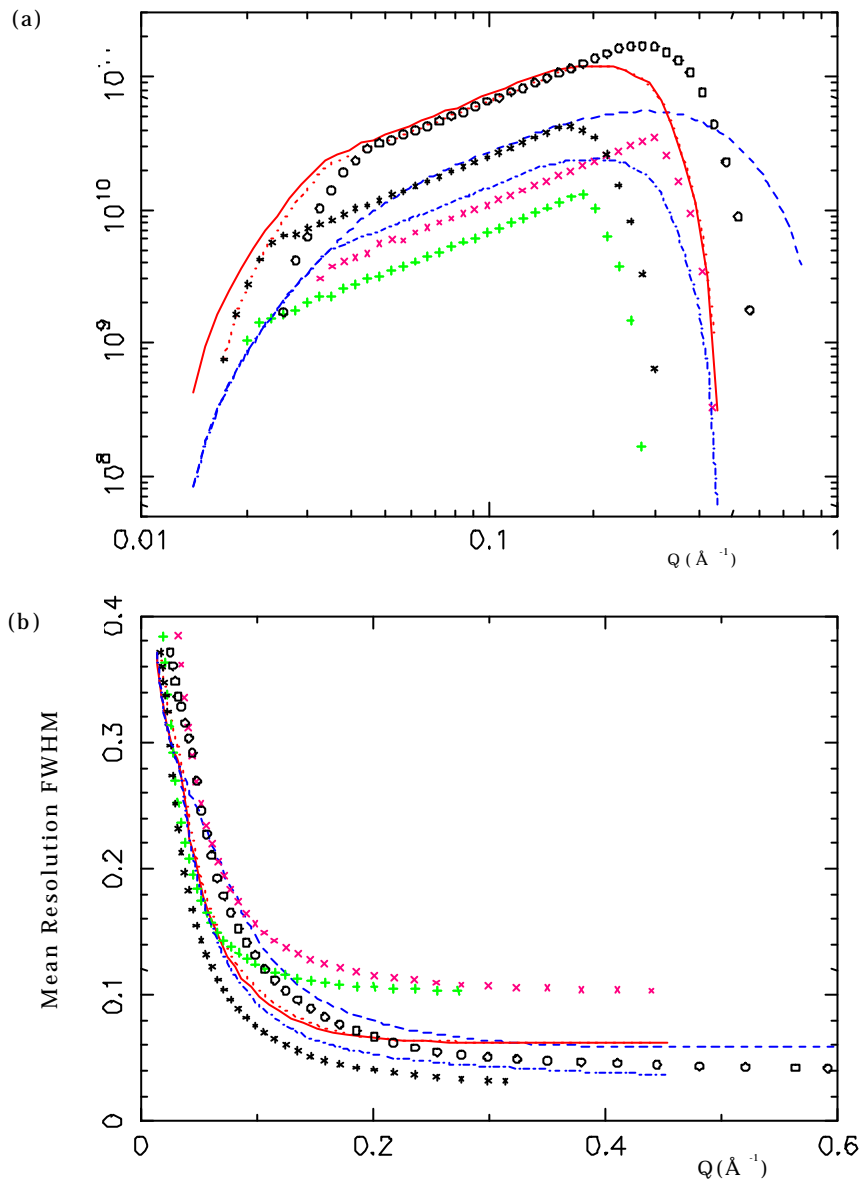


**Fig.3:** ESS - SANS At 23m (19/2/2), (a)  $1\text{cm}^{-1}$  flat scatterer, (b)  $\delta Q/Q$ , FWHM resolution coupled  $\text{H}_2$  moderator, 10mm diameter sample.

line -  $\lambda = 4.6\text{-}12 \text{\AA}$ , 5MW, 16.6Hz, long pulse

dots -  $\lambda = 4.6\text{-}9.9 \text{\AA}$ , (stopping before prompt spike at  $9.9 \text{\AA}$ ),

circles -  $\lambda = 3.6\text{-}6.6 \text{\AA}$ , 5MW, 50Hz

asterisk -  $\lambda = 6.8\text{-}9.9 \text{\AA}$ , 5MW, 50Hz

dashes -  $\lambda = 2\text{-}12 \text{\AA}$ , 1MW, 10Hz (full  $Q$  range truncated in (b)),

dot-dash -  $\lambda = 4.6\text{-}12 \text{\AA}$ , 1MW, 10Hz (improve resolution by omitting short  $\lambda$  near beam stop),

xxx -  $\lambda = 5 \text{\AA}$ , +++ -  $\lambda = 8 \text{\AA}$ , 10% FWHM, ~ "ILL reactor" assuming all other factors equal.

(Calculations are numerical integrations over detector and spectrum, assuming  $L_1 = L_2$ ,  $R_1 = 2R_2$ , detector FWHM  $\Delta R = 12\text{mm}$ ,  $R_{\text{min}} = 2.5 \times \text{penumbra}$ . A "1mm scintillator" detector efficiency has been included to make a realistic reduction of the short  $\lambda$  contribution.  $\delta Q(\text{FWHM})/Q$  is a simple mean of Gaussian approximations, actual resolution curves tend to have a relatively sharp peak and, where shorter  $\lambda$  are included, broader tails)

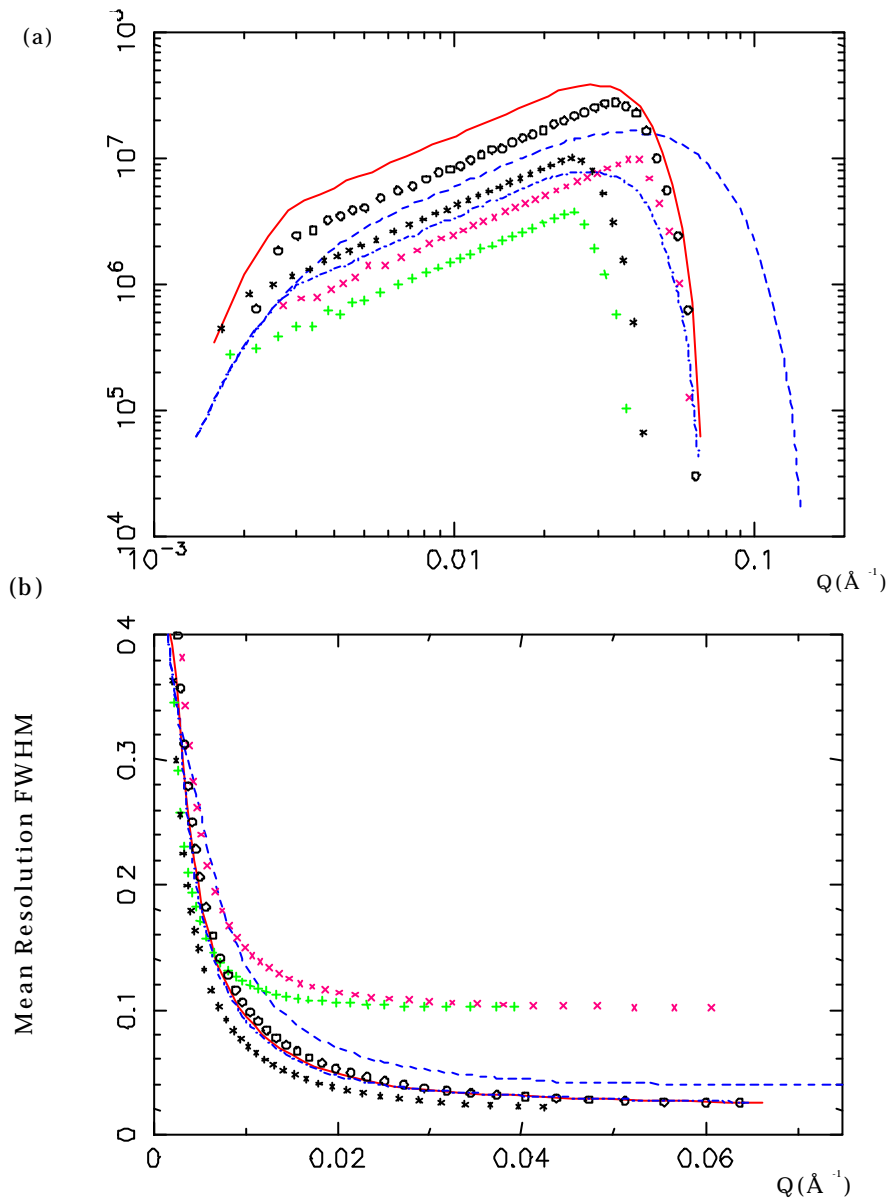


**Fig.4:** ESS - SANS At 36m (6/15/15), (a)  $1\text{cm}^{-1}$  flat scatterer, (b)  $\delta Q/Q$ , FWHM resolution (Gaussian approximations) coupled  $\text{H}_2$  moderator, 6mm diameter sample. Note changes to Q scales.

line -  $\lambda = 4.4 - 9.2 \text{ \AA}$ , 5MW, 16.6Hz, long pulse (Prompt spike at  $\lambda = 6.6 - 7.0 \text{ \AA}$  is still included here. Inelastic scatter from hydrogenous samples, separated by time-of-flight, reduces  $\lambda$  range from 4.4 to 11 down to say 4.4 - 9.2 or 7.5 - 11.0  $\text{\AA}$ ),

circles -  $\lambda = 4.6 - 6.6 \text{ \AA}$ , 5MW, 50Hz

asterisk -  $\lambda = 6.8 - 8.8 \text{ \AA}$ , 5MW, 50Hz

dashes -  $\lambda = 2-11 \text{ \AA}$ , 1MW, 10Hz (full Q range truncated in (b) ),

dot-dash -  $\lambda = 4.4-11 \text{ \AA}$ , 1MW, 10Hz (improve resolution by omitting short  $\lambda$  near beam stop)

xxx -  $\lambda = 5 \text{ \AA}$ , +++ -  $\lambda = 8 \text{ \AA}$ , 10% FWHM, ~"ILL reactor"

## **SANS at 50Hz, ~5MW**

At 50Hz count rates are good but only on a smaller Q range, particularly at longer distances, due to smaller  $\lambda$  band pass. Thus this case is most similar to a reactor. Three choppers are required in the collimation section to remove frame overlap, as a single chopper would not be allowed close enough to the moderator.

Removing pulses to operate at 25Hz, 12.5Hz, 10Hz expands the Q range, but could leave prompt spike(s) in the frame (Fig. 2). Working at progressively lower repetition rates would ultimately give roughly the same Q range and count rates as the curves shown for 10Hz and 1MW, though some intermediate compromises could be attractive for many experiments.

The guide/bender section could be made shorter than indicated in Figures 3 and 4 to minimise the overall length of the beam line and improve Q ranges over those shown here. This is however done at the risk of higher backgrounds, and worse geometrical constraints with neighbouring beams.

Other more exotic solutions to expand the Q range are to rapidly re-phase choppers during runs or to use a system of choppers that simultaneously passes two  $\lambda$  bands over a 40msec collection frame.

## **SANS at 10Hz, ~1MW**

The lowest repetition rate allows the largest  $\lambda$  band pass, as illustrated in Table 1, and gives the best simultaneous Q ranges (e.g. 0.0015 to  $> 0.1 \text{ \AA}^{-1}$ ), using the significant flux from  $\lambda$  down to  $\sim 2 \text{ \AA}$ . The fall off in count rate at very low Q does not suit weak scatterers but is fine for stronger ones where the higher counts at middle Q provide good detail where the cross section is lower. Inclusion of shorter  $\lambda$  close to beam stop worsens Q resolution due to a  $1/\lambda$  term, though these can easily be omitted in the final data reduction (as illustrated in Fig. 3b & 4b).

At the smallest Q, longest  $\lambda$ , a 5MW source at either 16.6Hz or 50Hz will always have more counts (Fig. 3 & 4). However even at 1MW there is potential to do better than the ILL over much of the Q range, particularly if the advantages of a wide simultaneous Q range are important. At 10Hz a single double disc chopper at  $L < 10\text{m}$  is sufficient to remove frame overlap. At longer  $L_2$  and longer  $\lambda$  time of flight could be used to partially separate the 30-50% inelastic component of supposed incoherent background from  $\text{H}_2\text{O}$  etc. thus improving signal/background for dilute samples.

## **Further opportunities for SANS.**

(i) At longer  $L_2$  and longer  $\lambda$  time of flight could be used to largely separate the 30-50% inelastic component of supposed incoherent background from  $\text{H}_2\text{O}$  etc., leaving a nearly pure coherent signal thus improving signal/background for weak scatterers. With a sample at 21m and detector at 36m suitable wavelength bands for which this might be achieved are for example: 4.0 - 4.5  $\text{\AA}$  (on a short pulse source), 6.0 - 7.0  $\text{\AA}$ , 7.5 - 9.0  $\text{\AA}$  or 8.3 - 10.0  $\text{\AA}$ . Some

reduction of repetition rate is also required, so count rates would be relatively low.

(ii) Further opportunities might be afforded using focussing mirror technologies currently under development to give improved count rates at very small  $Q$  with a relatively short beam line (Alefeld et.al.). The neutron beam is focussed at the detector to produce a two dimensional scattering pattern which is more useful and more appropriate for a white beam instrument than the slit smeared pattern from the Bonse-Hart, double crystal, method. To reach  $Q \sim 0.001 \text{ \AA}^{-1}$  should be relatively simple, the goal of  $Q$  to  $\sim 10^{-4} \text{ \AA}^{-1}$  is more technically challenging.

## In summary

In all cases where inhomogeneities on different length scale are present the required  $Q$  range of 2-3 orders of magnitude can only be realised by repeated measurements at different sample to-detector distances. In such widely encountered cases the  $Q$  range accessible in a single shot (which is largest in the 10Hz) is no longer the most important criteria for the optimisation of the target station. Instead we would search for the target which gives the highest intensity for a certain  $Q$ -range where the resolution in  $Q$  should be roughly constant. Comparing the results of Fig. 3 and 4 the overall intensities at the same distance is by a factor of 3 - 4 times better for the 16.6Hz long pulse solution. Careful compromise of instrument design gives  $Q$  resolution approaching that of a short pulse target and still better than on a reactor.

The very best  $Q$  resolution (e.g. for diblock copolymers at low  $Q$  or liquid crystals at higher  $Q$ ) is still however achieved on a short pulse target, selecting an appropriate wavelength band. Therefore a separate SANS instrument optimised for best  $Q$  resolution should be installed at the 50Hz, short pulse target station.

In other cases such as studies of anisotropic systems or ones changing in real time a wide simultaneous  $Q$  range is a distinct advantage of a pulsed source. Though 10Hz provides the best situation operation at sub-multiples of a 16.6Hz or 50Hz source frequency will be attractive for many experiments despite some issues of background signals.

Development and use of still larger area detectors is highly recommended in order to increase the simultaneously accessible  $Q$  range and count rate.

The combination of two instruments, one for lower wavelength resolution at a long-pulse 16.6Hz target station for main applications in conventional SANS and a second one (with the sample perhaps closer to the moderator) for high wavelength resolution at the 50Hz target would provide a world - leading experimental suite for SANS.

# Total Scattering Diffractometers

A.K. Soper<sup>1</sup> and R.L. McGreevy<sup>2</sup>

<sup>1</sup>Rutherford Appleton Laboratory, Chilton, Didcot, Oxon, UK, OX11 0QX

<sup>2</sup>Studsvik Neutron Research Laboratory, Uppsala University S-611 82 Nykoping, Sweden

Substantial gains in count rate and/or Q-range are achievable for total scattering diffractometers at the ESS compared to existing pulsed and reactor neutron sources. However neither of the options for 50Hz operation on a water moderator or 10Hz operation on a hydrogen moderator are ideal for the next generation of total scattering diffractometers. To make real progress this field needs very stable detectors and electronics, low backgrounds, and a very wide range of Q with appropriate resolution. Existing diffractometers on reactor sources provide good count rates and stability but do not permit very low or very high Q measurements. Diffractometers on pulsed neutron sources achieve a better Q range with variable count rates, but often have not achieved a detector stability comparable with the reactor instrument. (The true performance of GEM has yet to be established in this regard.)

The ideal total scattering diffractometer will need a liquid methane type moderator at 50Hz or a liquid hydrogen moderator at 25Hz. The preferred option is for a poisoned moderator, but decoupled/unpoisoned could be considered as well. There is no use for coupled/unpoisoned moderators for this work. The long pulse target could be used in reactor mode, with a monochromator, but there is little gain in either count rate, resolution or Q range in doing this.

## Introduction

Over the past several decades, Europe has led the World in the provision of diffraction facilities for liquids and non-crystalline solids. Diffractometers appropriate to this work include D4 and D20 at ILL, 7C2 at Saclay, and SANDALS at ISIS. In addition a state-of-the-art diffractometer, GEM, has recently been installed at ISIS, and there are somewhat lower flux facilities such as SLAD at Studsvik. Between them these instruments have studied a very broad range of disordered and crystalline materials science which has been widely disseminated in the scientific literature, including prestigious journals such as *Nature*, *Science*, and *Physical Review Letters*.

The theme of  $S(Q)$  measurements actually covers a rather broad front from the measurement of the radial distribution function in a simple fluid, like argon or krypton, through the study of a range of increasingly complex fluids and liquid mixtures, including supercritical fluids, molten salts, liquid metals, liquid semiconductors and ceramics, liquid mixtures and solutions, molten and amorphous polymers, heterogeneous systems (e.g. liquids absorbed in solids),

***European facilities for disordered materials neutron diffraction research are world leading.***

***The range of disordered materials covered is very broad and includes total scattering measurements on crystalline materials.***

amorphous and glassy solids. Total scattering studies of crystalline materials are also included in this list because they involve closely analogous measurement and data analysis techniques. Because of the diverse range of materials involved, the requirements on the diffractometer are equally diverse. High  $Q$  ( $\geq 60 \text{ \AA}^{-1}$ ) with high resolution is essential for amorphous and crystalline materials where the structure is often sensitive to subtle changes in the near-neighbour distances between atoms. On the other hand low or very low  $Q$  ( $\sim 0.01 \text{ \AA}^{-1}$ ) values are increasingly needed to probe the longer range order present in many technologically important complex fluids. What has not been achieved to date is the combination of very high and very low  $Q$  capability in a single diffractometer, and it is this possibility which will set an instrument built at the ESS apart from anything that can be envisaged at present day facilities.

### Requirements for a Total Scattering Diffractometer at the ESS

Based on the experience gained at existing facilities it is now possible to state clearly what features any new diffractometer(s) in this field will require:-

- A very wide  $Q$  range:-( $0.01 \text{ \AA}^{-1} < Q < 60 \text{ \AA}^{-1}$ )
- Good  $Q$  resolution (depending on the  $Q$  value):-( $5-10\% \geq \Delta Q/Q \geq 0.5\%$ ?)
- Good count-rate, at or above  $100 \text{ cts/s}/0.05 \text{ \AA}^{-1}/\text{per cm}^3$  vanadium over the whole  $Q$ -range.
- Acceptable recoil corrections.
- Low backgrounds.
- Very stable detectors ( $<0.1\%$  drift over 24hrs). This condition applies equally to the beam monitors. Assuming stable monitors and detectors are available small drifts in the incident spectrum are acceptable at the 1-2% level.
- Rapid means of changing samples and sample conditions.
- Rapid data accumulation (fast “begins” and “ends”) plus rapid data assessment/correction/reduction. It was felt that the rapid assessment of data is essential for any future diffractometer since how to proceed with any given experiment often depends on appreciating how a particular sample appears from the diffraction pattern.
- Sophisticated data interpretation tools, so that the structural consequences of any diffraction data can be assessed promptly as soon as they are accumulated.
- The diffractometer(s) should be dedicated to total scattering studies of materials. The instrumental requirements for crystalline structure refinement are distinct from those for total scattering structure refinements and in general both sets of requirements cannot be met with a single specification.

***A number of requirements need to be satisfied, particularly  $Q$  range,  $Q$  resolution and count rate***

### Consequences for a Total Scattering Diffractometer at the

## ESS

- **Q-range:** The very wide Q range can only be achieved with a combination of a range of scattering angles with full exploitation of the neutron energy range available at the ESS.
- **Large Q:** This is generally only achievable with high resolution in the backscattering direction. However lower resolution is achievable at large Q in the forward direction if the full moderator spectrum at high energies is available. This precludes the possibility of using a T0 chopper to block the fast neutrons from the experiment.
- **Low Q:** Requires longer flight path to reduce beam divergence and so keep resolution at low Q acceptable.
- **Resolution:** Neutron pulse width should ideally be matched to geometric resolution. This can be hard to achieve in an instrument which has both wide angle and low angle detectors. The notion of (almost) constant resolution detectors has proved useful at ISIS when banks of detectors are to be merged together. It is particularly important from the point of view of data interpretation of structures with sharp peaks that the resolution function is correctly included in the data interpretation process.
- **Count rate:** This can only be achieved by means of large solid angle detector arrays. If the source is short-pulsed the detectors do not need to be moved, which means the solid angle can be as large as cost and engineering constraints allow.
- **Recoil corrections:** Keeping these small means keeping the scattering angle below about 50° and neutron energies above the thermal energy of the sample. In some special cases (large scale structures for example or Bragg scattering) the latter condition can be relaxed somewhat.
- **Low backgrounds.** Effective collimation is needed on both the incident and scattered beams.
- **Detectors and data acquisition electronics:** As well as being STABLE these must also be FAST, i.e. low deadtimes. (On ISIS at ~160kW, the DAE\_I system falls over when the time averaged countrate exceeds about 1MHz.) With ESS running at roughly 20 times this countrate, there will be serious downtime problems unless much fast electronics can be incorporated. **It is particularly important to set up an electronics regime whose downtime is quantifiable, since the variation in downtime from different scattering samples will have serious deleterious effects on the overall reliability of the data if the downtime cannot be quantified.**

***The requirements lead naturally to the consequences for a total scattering diffractometer for the ESS. In particular it will be essential to make full use of the energy spectrum available. Lowest Q can only be achieved on a long total flight path.***

***Detectors and data acquisition electronics must be fast and stable***

## Comparative performance of two generic total scattering diffractometers.

Based on the spectral parameters produced by Feri Mezei (4-12-2000), two generic diffractometers were analysed with a

simple Monte Carlo routine to give comparative estimates of the likely resolution and count rates on the ESS. These are compared to estimates of what is currently available on the SANDALS diffractometer at ISIS, based on the published spectral parameters for the ISIS methane moderator. It should be stressed that the actual count rates (in particular) and resolution will depend on a number of factors which will only be known once experience with the actual target/moderator configuration becomes available.

**Two generic diffractometers, one short flight path the other long flight path, were analysed using the published moderator parameters for the ESS.**

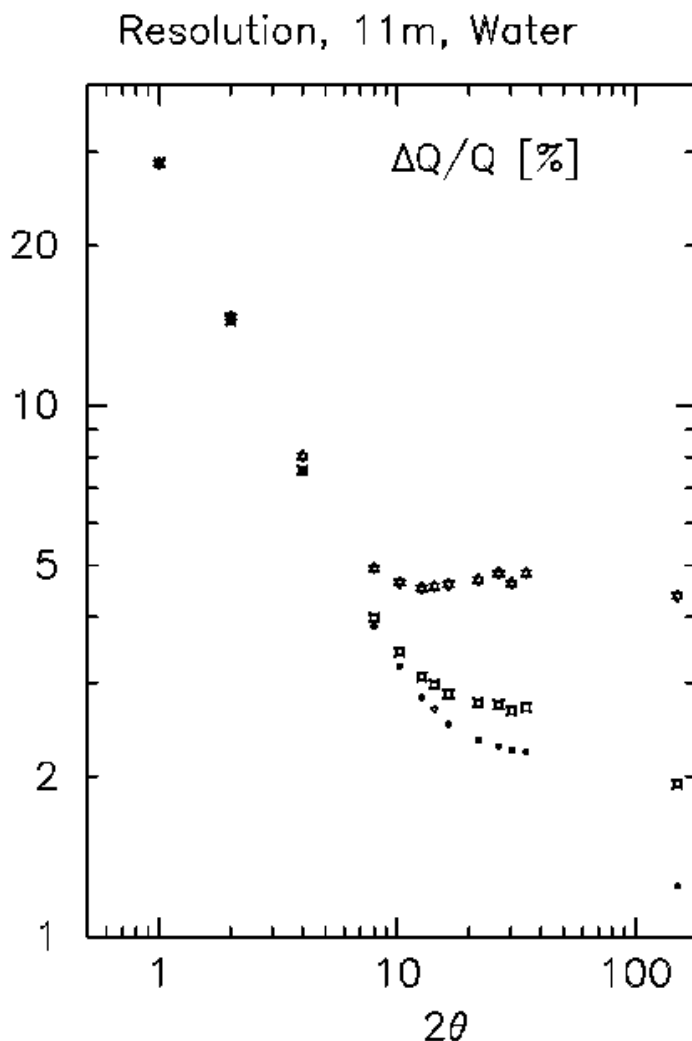


**Fig. 1:** Resolution of TSCAT-1, 11m incident flight path. The dots correspond to decoupled/poisoned moderator, the squares to the decoupled/unpoisoned moderator, and the stars to the coupled/unpoisoned moderator.

In both cases it was assumed the total scattering diffractometer (TSCAT) would consist of a large solid angle of detectors spanning the scattering angle range 0-40°, plus a smaller bank of detectors in the backscattering direction (150°). The detectors at low angles were arranged on the surface of a cylinder of radius 0.8m from the beam axis, for scattering angles above ~11°. For lower angles than this the secondary flight path was assumed to be ~6m from the sample. Individual detector elements were 200mm high by 100mm wide.

**The primary assumptions are that the neutron pulse is short, and the solid angle of the detectors is maximal, but concentrated at lower scattering angles.**

10mm wide (facing the sample) by 20mm deep, except at the very lowest angles, where they were assumed to be either 50mm or 100mm in height. The sample was a 1cm<sup>3</sup> of vanadium. It was assumed the incident beam would be circular in cross section, with the viewing area of the moderator a disk of diameter ~90mm. Absorbing apertures were placed 1.7m from the moderator and 0.3m from the sample to simulate the effect of the collimator on instrument performance.

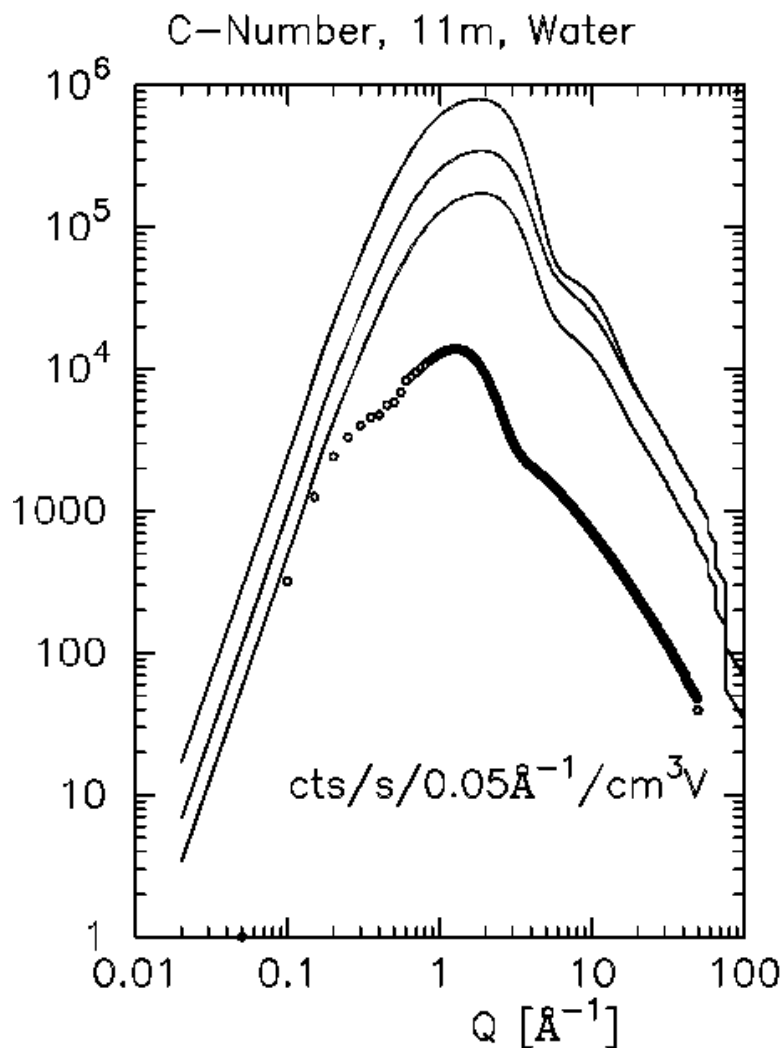


**Fig. 2:** Count rate number for TSCAT-I as a function of wave vector transfer. The circles correspond to the current SANDALS estimated using the same procedure as described here. The top line is for the coupled/unpoisoned moderator, and the bottom line is for the decoupled/poisoned moderator.

For TSCAT-I, the incident flight path was set to 11m, the ambient water moderator was viewed, and it was assumed the instrument would be on the 50Hz target. Figure 1 shows the estimated resolution for the three types of moderator (decoupled/poisoned, bottom; decoupled/unpoisoned, middle; coupled/unpoisoned, top). Figure 2 shows the estimated count rate (or “C-number”) for each moderator, and the circles show the comparative performance of the current SANDALS, estimated in the same way.

***The 50Hz instrument is on a 11m flight path.***

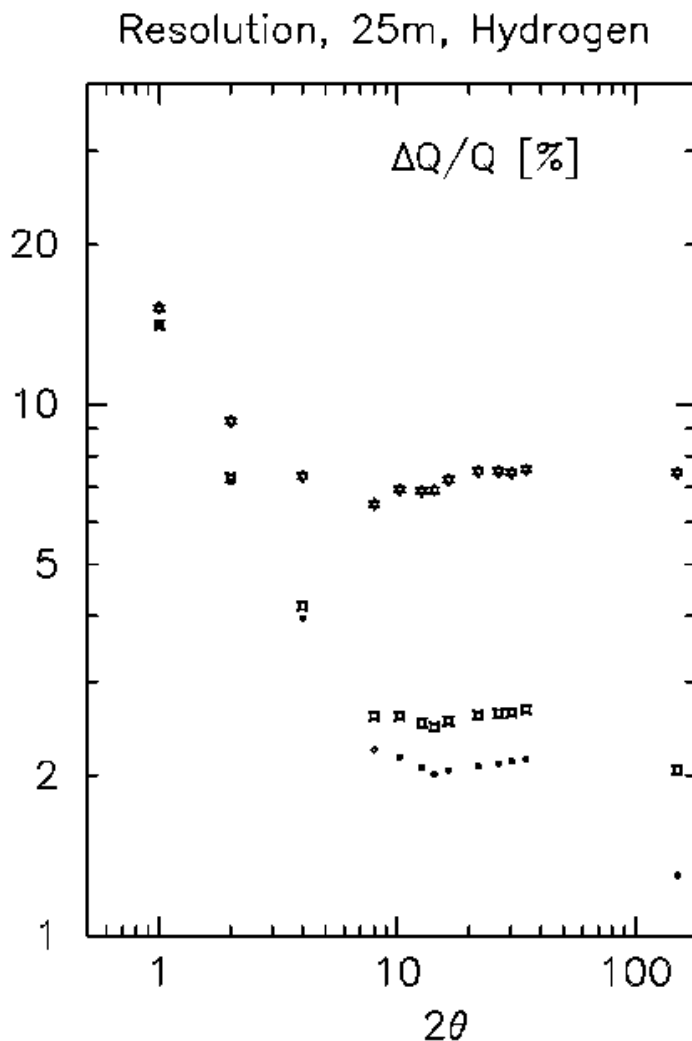


**Fig. 3:** Resolution for TSCAT-II. Symbols as for Fig. 1

For TSCAT-II, the incident flight path was set to 25m, the liquid hydrogen moderator was viewed, and the instrument was assumed to be on the 10Hz target. Figs. 3 and 4 are the sequel to Figs. 1 and 2 for this configuration.

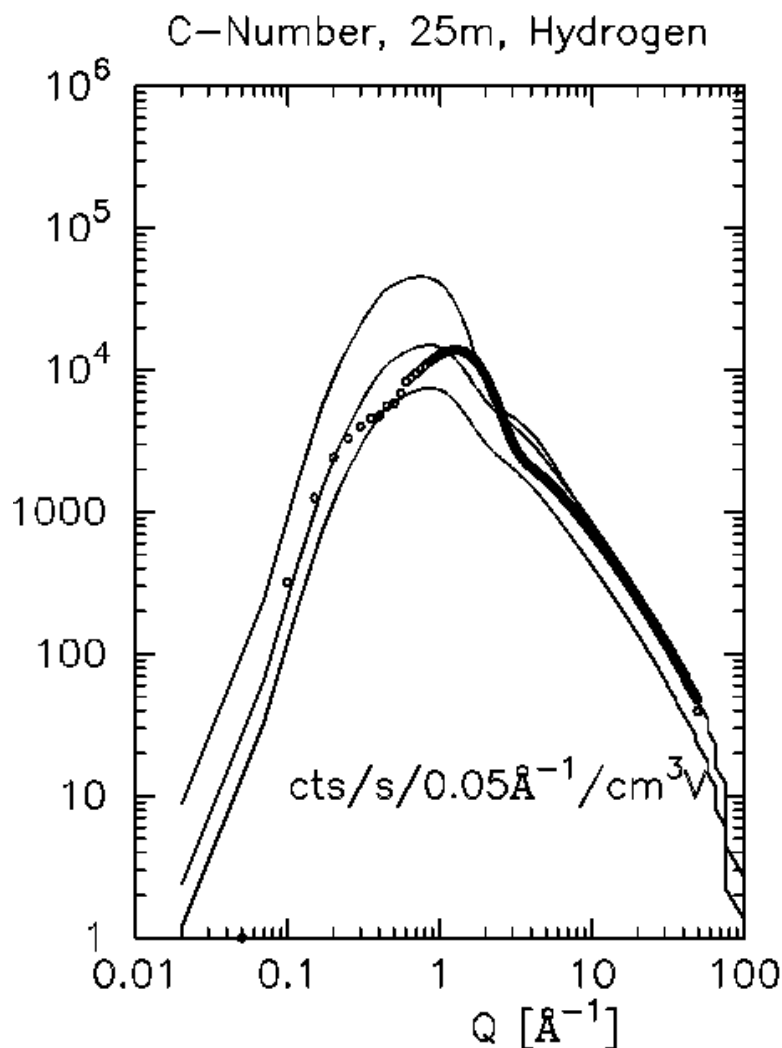
**The 10Hz instrument is on a 25m flight path**

### Discussion

It is clear that based on this rather simple comparison, a total scattering diffractometer on ESS will achieve count rates up to 20 times what is available at existing facilities, with an equivalent resolution. Such an instrument would also have a wider Q range with a given count rate than any existing diffractometer.

The 11m option TSCAT-I gives an exceedingly high count rate gain over existing machines, but there are only minor gains at low Q because the water moderator available cuts out too soon at low neutron energies. This could be in principle be won back by using a hydrogen moderator, but then there will be significant frame overlap which would necessitate the use of frame overlap choppers.

**The 50Hz option demonstrates a factor of ~20 enhanced count rate compared to existing facilities at ILL and ISIS over an equivalent Q range. The high Q resolution is probably better than a typical reactor diffractometer. The gains at low Q are not so apparent due to the water moderator's higher operating temperature**



*compared to the methane moderator available on ISIS.*

**Fig. 4:** C-number for TSCAT-II.

The 25m option TSCAT-II apparently gives very little count-rate advantage over existing machines, but the **minimum Q** that would be available on this machine would be at least a factor of 2 smaller than for TSCAT-I. This is because the longer flight path permits a narrower beam divergence, which in turn allows smaller scattering angles to be accessed. In addition by running on a 10Hz target the full range of neutron energies can be utilised.

The current view is that **neither** of these arrangements is optimal. TSCAT-I shows good count rate gains at large Q, but will not extend the minimum Q value significantly. TSCAT-II will achieve the required minimum Q but at substantial expense in count-rate. In fact on this flight path (~30m overall), the 10Hz repetition rate is too slow, and some of the flux loss could be recouped by running at say 25Hz instead. Use of frame choppers to chop alternate pulses on the 50Hz target in order to run at 25Hz could be explored although there is no experience of this on existing disordered materials diffractometers. Frame choppers will never completely attenuate the power pulse, leading to scattered neutron spectrum with a pronounced spike in it. By exploiting the wide angle range of the TSCAT it might be possible to eliminate this

***The 10Hz option gives little gain in count rate but will have a superb low Q range.***

***Neither option is optimal for total scattering studies of materials.***

in the final diffraction pattern, but there is no experience so far in attempting to do this.

The ideal would be to have a liquid methane type moderator on a 50Hz target, or else a liquid hydrogen moderator running at 25Hz.

As far as resolution is concerned it appears that the preferred moderator is decoupled and poisoned, although the unpoisoned moderator will deliver excellent count rates at slightly poorer resolution. The coupled moderators are definitely ruled out for S(Q) work.

***The ideal would be to have a liquid methane moderator on the 50Hz target, or a liquid hydrogen moderator on a 25Hz target.***

### **Long pulse target**

The 2 ms pulse width on the long-pulse target is too long to be used for S(Q) diffraction directly. Therefore it would be necessary to monochromate the beam, much in the same way as is done currently at a reactor source. Much of the gain from using a pulsed source is then thrown away with this option. The combined goals of obtaining a wider Q range with increased count rate could only be achieved in this case by repeating each diffraction measurement at a sequence of incident energies to get the fullest range possible. Given the often delicate nature of many of the new samples likely to be studied (examples of this are the recently executed levitator experiments) this is not always a practical method of operation. In addition the goal of reducing recoil corrections by going to low scattering angles and high neutron energies is not so easy to achieve in this case. Therefore for the purpose of this study, the exploitation of the long pulse target was ruled out as a possibility.

***The long pulse target is not useful for total scattering diffraction studies.***



## **ESS Instrument Performance Sheets**

Compiled by  
the ESS Instrumentation Task Group

Edited by:  
F. Mezei  
R. Eccleston  
T. Gutberlet



## Content:

### **Direct geometry spectrometers** (R. Eccleston et al.)

- High energy chopper spectrometer
- Thermal energy chopper spectrometer
- Variable resolution cold neutron chopper spectrometer
- Multi-chopper spectrometer

### **Indirect geometry spectrometers** (K. Andersen et al.)

- 0.8  $\mu\text{eV}$  backscattering
- 1.5  $\mu\text{eV}$  backscattering
- 17  $\mu\text{eV}$  backscattering
- Constant Q machine
- Vibrational spectroscopy machine
- Resonance high-energy spectrometer

### **NSE** (M. Monkenbusch et al.)

- High resolution NSE
- Large solid angle NSE

### **Single crystal and protein diffractometers** (C. Wilson et al.)

- Single crystal chemical crystallography
- High resolution single crystal diffraction
- Single crystal diffuse scattering
- Single reflection single crystal studies
- High resolution protein crystallography
- Low resolution protein crystallography

### **Powder diffractometers** (P. Radaelli et al.)

- High resolution powder diffraction
- High-Q powder diffraction
- Magnetic powder diffraction

### **Material sciences and engineering diffractometers** (P. Withers et al.)

### **Reflectometers** (H. Fritzsche et al.)

- High resolution reflectometer
- High intensity reflectometer

### **SANS** (R. Heenan et al.)

- High wavelength resolution SANS
- High intensity SANS

### **Total scattering diffractometers** (A. Soper et al.)



# Instrument performance sheet: High Energy Chopper Spectrometer

## **Instrument description:**

The instrument description is very similar to that of the MAPS spectrometer at ISIS. The beam is monochromated by a Fermi chopper, with T=0 chopper to reduce the prompt pulse. Detector coverage is as large as possible within space and cost constraints, using position sensitive detectors to provide a high degree of pixelation

## **Schematic set-up:**

Viewing decoupled poisoned water moderator. Moderator to sample distance 13m; sample to detector distance 6m. Detector array: position sensitive He-3 tubes

**Generic type.** Chopper Spectrometer

Incident Energy Range:  
25 meV - 2 eV

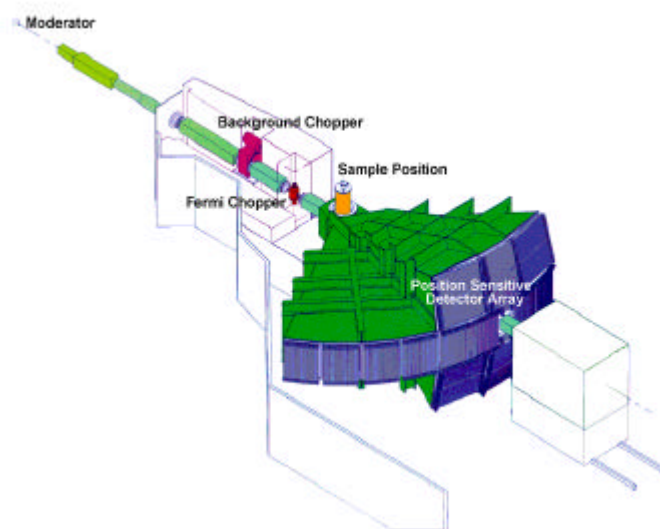
Energy Transfer

Resolution 1%-3%

Moderator Type:

Decoupled poisoned water

Target Station: 50Hz  
short pulse



## **Performance:**

The instrument performance in terms of incident flux will be approximately 30 times that of MAPS at ISIS. Greater improvements in terms of data rate can be achieved by increasing the detector area. Access to higher resolutions will be possible by extending the sample-detector distance and the primary flight path.

Nominal flux at 100 meV, 2%  $\Delta\epsilon/E$ :  $2 \times 10^5 \text{ n cm}^{-2} \text{ s}^{-1}$

**x ~ 30**

# Instrument performance sheet: **Thermal Energy Chopper Spectrometer**

## **Instrument description:**

The instrument description is very similar to that of the MAPS spectrometer at ISIS. The beam is monochromated by a Fermi chopper, with T=0 chopper to reduce the prompt pulse. Detector coverage is as large as possible within space and cost constraints, using position sensitive detectors to provide a high degree of pixelation

## **Schematic set-up:**

Viewing coupled water moderator. Moderator to sample distance ~20m; sample to detector distance 2.5m. Supermirror Guide.

Detector array: position sensitive He-3 tubes. Solid angle of  $>\pi$ Sr; 50000 detector pixels

## **Generic type.** Chopper Spectrometer

Incident Energy Range:

10 meV – 140 eV

Energy Transfer

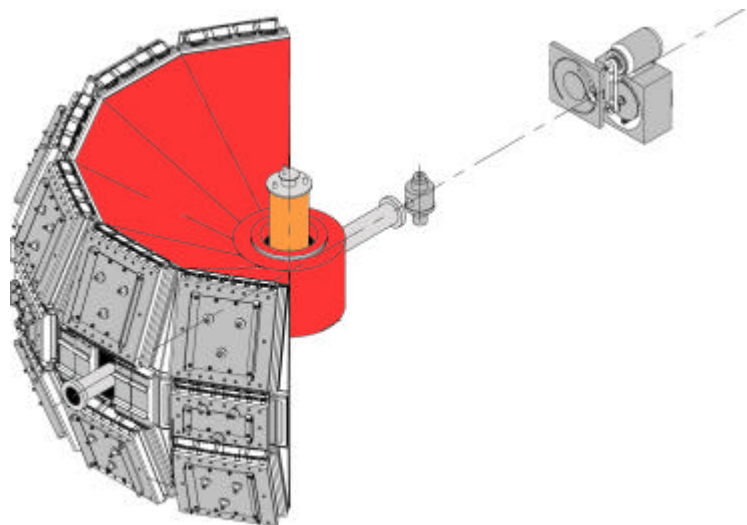
Resolution 2%-10%

Moderator Type:

Coupled water

Target Station:

50Hz short pulse



## **Performance:**

A medium resolution high intensity chopper spectrometer.

Performance in terms of intensity relative to HET at ISIS: x 240 (source 30x; moderator 2x; instrument 4x). Large angular coverage provides additional performance in terms of data rate.

Nominal flux at 50 meV, 2.5%  $\Delta\epsilon/E$ :  $9 \times 10^5$  n cm<sup>-2</sup> s<sup>-1</sup>.

**x ~ 240**

# Instrument performance sheet: Variable resolution cold neutron chopper spectrometer

## **Instrument description:**

Time-of-flight spectrometer with detectors covering a large solid angle and a large angular range from about  $2^\circ$  to  $140^\circ$ . The secondary resolution is assured by a disc chopper in front of the sample, the primary resolution by the source pulse and/or a pulse shaping chopper up-stream. Chopper speed, choice of slit width and/or adjustable pulse tail cutting determines the resolution. Resolution ratio between best intensity and best resolution modes: 1:6. Best elastic resolution at  $7\text{\AA}$  incoming wavelength:  $20\text{ }\mu\text{eV}$

## **Schematic set-up:**

Source to sample distance:  $\sim 40 - 80\text{m}$ , bridged by ballistic guide. This distance allows to have detectors on both sides with little interference of neighbouring beams. Repetition Rate Multiplications allows max 300Hz pulse rate on sample. Detector to sample distance:  $\sim 3\text{m}$ , detector area  $\sim 20\text{m}^2$ .

**Generic instrument type** for comparison: IN5 (ILL), as in Dec. 2000

Choice of incoming wavelength:  $2\text{\AA} < \lambda_{\text{in}} < 20\text{\AA}$

Moderator type: cold coupled moderator

**Q-w-range and resolution:** varies with wavelength

Q: from  $0.01\text{\AA}^{-1}$  (at  $\lambda_{\text{in}}=20\text{\AA}$ ) to  $6\text{\AA}^{-1}$  (at  $\lambda_{\text{in}}=2\text{\AA}$ )

$\omega$ : from  $1\text{ }\mu\text{eV}$  (best elastic resolution at  $\lambda_{\text{in}}=20\text{\AA}$ ) to  $100\text{ meV}$  maximum energy change in up-scattering and  $15\text{ meV}$  in down-scattering (at  $\lambda_{\text{in}}=2\text{\AA}$ )

## **Source gain:**

Target	50Hz	10Hz	16.6Hz
High resolution setting	<b>40</b>	<b>15</b>	<b>20</b>
High intensity setting	<b>7</b>	<b>3</b>	<b>15</b>

*Additional gain by modern/new design:  $\sim 35-70$*

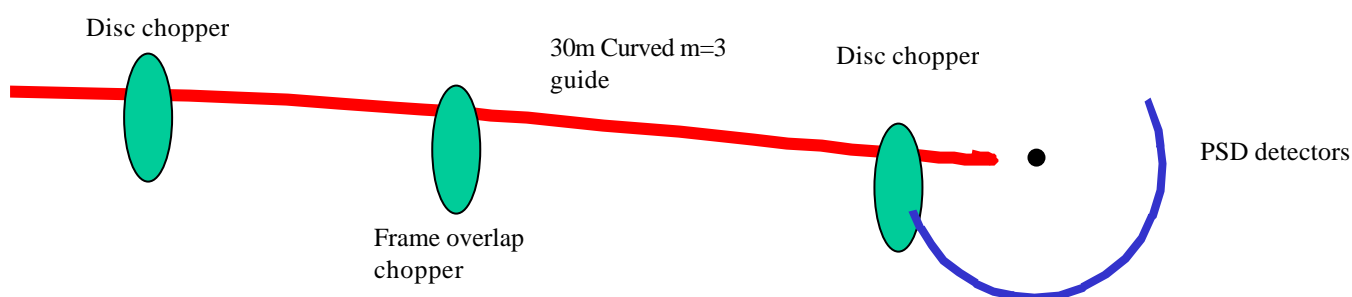
**x ~ 800**

# Instrument performance sheet: Multi-Chopper Spectrometer

## Instrument description:

A direct geometry multi-chopper instrument. The multiple choppers give full control over the resolution and allows one to 'match' the resolution contributions from the moderator and chopper, thus giving maximum flux for a certain resolution. The instrument would be on a 30m curved supermirror guide.

## Schematic set-up:



**Generic type:** IN5, NEAT, direct geometry multi-chopper

**Wavelengths used:**  $1 < \lambda < 16 \text{ \AA}$

**Moderator Type:** cold coupled

**Resolution:**  $\Delta\varepsilon/E_i = 1-6\%$

**Q- $\omega$ -range:**  $.03 < Q < 13.0 \text{ \AA}^{-1}$

$1 < E_i < 100 \text{ meV}$

Gain for LET at 4.86 meV for 2% resolution

## Source Gain:

Target	50Hz	10Hz	16.6Hz
Moderator	Coupled Cold	Coupled Cold	Coupled Cold
Gain relative to IN5*	60	10	10
Gain relative to IN6	112	20	20

\*IN5 upgrade. autumn 2001

Further instrumental gains are possible: larger detector areas (PSDs) x 4; rep. rate multiplication x2-4. Additional advantages arising from the use of position sensitive detectors are not easily quantifiable but provide considerable additional experimental capability.

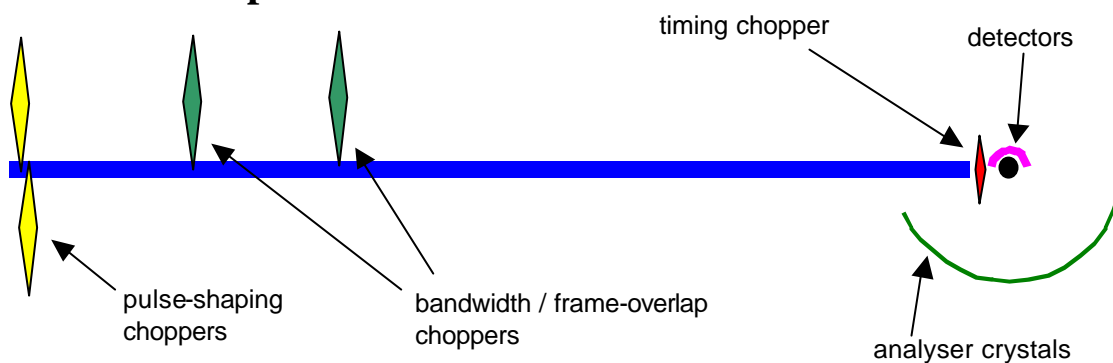
**x ~ 1000**

# Instrument performance sheet: 0.8 meV Backscattering

## Instrument description:

An inverse-geometry instrument using Si 111 crystals arranged in direct backscattering to give an energy resolution of 0.8  $\mu\text{eV}$ . A pulse-shaping chopper is used to provide a very sharp time structure. The instrument is 200m long and optimised for quasielastic measurements with a dynamic range of about 300  $\mu\text{eV}$ .

## Schematic set-up:



**Generic type:** IN16 direct backscattering Si 111

Wavelengths used: 4  $\rightarrow$  7  $\text{\AA}$

Moderator Type: cold coupled

**Q-w-range:**  $0.3 < Q < 2.0 \text{ \AA}^{-1}$

$\hbar\omega$ -range  $\sim 300 \mu\text{eV}$

usually quasielastic, i.e.  $-150 \rightarrow +150 \mu\text{eV}$

Gain (relative to IN16)

$g_0$  = flux gain at the elastic wavelength

$d_0$  = gain in dynamic range

## Source gain:

Target	50Hz	10Hz	16.6Hz
moderator	coupled cold	coupled cold	coupled cold
$g_0$	<b>25</b>	<b>5</b>	<b>4</b>
$d_0$	<b>10</b>	<b>12</b>	<b>30</b>

Additional gain due to modern/new design:  $\sim 2$

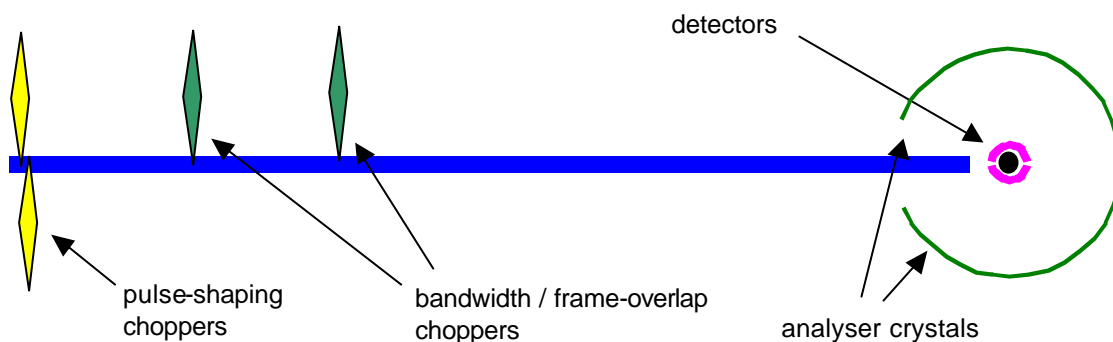
**x = 50**

# Instrument performance sheet: 1.5 meV Backscattering

## Instrument description:

An inverse-geometry instrument using Si 111 crystals arranged in near-backscattering to give an energy resolution of 1.5  $\mu\text{eV}$ . A pulse-shaping chopper is used to match primary and secondary resolution at inelastic energy transfers. The instrument is 200m long and optimised for inelastic measurements with a dynamic range of about 300  $\mu\text{eV}$ .

## Schematic set-up:



**Generic type:** IRIS/IN16 near-backscattering Si 111

Wavelengths used: 2  $\rightarrow$  7  $\text{\AA}$

Moderator Type: cold coupled

**Q-w-range:**  $0.3 < Q < 2.0 \text{ \AA}^{-1}$   
 $\hbar\omega$ -range  $\sim 300 \mu\text{eV}$   
 if quasielastic:  $-150 \rightarrow +150 \mu\text{eV}$

Gain (relative to IN16, which has a slightly better resolution of 0.9  $\mu\text{eV}$ )  
 $g_0$  = flux gain at the elastic wavelength  
 $d_0$  = gain in dynamic range

## Source gain:

Target	50Hz	10Hz	16.6Hz
moderator	coupled cold	coupled cold	coupled cold
$g_0$	<b>100</b>	<b>20</b>	<b>15</b>
$d_0$	<b>10</b>	<b>12</b>	<b>30</b>

Additional gain due to modern/new design:  $\sim 3$

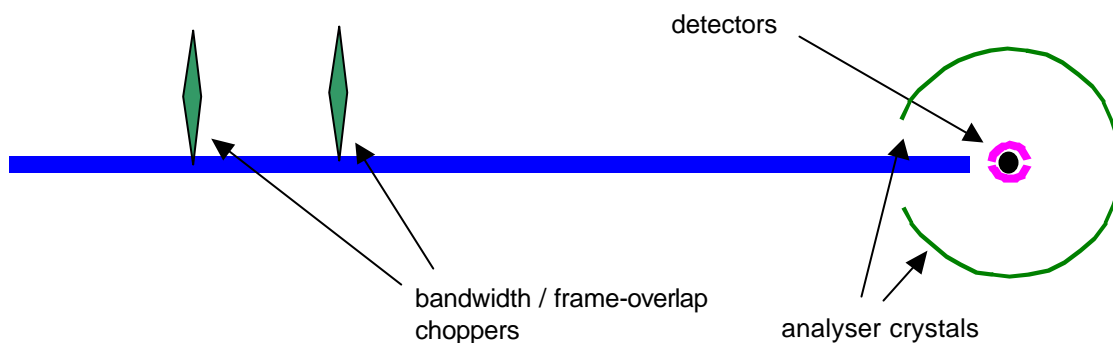
**x = 300**

# Instrument performance sheet: 17 meV Backscattering

## Instrument description:

An inverse-geometry instrument using PG 002 crystals arranged in near-backscattering to give an energy resolution of 17  $\mu\text{eV}$ , similarly to IRIS at ISIS. The instrument is 22m long and optimised for inelastic measurements with a dynamic range of about 3 meV.

## Schematic set-up:



**Generic type:** IRIS near-backscattering PG 002

Wavelengths used: 2  $\rightarrow$  7  $\text{\AA}$

Moderator Type: cold decoupled (50Hz) or coupled (10Hz)

**Q-w-range:**  $0.3 < Q < 1.9 \text{ \AA}^{-1}$

$\hbar\omega$ -range  $\sim 3 \text{ meV}$

if quasielastic:  $-1.5 \rightarrow +1.5 \text{ meV}$

Gain (relative to IRIS)

$g_0$  = flux gain at the elastic wavelength

$d_0$  = gain in dynamic range

## Source gain:

Target	50Hz	10Hz	16.6Hz
moderator	decoupled cold	coupled cold	coupled cold
$g_0$	<b>150</b>	<b>100</b>	<b>150</b>
$d_0$	<b>2</b>	<b>3</b>	<b>0.5</b>

Additional gain due to modern/new design:  $\sim 4$

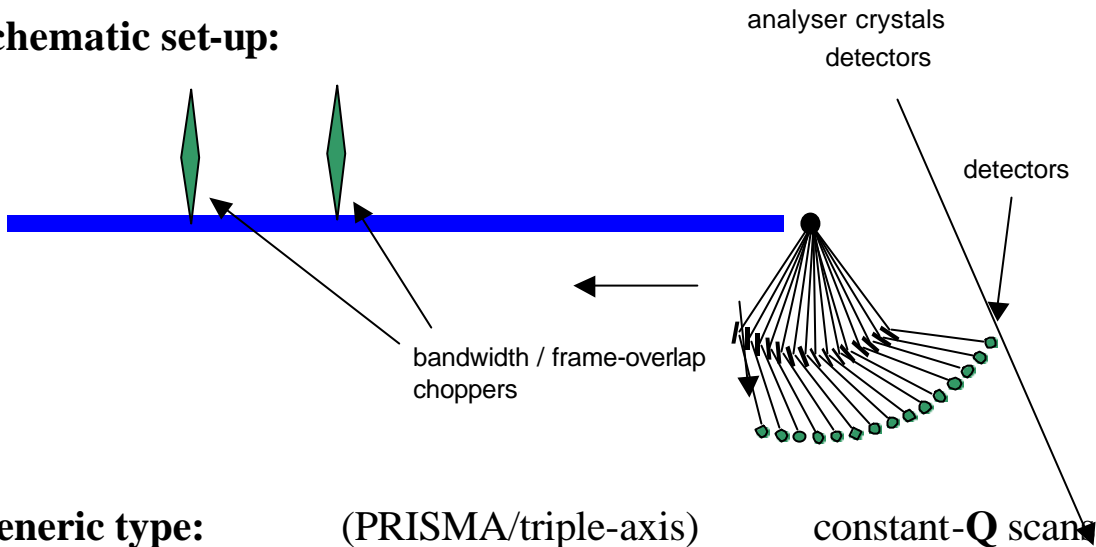
**x = 600**

# Instrument performance sheet: constant-Q Machine

## Instrument description:

An inverse-geometry instrument for measuring constant-Q scans in single crystals. A multianalyser array of PG002 crystals is used, consisting of at least 20 arms with at most  $1^\circ$  separation with individually adjustable take-off angles.

## Schematic set-up:



**Generic type:** (PRISMA/triple-axis)

Wavelengths used:  $1 \rightarrow 6 \text{ \AA}$

Moderator Type: decoupled hydrogen

**Q-w-range:**  $0.2 < Q < 4 \text{ \AA}^{-1}$   
 $-30 < \hbar\omega < 80 \text{ meV}$

Gain (relative to PRISMA)

$g_0 = \text{flux gain}$

Target	50Hz	10Hz	16.6Hz
moderator	decoupled cold	coupled cold	coupled cold
$g_0$	<b>100</b>	<b>50</b>	<b>30</b>

*Additional gain due to modern/new design:  $\sim 5$*

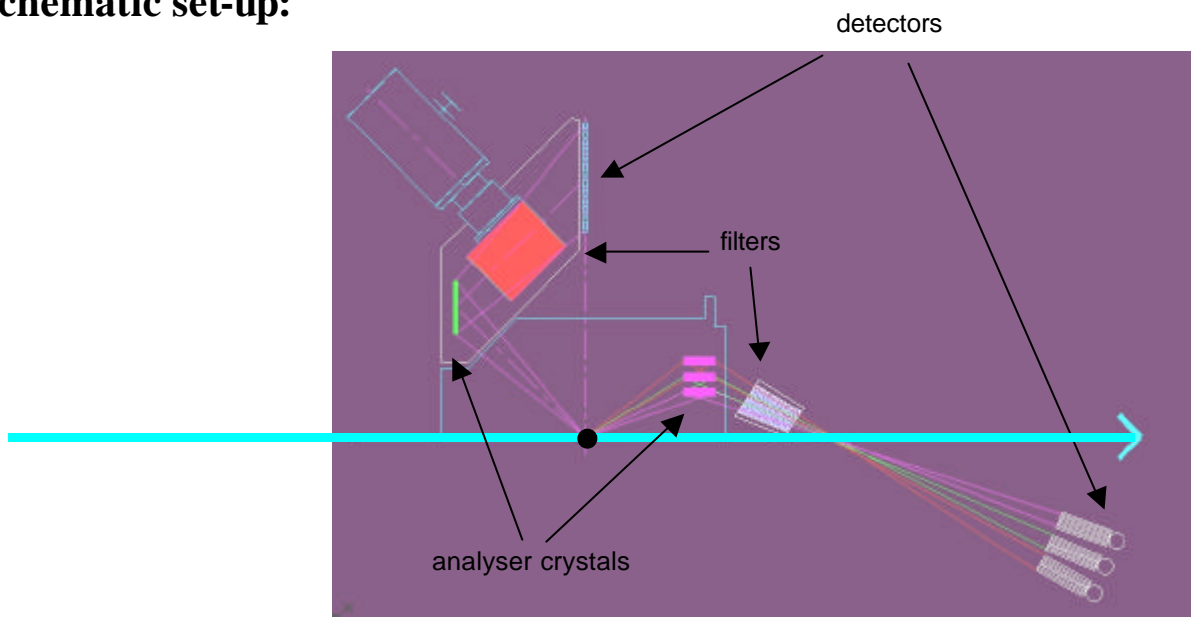
**x = 500**

# Instrument performance sheet: **Vibrational Spectroscopy Machine**

## **Instrument description:**

An inverse-geometry instrument for measuring the vibrational density of states, particularly in hydrogenous systems. A multianalyser array of PG002 crystals is used at fixed  $k_f$ , covering as much solid angle as possible. Cooled Be filters remove higher-order contamination.

## **Schematic set-up:**



**Generic type:** TOSCA      Vibrational Spectroscopy  
**Wavelengths used:** 0.2 → 5 Å  
**Moderator Type:** decoupled hydrogen

**Q-w-range:**  $0 < \hbar\omega < 1000$  meV

## **Source gain:**

Target	50Hz	10Hz	16.6Hz
moderator	decoupled cold	decoupled cold	
flux gain relative to TOSCA	<b>50</b>	<b>20</b>	<b>0</b>

*Additional gain due to modern/new design: ~2*

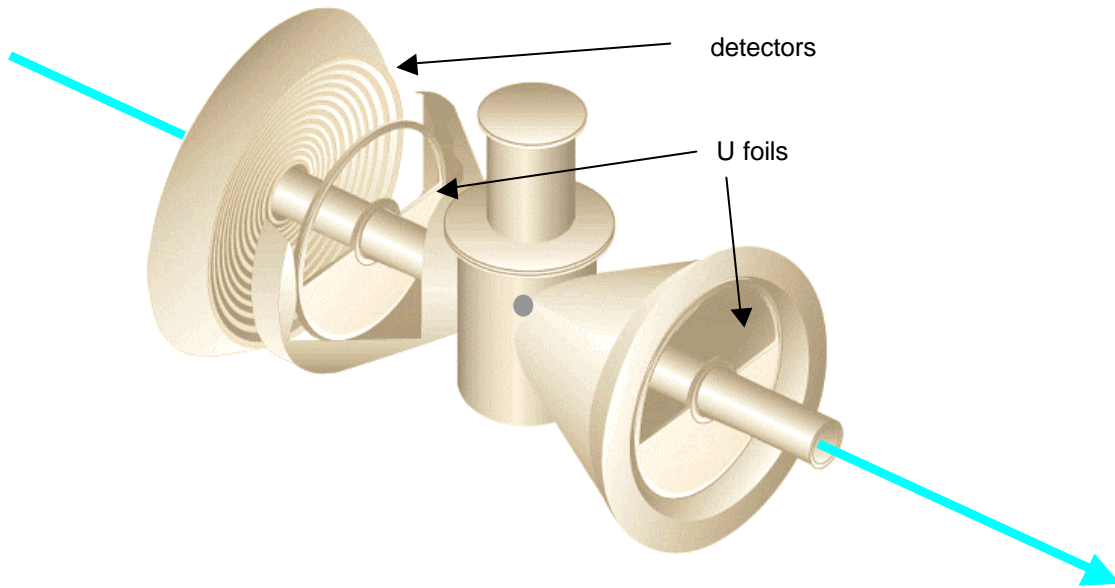
**x = 100**

# Instrument performance sheet: Resonance High-Energy Spectrometer

## Instrument description:

An inverse-geometry instrument for measuring atomic momentum distributions by neutron Compton scattering. It uses the resonant neutron absorption of  $^{238}\text{U}$  at 6.67 eV as energy analyser.

## Schematic set-up:



**Generic type:** eVS Neutron Compton Scattering  
**Wavelengths used:** 0.04 → 0.11 Å (5 to 64 eV)  
**Moderator Type:** poisoned water or hydrogen

**Q-w-range:**  $30 < Q < 200 \text{ \AA}^{-1}$   
 $1 < \hbar\omega < 30 \text{ eV}$

## Source gain:

Target	50Hz	10Hz	16.6Hz
moderator	poisoned	poisoned	
flux gain relative to eVS	<b>30</b>	<b>6</b>	<b>0</b>

*Additional gain due to modern/new design: ~10*

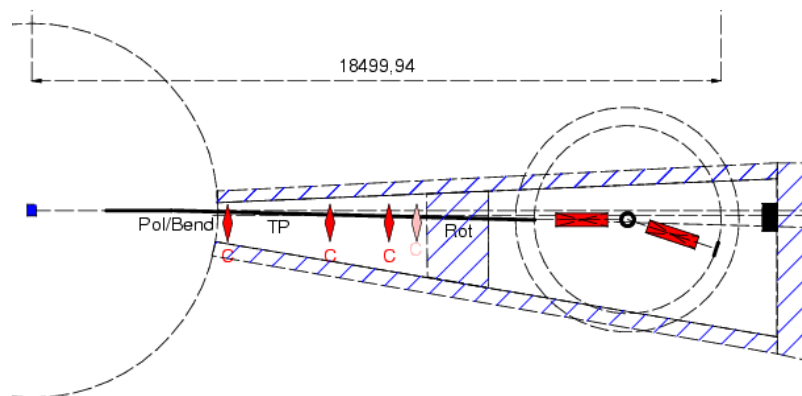
**x = 300**

# Instrument performance sheet: High Resolution NSE

## Instrument description:

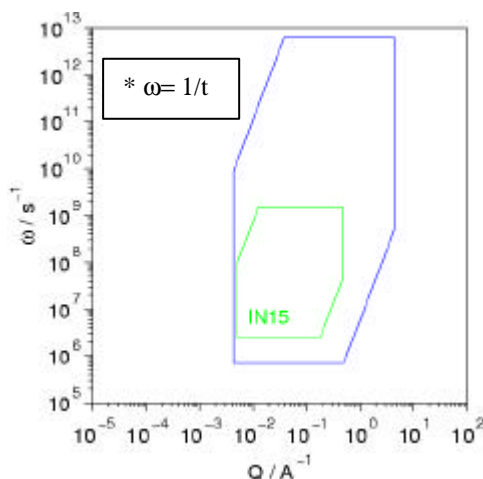
Neutron Spin-echo instrument, the exact layout depends on the target station (repetition frequency); new design features to achieve long Fourier times; resolution depends on long wavelength NOT on short pulses.

## Schematic setup:



**Generic type:** IN11 ; Fourier method  $\rightarrow S(Q,t)$   
**Wavelengths used:**  $0.2 \text{ nm} < \lambda < 2 \text{ nm}$   
**Moderator type:** cold coupled hydrogen

## Q-w -range:



Intensity gain (relative to reactor)

$$g_0 = \ln(\lambda_{\max} / \lambda_{\min}) / (\text{rel.FWHM})$$

Target	50Hz	10Hz	16.6Hz
$g_0 * (\Phi_{\text{ESS}} / \Phi_{\text{ILL}})$	<b>2.7-7.4</b>	<b>2.8</b>	<b>14 !</b>

*Additional gain due to modern/new design: ~10*

**x = 140**

# Instrument performance sheet: Wide Angle NSE

## Instrument description

The spectrometer will be of SPAN (HMI) generic design. It will have an overall diameter of 8-9m and the set-up should allow for the maximum detection solid angle. Due to its large dimensions the spectrometer should be located at ~40m from the source, i.e. far from the crowded area around the shielding.

## Generic type: SPAN

Wavelength range : 0.2 nm  $\lambda$  2 nm

Energy range at  $\lambda = 0.2$  nm : from 2  $\mu$ eV up to 4 meV

$\lambda = 1$  nm : from 16 neV up to 32  $\mu$ eV

$\lambda = 2$  nm : from 2 neV up to 4  $\mu$ eV

## Schematic set-up:

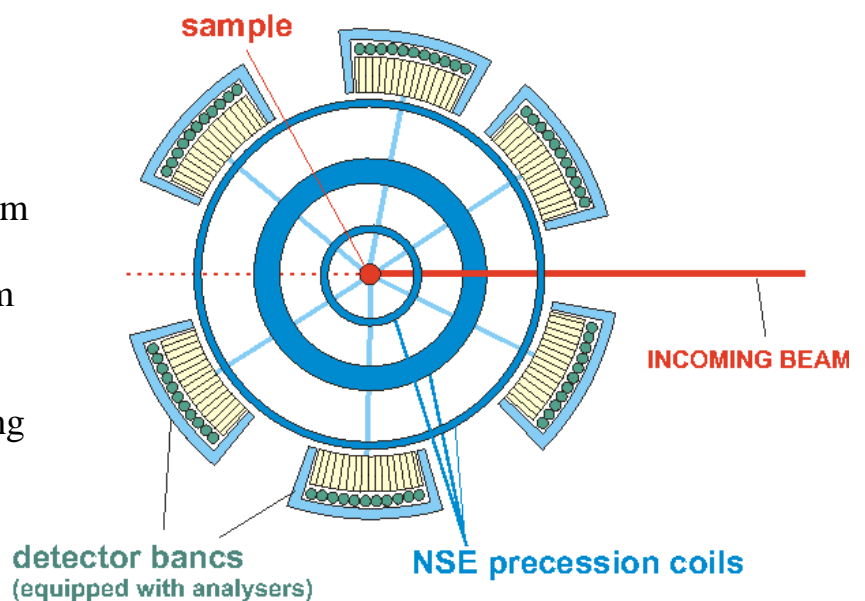
Spectrometer seen from the top

Angular range for NSE:  
from -150 deg to 150 deg

Detector – moderator distance 40m

Distance sample – detectors 4.5m

Detecting system :  
benches of single detectors moving  
around the sample



## Source gain:

Target	50Hz	10Hz	16.6Hz
$g_0^*(\Phi_{ESS} / \Phi_{ILL})$	<b>4</b>	<b>2</b>	<b>9</b>

Additional gain due to modern/new design (ref. IN11C): ~35

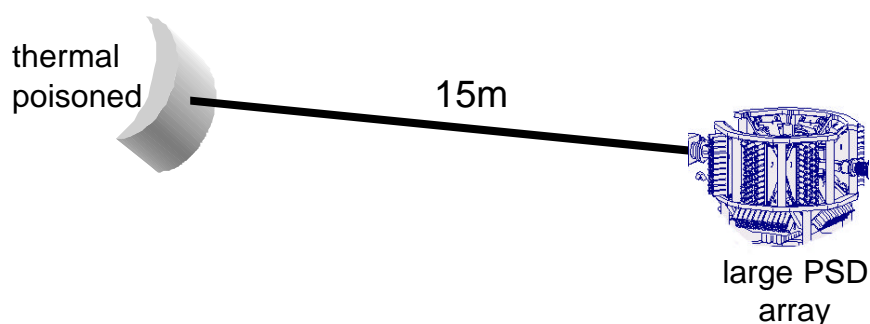
**x = 300**

# Instrument performance sheet: Single Crystal Chemical Crystallography

## Instrument description:

"Standard" chemical crystallography and materials science, rapid structure determination for unit cells up to 30 Å cell edge, parametric studies e.g. function of T, small crystal samples. Hydrogen atom positions, atomic disorder, thermal parameters, charge and spin density studies etc.  $d_{\min}$  to 0.35-0.4 Å. Good Q-space resolution to allow peaks to be separated and integrated.

## Schematic set-up:



**Generic type.** D9 (ILL); SXD (ISIS)  
**Wavelengths used:** 0.5-5 Å  
**Moderator Type:** thermal, poisoned, decoupled (option of 130K)

## Q-w-range:

$$d_{\min} \sim 0.35-0.4 \text{ \AA}$$

$$\sin\theta/\lambda \leq 1.4 \text{ \AA}^{-1}$$

$$(Q \leq 18 \text{ \AA}^{-1})$$

Gains (relative to reactor/best spallation) - very dependent on sample / background / application etc). Not just flux.

## Source gain:

Target	50Hz	10Hz	16.6Hz
Gains	<b>optimal, »10</b>	<b>2<sup>nd</sup> choice</b>	<b>3<sup>rd</sup> choice</b>

*No additional gain by modern design*

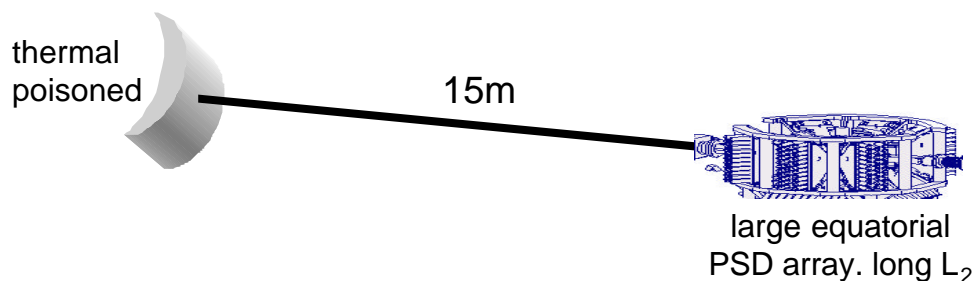
**x >>10**

# Instrument performance sheet: High Resolution Single Crystal Diffraction

## Instrument description:

High resolution (both short d-spacing and good  $\Delta Q/Q$ ) single crystal diffraction. Studies of anharmonicity, critical scattering, incommensurate structures, satellite reflections, magnetic structures, phase transitions.  $d_{\min}$  of 0.2 Å. Very high Q-space resolution required to allow for features close to Bragg peaks to be resolved. High positional resolution area detectors important.

## Schematic set-up:



**Generic type:** D9, D10 (ILL); SXD (ISIS), SCD (IPNS)

**Wavelengths used:** 0.25-2 Å

**Moderator Type:** thermal, poisoned, decoupled (dt~10μs)

## Q-w-range:

$$d_{\min} \sim 0.2 \text{ \AA}$$

$$\sin\theta/\lambda \leq 2.5 \text{ \AA}^{-1}$$

$$(Q \leq 31 \text{ \AA}^{-1})$$

Gains (relative to reactor/best spallation) - very dependent on sample / background / application etc). Not just flux.

## Source gain:

Target	50Hz	10Hz	16.6Hz
Gains	<b>optimal, »10</b>	<b>2<sup>nd</sup> choice</b>	<b>3<sup>rd</sup> choice</b>

*No additional gain by modern design*

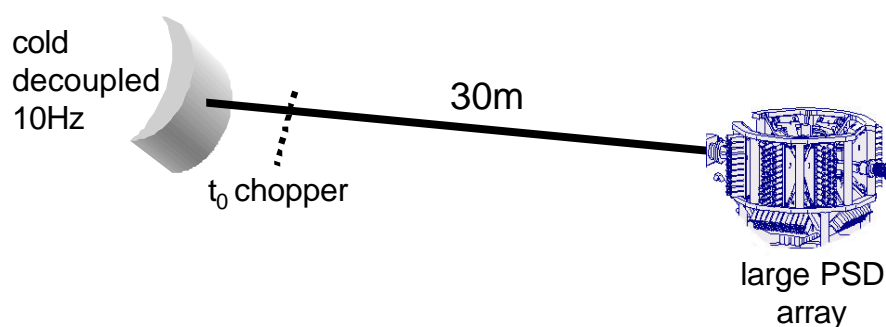
**x >>10**

# Instrument performance sheet: Single Crystal Diffuse Scattering

## Instrument description:

Diffuse scattering studies, particularly away from the Bragg peaks. Studies of (static and dynamically) disordered single crystals - fast-ion conductors, GMR/high  $T_C$  materials etc. Analysis techniques such as Reverse Monte Carlo, pair distribution function etc. Good intensity at high/low  $Q$ , continuous coverage of reciprocal space at good  $Q$ -space resolution. Fully resolved 3D volumes accessed.

## Schematic set-up:



**Generic type:** SXD (ISIS), D10 (ILL)  
**Wavelengths used:** 0.5-5 Å  
**Moderator Type:** medium cold (130K) or cold, decoupled

## Q-w-range:

$$d_{\min} \sim 0.4 \text{ \AA}$$

$$\sin\theta/\lambda \leq 1.2 \text{ \AA}^{-1}$$

$$(Q \leq 15 \text{ \AA}^{-1})$$

Gains (relative to reactor/best spallation) - very dependent on sample / background / application etc). Not just flux.

## Source gain:

Target	50Hz	10Hz	16.6Hz
Gains	<b>optimal, »10</b>	<b>2<sup>nd</sup> choice</b>	<b>3<sup>rd</sup> choice</b>

*No additional gain by modern design*

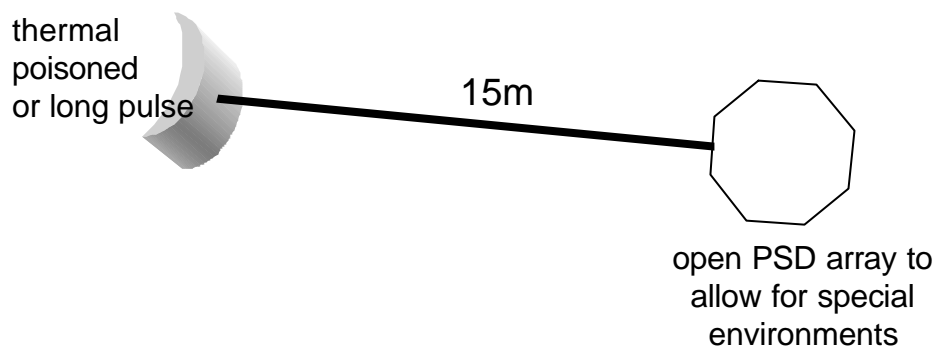
**x >>10**

# Instrument performance sheet: Single Reflection Single Crystal Studies

## Instrument description:

Rapid and/or accurate studies of individual peaks through e.g. a phase transition under the influence of changing external environment e.g. temperature, pressure, magnetic field. Important in physics area. Need for high point-by-point flux, good resolution to resolve e.g. splitting peaks, appearance of satellites. Complementary (simultaneous) structural measurements also necessary.

## Schematic set-up:



**Generic type:** D10 (ILL), 6T2 (Saclay), TAS in elastic mode  
**Wavelengths used:** 0.5-5 Å  
**Moderator Type:** thermal, decoupled

## Q-w-range:

$$d_{\min} \sim 0.4 \text{ \AA}$$

$$\sin\theta/\lambda \leq 1.2 \text{ \AA}^{-1}$$

$$(Q \leq 15 \text{ \AA}^{-1})$$

Gains (relative to reactor) - very dependent on sample / background / application etc). Not just flux.

## Source gain:

Target	50Hz	10Hz	16.6Hz
Gains	<b>0.3-3</b>	<b>3<sup>rd</sup> choice</b>	<b>0.3-3</b>

*No additional gain by modern design*

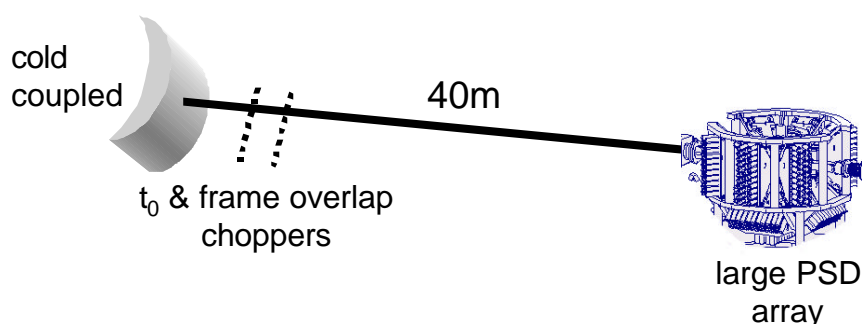
**x = 0.3-3**

# Instrument performance sheet: High Resolution Protein Crystallography

## Instrument description:

Macromolecular (protein) crystallography, unit cells up to 150-200 Å, crystals of 1mm<sup>3</sup> or less. Determination of H/D positions in active sites, mobile protons, studies of H/D exchange, solvent structure around biological macromolecules. High d-space resolution -  $d_{\min}$  of 1.2-2.4 Å depending on application and crystal diffraction quality. Good Q-space resolution for reliable peak integration.

## Schematic set-up:



**Generic type:** LADI, D19 (ILL); PX-station (LANSCE)  
**Wavelengths used:** 1.8-5 Å  
**Moderator Type:** cold, coupled (but 3-5 x gain if 130K mod.)

## Q-w-range:

$$d_{\min} \sim 1.2-2.4 \text{ \AA}$$

$$\sin\theta/\lambda \leq 0.4 \text{ \AA}^{-1}$$

$$(Q \leq 5.0 \text{ \AA}^{-1})$$

Gains (relative to reactor/best spallation) - very dependent on sample / background / application etc). Not just flux.

## Source gain:

Target	50Hz	10Hz	16.6Hz
Gains	<b>optimal, &gt;10</b>	<b>2<sup>nd</sup> choice</b>	<b>3<sup>rd</sup> choice</b>

*No additional gain by modern design*

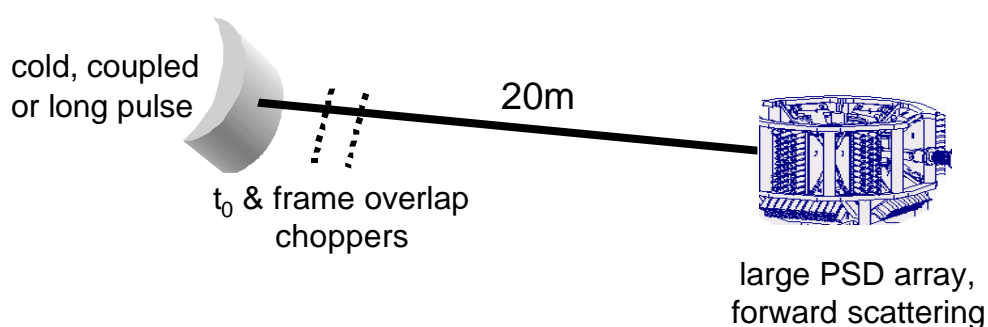
**x >10**

# Instrument performance sheet: Low Resolution Protein Crystallography

## Instrument description:

Low resolution biological crystallography, studies of partially ordered components of molecular complexes and assemblies, membranes, protein-nucleic acid interactions. Use of contrast variation/D labelling. Small single crystals ( $<0.1\text{mm}^3$ ) or large unit cell ( $>300 \text{ \AA}$ ) studied to low d-spacing resolution ( $d_{\text{min}}$  of 6-10  $\text{\AA}$ ). An important area under exploited with current instrumentation.

## Schematic set-up:



**Generic type.** DB21 (ILL)  
**Wavelengths used:** 5-15  $\text{\AA}$   
**Moderator Type:** cold, coupled

## Q-w-range:

$$d_{\text{min}} \sim 6-10 \text{ \AA}$$

$$\sin\theta/\lambda \leq 0.08 \text{ \AA}^{-1}$$

$$(Q \leq 1 \text{ \AA}^{-1})$$

Gains (relative to reactor) - very dependent on sample / background / application etc). Not just flux.

## Source gain:

Target	50Hz	10Hz	16.66Hz
Gains	<b>3-5</b>	<b>3<sup>rd</sup> choice</b>	<b>3-5</b>

*No additional gain by modern design*

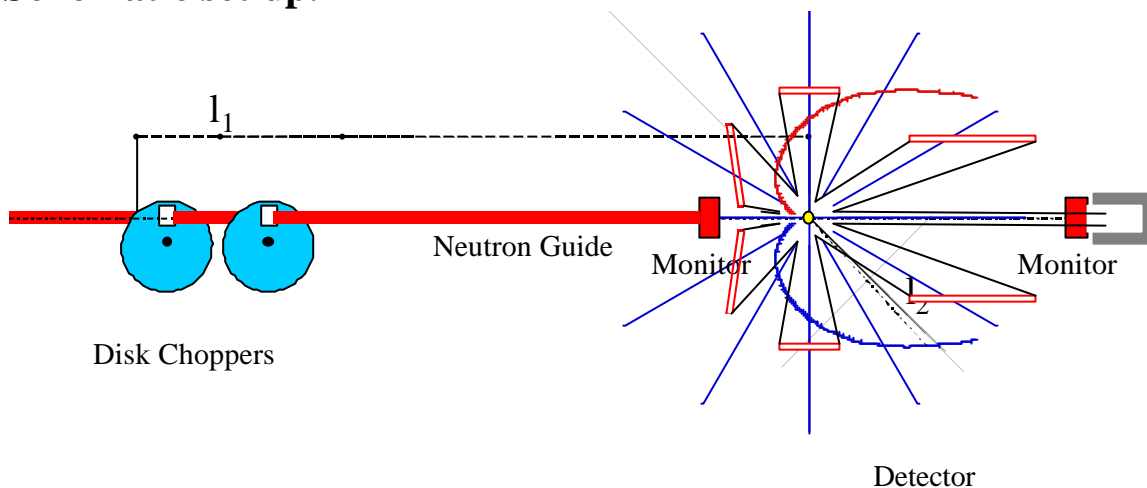
**x = 3-5**

# Instrument performance sheet: High Resolution Powder Diffraction

## Instrument description:

High resolution powder diffractometer, with either a continuous detector or discrete banks. The primary flight-path is 200m. It can be operated in narrow- or wide-bandwidth mode. The resolution on an H<sub>2</sub> moderator (0.04%) will be similar to that of HRPD at ISIS in the 2m position, and can be improved on an advanced cold moderator.

## Schematic set-up:



**Generic type:** High-resolution powder diffractometer

Wavelengths used:  $0.7 \text{ \AA} < \lambda < 10 \text{ \AA}$ .  $\Delta\lambda \sim 0.4 \text{ \AA} @ 200\text{m}$

Moderator Type: decoupled cold poisoned (H<sub>2</sub> or advanced)

**Q-w-range:**

$$0.5 \leq Q \leq 12.0$$

Intensity gain (relative to ISIS)  
 Additional gain ( $\times 2-4$ ) can be achieved  
 in back-scattering by using a  
 supermirror guide.

**Source gain:**

Target	50Hz	10Hz	16.6Hz
g0	<b>50</b>	<b>50</b>	<b>50</b>

*Additional gain due to modern/new design: 2-4*

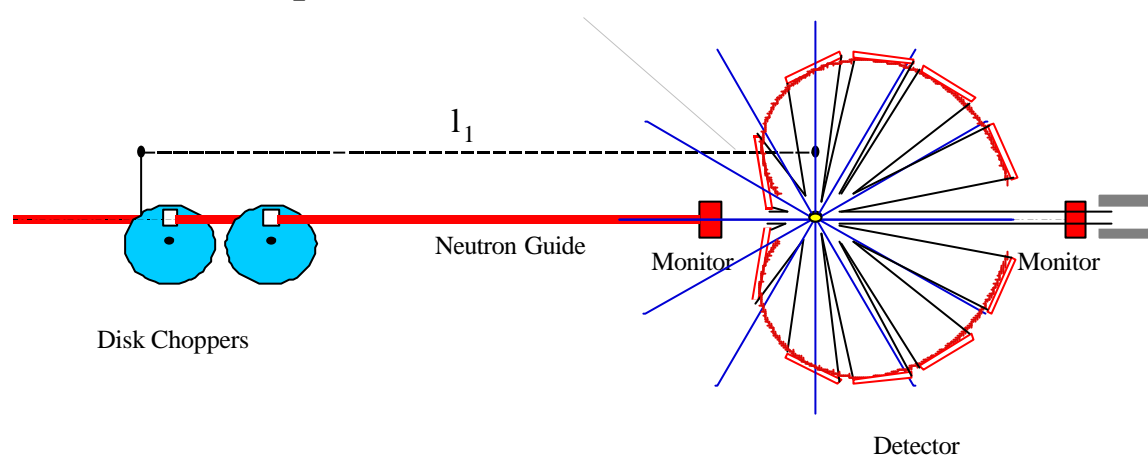
**x = 100-200**

# Instrument performance sheet: High-Q Powder Diffraction

## Instrument description:

Medium-resolution powder diffractometer for fast crystallographic and PDF data collection to high Q. The primary flight-path is 40m. It can be operated in narrow- or wide-bandwidth mode, with either multi-bank or continuous detector. The resolution is ~0.2% on a poisoned H<sub>2</sub>O moderator, 0.1% on an advanced cold moderator.

## Schematic set-up:



**Generic type:** Medium-resolution powder diffractometer  
crystallographic applications

Wavelengths used:  $3 \text{ \AA} < \lambda < 8 \text{ \AA}$ .  $\Delta\lambda \sim 2.1 \text{ \AA} @ 50\text{m}$

Moderator Type: decoupled ambient poisoned H<sub>2</sub>O/advanced cold

## Q-w-range:

$0.2 \leq Q \leq 80$

Intensity gain (relative to ISIS)  
Vertical focussing can be optimised for  
a  $\times 2$  gain.

## Source gain:

Target	50Hz	10Hz	16.6Hz
g0	<b>60</b>	<b>60</b>	<b>n.a.</b>

*Additional gain due to modern/new design: ~2*

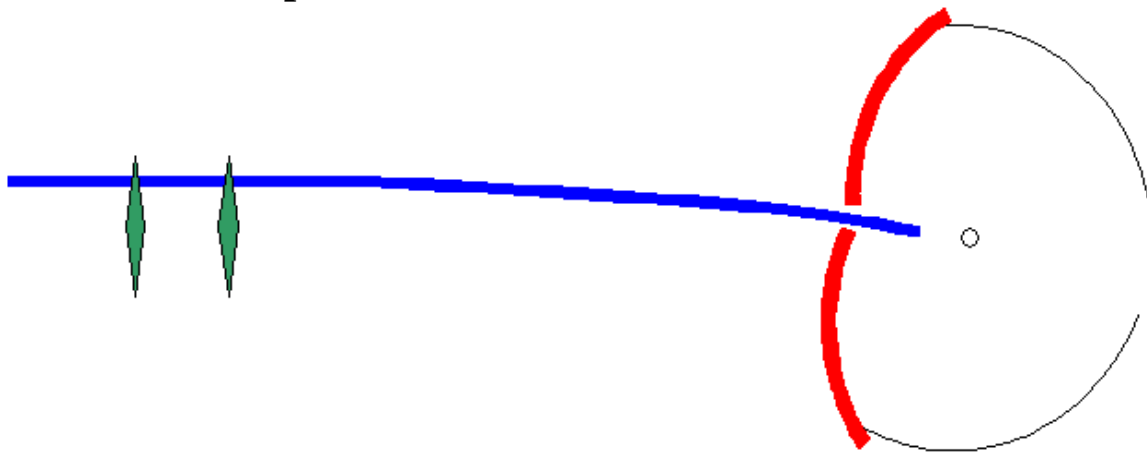
**x = 120**

# Instrument performance sheet: Magnetic Powder Diffraction

## Instrument description:

Medium-resolution powder diffractometer for magnetic diffraction, with continuous detector in back-scattering. The primary flight-path is 80m. The resolution on an unpoisoned H<sub>2</sub> moderator is ~0.2%.

## Schematic set-up:



**Generic type:** Medium-resolution powder diffractometer for magnetism

Wavelengths used:  $1.2 \text{ \AA} < \lambda < 30 \text{ \AA}$ .  $\Delta\lambda \sim 1 \text{ \AA} @ 50\text{m}$

Moderator Type: decoupled cold unpoisoned H<sub>2</sub>

## Q-w-range:

$0.2 \leq Q \leq 6.0$

Intensity gain (relative to ISIS)  
Osiris guide is already optimized.  
Extended detector design yields a  $\times 2$  gain.

## Source gain:

Target	50Hz	10Hz	16.6Hz
g0	<b>60</b>	<b>60</b>	<b>25-50*</b>

*Additional gain due to modern/new design: ~1*

**x = 60**

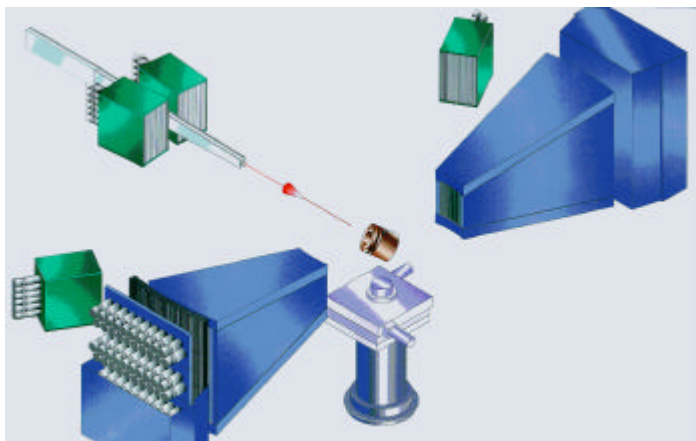
# Instrument performance sheet: **Engineering**

## **Diffractometer**

### **Instrument description:**

Medium-high resolution powder diffractometer optimised for strain measurement, similar to ENGIN-X at ISIS. The primary flight path is ~50m, on a curved guide. The final section of the guide can be interchanged with absorber to provide tuneable resolution in the 90° detector banks. Large 90° detector banks, also backscattering and transmission detectors. The sample area is large and open to the air, to allow large samples and sample environment equipment.

### **Schematic set up:**



Moderator to sample distance 40-50m, supermirror guide, frame definition choppers.

Large sample environment space. Variable incident horizontal divergence. Variable incident and exiting collimation.

### **Generic type:**

Medium resolution powder diffractometer

Wavelength.  $0.7 \text{ \AA} < \lambda < 3 \text{ \AA}$ .  $\lambda$  range  $\sim 1.5 \text{ \AA}$ .  
 $0.2\% < \Delta\lambda/\lambda < 0.7\%$  in 90°.

Moderator type: decoupled, poisoned H<sub>2</sub>O or new cold one

Target station: 50Hz short pulse

### **Performance:**

High resolution engineering diffractometer. Performance gains vs. ENGIN-X instrument presently under construction at ISIS x30 (source), further x2-3 for some types of experiments from instrument design.

**x=90**

## Instrument performance sheet: Reflectometers

### **Instrument description:**

Instrument which measures reflectivity curves down to reflectivities of the order  $10^{-8}$  in the small angle range up to  $q = 0.5 \text{ \AA}^{-1}$ . For solids it is possible to measure atomic Bragg peaks at large  $q$ -values.

In order to optimize the instrument with respect to both resolution and intensity **two** instruments are needed, a high intensity reflectometer on the 16.6Hz LPSS and a high resolution reflectometer at the 50Hz SPSS.

### **Schematic set-up:**

The exact set-up strongly depends on the source parameters, the wanted resolution and the samples which should be investigated: solid magnetic/non-magnetic samples or liquid samples. Polarized neutrons should be available.

Length of instrument at a LPSS: 40-80m

Length of instrument at a SPSS: 12m

**Generic type:** high resolution: SURF (ISIS)

high intensity: ADAM (ILL)

Wavelengths used:  $0.2 \text{ nm} < \lambda < 0.9 \text{ nm}$

Moderator Type: cold coupled moderator

### **Q-w-range:**

$0.01 \text{ \AA}^{-1} < q < 3 \text{ \AA}^{-1}$

### **Source gain:**

Target	50Hz	10Hz	16.6Hz
g0 (high resolution)	<b>120</b>	<b>25</b>	<b>90</b>
g0 (high intensity)	<b>10</b>	<b>2</b>	<b>15</b>

*Additional gain due to modern/new design: ~2*

**x = 30-200**

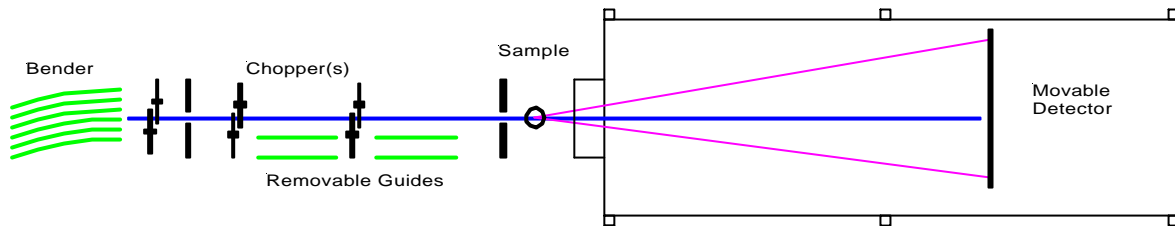
# Instrument performance sheet: **SANS**

## Instrument description:

Neutron Small Angle Instrument, the exact layout depends on the target station (repetition frequency).

## Schematic set-up:

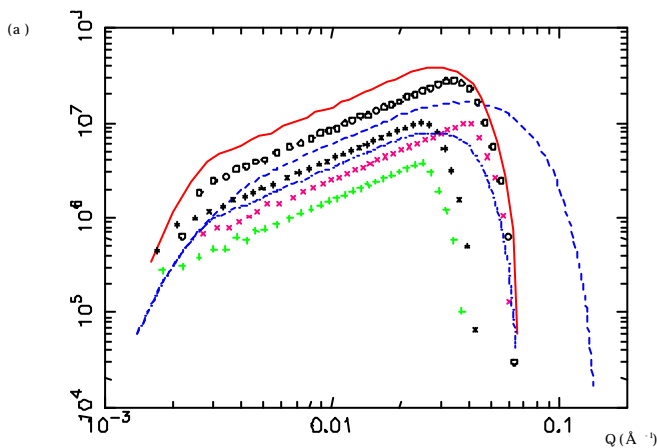
Generic SANS instrument for ESS:



**Generic type** (c.f. D22 at ILL): total length ~ 40m; large area detector (> 1m x 1m); curved guide and/or bender removes direct view of moderator, optional polariser.

Wavelengths used:  $0.2 \text{ nm} < \lambda < 2 \text{ nm}$

Moderator type: cold coupled hydrogen



SANS at 36m (6/15/15), collimation and sample to detector distance of 15m,  $1 \text{ cm}^{-1}$  flat scatterer

line (-):  $\lambda = 4.4\text{-}9.2 \text{ \AA}$ ; 5MW, 16.6Hz

circles:  $\lambda = 4.6\text{-}6.6 \text{ \AA}$ ; 5MW, 50Hz

asterisk:  $\lambda = 6.8\text{-}8.8 \text{ \AA}$ ; 5MW, 50Hz

dashes (-):  $\lambda = 2\text{-}11 \text{ \AA}$ ; 1MW, 10Hz

dot-dash (-·):  $\lambda = 4.4\text{-}11 \text{ \AA}$ ; 1MW, 10Hz

xxx:  $\lambda = 5 \text{ \AA}$ ; +++:  $\lambda = 8 \text{ \AA}$ , 10% FWHM; ~ ILL reactor

**Source gain:** Approximate improvements in count rate  $g_0$ , and Q resolution  $\sigma_0$  (FWHM) over ILL, which are then coupled with an expanded simultaneous Q range:

Target	50Hz	10Hz	16.6Hz
$g_0^*(\Phi_{\text{ESS}} / \Phi_{\text{ILL}})$	<b>4-5</b>	<b>2-4</b>	<b>7-10</b>
$\sigma_0^*(\sigma_{\text{ILL}} / \sigma_{\text{ESS}})$	<b>3.5</b>	<b>3.5</b>	<b>2</b>

*No additional gain due to modern design*

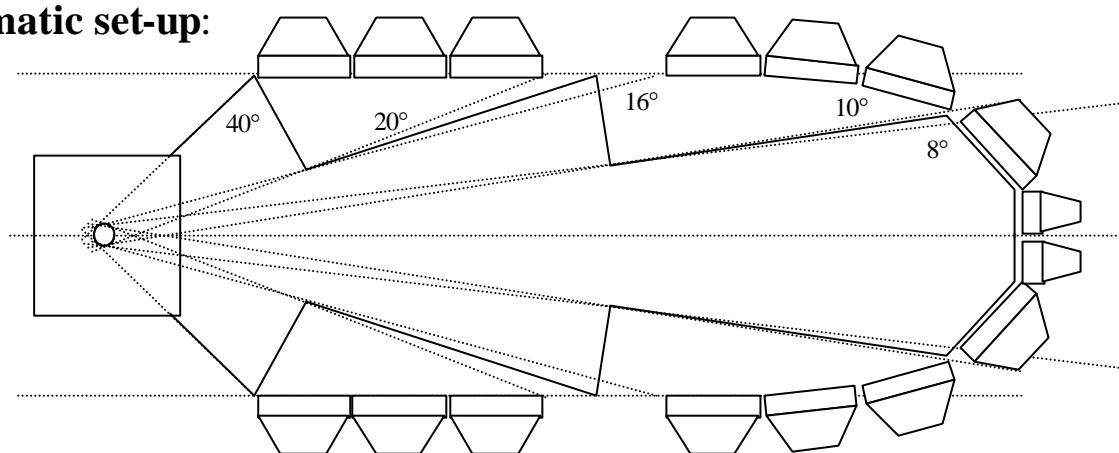
**x = 10**

# Instrument performance sheet: Total Scattering Diffractometer

## Instrument description:

Total Scattering diffractometer for disordered materials and crystalline materials. Can be 11m incident flight path (50Hz target) or up to 25m incident flight path (10Hz Target). 50Hz option is preferred. Most detector solid angle is at low scattering angles, but **backscattering** detectors are needed for higher resolution at large Q. This instrument(s) should be kept separate from any crystallographic powder diffractometers because the flight path requirements are different.

## Schematic set-up:



## Generic type.

SANDALS/GEM TOF diffractometer

Wavelengths used:

0.05 Å – 5.0 Å

Moderator Type:

water (50Hz) – preferred

Q-range:

$0.01 \text{ \AA}^{-1} < Q < 60 \text{ \AA}^{-1}$

## Source gain (relative to ISIS):

“C-number” is the peak count rate from  $1 \text{ cm}^3$  vanadium in units of  $\text{cts/s}/0.05 \text{ \AA}^{-1}/\text{cm}^3 \text{ V}$

Current value at D4 (ILL) is 50-500, at SANDALS (ISIS) is ~600

We quote the ratio C-number(ESS)/C-number(SANDALS)

Target	50Hz	10Hz	16.6Hz
C-number ratio	~20	4	-

*Additional gain due to modern/new design: ~1*

**x = 20**

